BIDDING STRATEGY OF DISTRIBUTED ENERGY RESOURCES PARTICIPATING IN ELECTRICITY MARKET AS PRICE-MAKERS

GAO XIANG

PhD

The Hong Kong Polytechnic University

2021

The Hong Kong Polytechnic University

Department of Electrical Engineering

Bidding Strategy of Distributed Energy Resources Participating in Electricity Market as Price-makers

GAO XIANG

A thesis submitted in partial fulfillment of the requirements for the degree of Doctor of Philosophy

Dec 2020

CERTIFICATE OF ORIGINALITY

I hereby declare that this thesis is my own work and that, to the best of my knowledge and belief, it reproduces no material previously published or written, nor material that has been accepted for the award of any other degree or diploma, except where due acknowledgment has been made in the text.

_____(Signed)

GAO Xiang (Name of student)

Abstract

Over the last decade, the world has witnessed a rapid growth in the capacity of distributed energy resources (DERs). The rapid expansion of their scales and their green contribution to energy conservation and environment protection have resulted them playing increasingly important roles in the electricity market. While those DERs can be aggregated to increase their own profits via strategically bidding, an effective approach to model their market behaviors shall also be developed to investigate their systemwide impacts.

Wind power producers (WPPs) as aggregated large quantities of distributed wind turbines have occupied a dominant position in electricity generation of renewable DERs. Meanwhile, rapidly growing number of distributed electric vehicles (EVs) could be aggregated as a new demand response (DR) resource for providing energy through a coordinator called the EV aggregator, which dispatches the charging of EVs and exchanges information between the electricity market and individual EV owners. In recent years, there also exists a rapid increase in generating electricity by natural gas, which is expected to overtake coal by 2030 due to its lower price, less pollution, and higher energy conversion efficiency. The proliferation of natural gas generating units (NGGs) and the emerging of power-to-gas conversion (P2G) technology have enabled the bidirectional energy flows between the electric power and natural gas systems via integrated NGG-P2G facilities. However, DERs such as wind energy and EVs are easily influenced by the weather or depend on human behaviors, there are uncertainties in their outputs which would further influence their profits. The resulted bidding problem would therefore be an optimization problem involving uncertainties, and a stochastic optimization method is adopted in this thesis to handle this problem. Also, large-scaled DERs could be cooperated with or competed against each other to

influence electricity prices according to their own interests, this thesis would conduct studies and develop bidding strategies for large-scaled DERs in the electricity market.

For the bidding strategy of same-commodity cooperative arbitrage, this thesis firstly proposes a bi-level stochastic optimization model for an aggregated WPP-EV hybrid power plant (HPP) as a price-maker in the day-ahead (DA) market with consideration of the uncertainties of the wind power capacity and the electricity price in the real-time (RT) market. The profit of HPP is maximized in the upper level using the conditional-value-at-risk (*CVaR*) to manage the risk of the expected revenue, while the lower level is used to maximize the social welfare from the perspective of the grid. The formulated bi-level model is first transformed into a single-level mathematical program with equilibrium constraints (MPEC) and then further transformed to a mixed-integer linear programming (MILP) problem for solution. Simulation results have demonstrated the effectiveness of the proposed HPP model with strategically bidding prices to increase the profits and reduce its volatility caused by uncertainties through considering the risk-metric.

As to cross-commodity cooperative arbitrage, the integrated energy system has attracted more and more attention in recent years as it is beneficial to use the synergies between electricity and other energies for balancing the fluctuation of renewable DERs. In this thesis, a bidding strategy is developed for a coordinated WPP and NGG-P2G facility in DA market and RT market as well as providing auxiliary services employed in real-time. The WPP and NGG-P2G unit are coordinately operated in a virtual multi-energy plant (VMP) with the feature of natural gas, heat and electricity integration. A bi-level stochastic optimization model is proposed to determine the bidding strategy. The profit of the coordinated unit is maximized in the upper level with consideration of the uncertainties of WPP output and RT electricity prices, while the lower level is used to maximize social welfare from the perspective of the grid. Simulation results have demonstrated that uncertainties of the WPP are mitigated with flexible operation of NGG-P2G unit and the waste of wind resources is reduced, which is more profitable and environmentally friendly. The payoff in the proposed model is mostly provided by

the WPP in DA market, where the integrated P2G-G2P unit enhances payoffs further by providing auxiliary services.

Although numerous cooperative models have been demonstrated to bring more revenue with strategical bidding based on collaborators' compensation for peak shaving. They depend highly on the centralized control and scheduling of a central aggregator, in which the privacy of players cannot be guaranteed, and have little flexibility to cope with any self-decisions. Considering the bidding strategy with decentralized control which respects personal privacy and autonomy of energy suppliers, a competitive model is further formulated for WPPs and EV aggregators in a pool-based day-ahead electricity market. A bi-level multi-agent-based model is proposed to study their bidding behaviors, with market-clearing completion in the lower level and revenue maximization in the upper level. A stochastic framework is developed to incorporate the uncertainties in bid prices of other participants and the power production of WPPs and EV aggregators. The process of bidding decision is formulated as a stochastic game with incomplete information. Their lack of information in this stochastic market environment is counterbalanced by a multi-agent reinforcement learning (MARL) algorithm named win or learn fast policy hill climbing (*WoLF-PHC*) with maximizing their own profits by self-game. The feasibility and effectiveness of the proposed model and the *WoLF-PHC* solution approach are successfully illustrated using IEEE 6-bus and 118-bus systems. Multiple participants could respectively optimize their bids by learning with using the *WoLF-PHC* algorithm in competitive markets. Besides, compared with the cooperative model of the WPP and EV aggregator in the previous study, the proposed competitive model can adapt to a more flexible market environment in which every strategic player has full autonomy in biddings with incomplete information to maximize its own profit.

Acknowledgments

First and foremost, I would like to express my most sincere gratitude to my chief supervisor, Dr. Kevin K. W. Chan, for his continuous support, care and encouragement throughout my PhD study and research. He kindly offered me the chance to study and patiently guided me to solve all kinds of academic problems. His knowledge, experience and intelligence always impress me and enlighten me. It is my honor to study under his guidance.

I also would like to express my special appreciation to my good friend Dr. Shiwei Xia, for the patient suggestions throughout my entire PhD study, for the stimulating discussions we had, for the can-do attitude and hardworking spirit brought to me. My thanks also go to other members in the research team Dr. Bin Zhou, Dr. Xian Zhang, Dr. Xi Lu, Dr. Ming Liu, Dr. Wenzheng Xu, Mr. Jiahan Zhou, Mr. Ziqing Zhu and research colleagues Miss. Qian Hu, Mr. Jiaxin Wen, Mr. Jianqiang Luo, Mr. Zilin Li. They accompanied and inspired me when I was frustrated, made progress and became better together with me during my precious PhD study. In addition, I am very grateful to research assistants Dr. Xiaoshun Zhang, Dr. Qianwen Xu, Dr. Zhekang Dong, Dr. Da Xu and Mr. Kuan Zhang. They have given me many valuable advices and practical helps on my life and research. I will always remember this wonderful and unforgettable research journey in Hong Kong.

Moreover, I would like to thank my dear parents Liming Gao and Jianping Liu for their selfless and unconditional love ever since I was born, for financial support and spiritual encouragement to fulfill my desire to continue the study.

Last but not the least, I would like to acknowledge the support from The Hong Kong Polytechnic University.

Table of Contents

Lists of Figures, Tables and Abbreviations

List of Figures

List of Tables

List of Abbreviations

WPP	Wind power plant
EV	Electric vehicle
HPP	Hybrid power plant
DA	Day-ahead
RT	Real-time
CVaR	Conditional-value-at-risk
MPEC	Mathematical program with equilibrium constraints
MILP	Mixed integer linear programming
DR	Demand response
G2V	Grid-to-Vehicle
V2G	Vehicle-to-Grid
ISO	Independent system operator
LMP	Locational marginal prices
OPF	Optimal power flow
KKT	Karush-Kuhn-Tucker
SDT	Strong duality theorem
DER	Distributed energy resources
NGG	Natural gas generating
P2G	Power-to-gas
VMP	Virtual multi-energy plant
UL	Upper level
LL	Lower level
MARL	Multi-agent reinforcement learning
WoLF-PHC	Win or learn fast policy hill climbing
ABM	Agent-based model

Chapter I

Introduction

1.1 Background

Towards low carbon emission and conservation of fossil fuels, the integration of various DERs to the grid has been actively researched in the past few decades for sustainable electricity [1, 2]. Renewable DERs are able to replenish itself relied on the natural process and have been predicted to account for 80% of the total electricity production by 2030 and 100% by 2050, of which 37% will be provided by wind energy [3, 4]. Wind energy has obvious advantages in carbon emission, production cost and developed technology [5]. With significant growth in the installed capacity of wind turbines and greatly improved wind generation technologies, distributed wind energy resources could be aggregated as WPPs and have played a major role in some electricity markets such as in Denmark, in which it could bid strategically to influence the electricity price according to its own interest [6-8]. Compared with traditional vehicles, EVs have less environmental pollution, lower noise, and greater starting torque. Besides, EVs are new DR resources which not only could buy the electricity as consumers in G2V (Grid-to-Vehicle) mode but also sell the electricity back to the grid in V2G (Vehicle-to-Grid) mode. Thus, with the number of distributed EVs dramatically increased, such flexible consumers are expected to be aggregated to supply energy on a large scale [9]. In recent years, there also has a rapid increase in the use of natural gas for generating electricity by power plants, domestic cooking and heating. The natural gas is supposed to overtake coal in energy supply by 2030 due to its lower natural gas prices, less pollution and higher energy conversion efficiencies [3]. The green contribution of these DERs to energy conservation and environment protection, as well as the rapid expansion of their scales, would result in them being oligopolists in the

wholesale electricity market [10-12].

Researches on electricity market refer to load forecasting [13, 14], price forecasting [15, 16], plan and operation of unit commitment [17], bidding strategy [18], asset valuation and risk management [19, 20], transmission congestion management and pricing [21]. This thesis mainly focuses on the bidding strategy with consideration of uncertainties of large-scaled DERs. In a perfectly competitive electricity market, any participant can only simply bid marginal cost and act as a price-taker according to the microeconomic theory [22]. When a participant bids other than marginal cost for increasing its profit, the behavior is called strategic bidding. In fact, emergent market structures are more likely to be oligopoly than perfectly competitive markets. In oligopoly electricity market, large-scale energy suppliers can improve their profits by strategically bidding and have a vital influence on market prices and power production [23-25]. The bidding information submitted by electricity producers and consumers could be only the bidding price or the bidding curve including the price and power generation [26]. The integration of a large amount of DERs into the electricity market in recent years has resulted in important research challenges. As a result, it is worthy of developing an effective approach to model bidding strategies for these large-scaled DERs.

The bidding in the electricity market involves contract trades and pool trading [27]. Bilateral contracts are negotiable agreements on delivery and reception of electricity between two market players, which is flexible and not dependent on ISO (Independent System Operator). However, it has disadvantages of contracts with high costs and risks caused by counterparties with the loss of credits. In the pool-based market, the market operator/ISO collects bidding information from electricity producers and consumers, completes market clearing, and then obtains the estimated electricity production and consumption as well as the market prices [28]. The prices and electricity production depend on the electricity trading occurring on different trading stages, which contains the day-ahead (DA), real-time (RT), and futures markets [16]. In DA market, the clearing is usually done on hourly basis and one day in advance. The RT market usually

is used to compensate for the difference between the scheduled electricity and actual electricity delivery within a short period of time (e.g., half an hour). The futures market refers to medium and long-term transactions. In these three trading stages, the largest volume of trading exists in the DA market. In addition, market types include the energy market, ancillary service market and transmission market. The DA pool-based energy market is where trading of electricity occurs, which has an independent clearing and settlement function, is studied in this thesis. The key components in DA energy market are the ISO and market participants, which can be separately considered in the lower and upper levels.

From the perspective of the ISO, there are MinISO and MaxISO models in literatures. In the MinISO model, the ISO accepts the bid curve with a price and quantity pair from every market participant and determines the market clearing price (MCP) by finding the intersection point of supply and demand curves; whereas in the MaxISO model, all participants first submit information such as energy bid, start-up cost, ramp rates to the ISO and then the ISO maximizes the social welfare by setting the locational marginal prices (LMPs) as dual variables of the load balance constraints [27]. In this thesis, the bidding problem will be fully modelled as the MaxISO model in the lower level. Network constraints only refer to the DC power flow and line losses are not considered. Other constraints include the power balance at each node, thermal capacity limits in transmission lines, generation and consumption limits for power producers and loads separately, and voltage angle limits.

For the market participant in the upper level, the aim is to maximize its profit by strategically bidding. There are two methods including same-commodity arbitrage and cross-commodity arbitrage in the electricity market. The same-commodity arbitrage aims at electricity trading at different time horizons. While the cross-commodity arbitrage refers to different products in a market or different markets. For example, the arbitrage can be obtained between power and natural gas resources, electricity and gas markets, energy market and ancillary service [27]. In [19], it is pointed out that “An energy supplier could get more revenues from the arbitrage cross the energy and

ancillary service than only selling electricity as a commodity." This is because the producer could choose to sell more electricity to ancillary services and less to the energy market when the price of providing ancillary services is higher than in trading in the energy market. Different from the traditional units developing bidding strategy, renewable wind energy resources as market participants are easily influenced by the external environment such as the weather and thus it is hard to predict their outputs. In other words, renewable wind energy resources bring uncertainties to the bidding problem of the electricity market. In addition, the integration of EVs brings flexibility for the operation of the power system. On one hand, EVs can be aggregated to balance the uncertainties caused by the renewable wind energy resource. On the other hand, it is hard to forecast information such as the arrival and departure time of EVs accurately because of the unpredictability of human decisions and the complexity of traffic situations. Thus, EVs also bring uncertainties to the operation of the electricity market. The uncertainties brought by the wind energy resources and EVs can cause some serious consequences such as power imbalance and overloaded lines, which may further result in widespread power outages. For the DERs making bidding decisions, uncertainties of them may affect their own incomes [20]. Besides, the uncertainties associated with these stochastic resources can introduce risk into the bidding problem. In this case, risk measurement is important for uncertainty and can provide guidance to DERs decision makers. Risk measuring can be categorized into risk-neutral and risk-averse according to different design parameters. The risk-neutral approach maximizes profits of decision makers and ignores the volatility of profits, while the risk-averse method enables us to consider the risk of profit fluctuations associated with the bidding strategy.

Thus, it is essential to research the bi-level bidding model in electricity market with consideration of uncertainties of DERs.

1.2 Research Motivations

1.2.1 Current models of bidding strategy in literature

In general, there are cooperative and competitive models researched for developing bidding strategy of DERs to improve their revenues in pool-based DA energy market. [29-31]. Previously, DERs could not affect electricity prices as their proportions in the market were small and negligible [32]. As installed capacity of WPPs and gas facilities, and the number of EVs increased, these DERs could be aggregated to become large-scale market participants and make bidding strategies as price-takers [33, 34]. [35] shows DERs as price-takers achieve profits depending on load and price forecasting. Furthermore, market participants acting alone or colluding with their counter-parts, may own enough share of the supply or the demand to exercise market power for increasing their profits. The market power, which is known as a seller or a group of sellers, is able to exert a significant influence (monopoly) on electricity prices and output of electricity, which prevents competitors in electricity market. Bidding strategies for large-scaled energy suppliers as price-makers in an oligopoly market are initially researched for traditional thermal generators [36, 37], which are then extended to the hydro-generator combined with the pumped storage plant in [38]. Models of these traditional electricity suppliers are usually considered as controllable and deterministic. Bidding strategies of renewable WPPs as price-makers improving their own interests with consideration of uncertainty of wind energy resources have been researched in recent years [39, 40]. Moreover, numerous cooperative models have been proposed to develop bidding strategies based on collaborators' compensation for peak shaving in a centralized marketplace.

For the same-commodity cooperative arbitrage, the bidding strategy with managing wind fluctuations originally refers to WPPs combing with hydro units in [41], with bulk energy storage devices in [42] and with compressed air storage devices in [43]. As the development of DR resources in recent years, aggregated DR resources were suggested to balance the volatility of wind energy production. The influence of

DR resources on wind generation is researched in [40] and [44]. DR loads traded in a separate intra-day market to increase revenues of WPPs are studied in [45]. [46] researches profits of DR sides from the perspective of WPPs, and [47] proposes the bidding strategy model of the DR aggregator as a price-maker. In the future smart grid, increasing numbers of EVs with flexible charging and discharging characteristics can be aggregated as DR programs to deal with the uncertainty of WPPs [48, 49]. Thus, it is expected to develop the bidding strategy of cooperative WPPs and EVs.

For the cross-commodity cooperative arbitrage, recent research on the synergies of electricity and other energy in the multi-energy system has attracted a lot of attention [50-52]. A bi-level economic dispatch model for integrated natural gas and electricity systems considering wind power and the power-to-gas process is proposed in [53]. The optimal operation strategy of coupled electricity, heating and natural gas networks is proposed in [54]. Considering the marketing perspective of the multi-energy system, [55] investigates the strategic behavior of a multi-energy player aggregating demand-side resources and participating in the wholesale electricity market. [56] focuses on developing the coordinated operation strategy of electricity and natural gas networks considering DR based virtual power plant (VPP). The optimal operation strategy of an integrated NGG-P2G unit in the coupled electricity and gas market is developed in [57]. To consider DERs operating cooperatively to eliminate fluctuations of renewable resources in the multi-energy electricity market, a complex bidding strategy for an energy hub with multi-energy inputs and outputs is modeled in [58] where the optimized operation of energy hub is used to handle the uncertainty of renewable generation. A growing number of natural gas facilities are promising to manage the wind energy fluctuation in a virtual multi-energy plant (VMP). This leads to the emphasis on the bidding strategy developed for the natural gas unit coordinating with the WPP in multi-energy system.

As to the competitive market model, there are three common approaches to develop the bidding strategy. The first one is forecasting electricity prices in the next trading period, which is suitable for DERs as price-taker in the perfectly competitive electricity

market. The second one relies on estimating bidding behaviors of the rival participants. In [11], bidding behaviors of multi-agent large-scale renewable resources in oligopoly electricity markets were formulated as mathematical programming with equilibrium constraints (MPEC) with consideration of the uncertainty of market competitors. However, the equilibrium solution is often not easy to obtain or does not exist based on a set of equations in the equilibrium model, especially in large systems. The complexity of these models increases when it is applied to a real market with consideration of related assumptions and constraints [59]. Moreover, the penetration of renewable resources in the grid results that any slight changes in the power production of them would disturb the market equilibrium. In this way, it is necessary to solve this complex set of equations again for finding the equilibrium of the market under the new situation [60]. The last one is game theory-based bidding strategy. Compared to the equilibrium model of forecasting behaviors of the rivals, agent-based model (ABM) is more flexible and has been widely adopted to develop game theory-based bidding strategy [61]. All market players could be modeled as the artificial autonomous agents, who learn through repetitive interactions with a simulated market environment. It is more similar to a real electricity market. Existing researches on large-scaled players bidding in the competitive environment refer to the WPP and DR in [62], GENCOs and large consumers in [18], a DR virtual power plant in [63], and plug-in EV owners in [64]. As a description of large numbers of wind energy resources and EVs before, it is expected to explore a competitive bidding strategy for WPP and EV aggregator in an agent-based market.

1.2.2 Gap of models and potentials in developing bidding strategy

Consider the influence of large-scaled DERs on the electricity market and uncertainties of DERs, this thesis focuses on developing bidding strategies for the cooperative EV and the WPP, the natural gas unit combining with the WPP in multi-energy VPP, and the EV aggregator competing with the WPP in the agent-based electricity market.

(1) The flexibility of EVs has been researched to be combined with WPPs, [65] proposes the operation strategy of EVs to balance the volatility of wind output; whereas, this work considers specific EVs. In this way, it is difficult to manage the increasing numbers of EVs in the future electricity market due to the complexity of collecting all information from every EV and performing time-consuming calculations. Thus, it is more reasonable to have an intermediary EV aggregator, which dispatches aggregated EVs and exchanges information between the ISO and individual EV owners. Considering cooperative EV aggregators and WPPs, [66] increased profits by using unidirectional G2V services (night residential EV charging) to manage energy deviations while [67] investigated the coordination of unidirectional V2G units, traditional generating units and wind generating units to influence market prices and energy outcome. However, little research has been done for the EV aggregator with both G2V and V2G services cooperating with WPPs as a price-maker in the electricity market to increase their overall profits.

Therefore, it is the first incentive of this thesis to cooperate WPPs with EV aggregators to form an HPP, in which flexible EV charging/discharging characteristics enable EV aggregators to manage fluctuations of renewable wind energy resources. The HPP is promising to strategically bid to fix electricity prices and increase their overall profits. Therefore, a risk-constrained offering strategy for the aggregated HPP consisting of WPP and EV aggregator as a price-maker in an oligopoly electricity market, with consideration of the uncertainties of the energy production and RT prices, is proposed here.

(2) Recently, natural gas facilities have been researched in electricity market. An optimal bidding strategy for WPPs and G2P devices is developed in [43], where G2P is used to compensate wind energy fluctuations. [68] focuses on the coordinated operation among small owners of DERs in coupled transactive power and gas systems, in which the unexpected power fluctuations of renewable sources and demands are mitigated. However, market participants in these kinds of literature are usually in a small-scale and are treated as price-takers in electricity markets. So far, to the best of

knowledge, there is no research considering the NGG-P2G unit coordinating with the WPP as a price-maker to increase their overall profits by strategically bidding.

The proliferation of natural gas generating units (NGGs) and the emerging power-to-gas conversion (P2G) technology which converts electric energy into natural gas to storage or use in recent years, have enabled the bidirectional energy flows between electric power and natural gas systems [69]. In the electricity market, WPP and NGG-P2G are expected to bring more profits as flexible NGG-P2Gs could accommodate WPP uncertainties and provide large capacities for ancillary services. Therefore, it is the second incentive of this thesis to develop bidding strategy of coordinated WPP and NGG-P2G unit with considering uncertainties of wind output capacities and RT prices, where the coordinated supplier is considered as a price-maker in DA market and a price-taker in RT market as well as providing ancillary services employed in real-time through the NGG-P2G unit to enhance their common interests.

In the above cooperative model, the centralized control and scheduling of a central aggregator who owns lots of bidding information of participants are highly dependent [30, 70, 71]. Thus, the privacy of players cannot be guaranteed and they have little flexibility to cope with any self-decisions [72]. In the future electricity market with great respect for personal privacy and autonomy of energy suppliers, a bidding strategy accustomed to a more flexible market environment without any central agent or aggregator would be more attractive [73]. Since energy suppliers would not share any personal data with each other for the sake of privacy, they would have the freedom to make their own bidding decisions to increase their respective profits in a competitive market.

(3) In the agent-based competitive market, model-based adaption algorithms with naive or intuitive learning formulations and genetic algorithms inspired by the biological evolution have been applied to find the optimal bidding curves in [74] and [75]. However, these algorithms are designed to obtain the bidding strategy of a single agent, in which each agent makes the decision without regard to other rivals. Thus, they are inappropriate for the competitive oligopoly market with each agent achieving its

independent goal by adapting its behavior in the presence of other agents. As a class of reinforcement learning methods, various *Q*-learning algorithms have been widely used in the multi-agent electricity market to explore bidding strategies [76]. A decentralized multi-agent model of EV owners bidding in electricity market was developed based on a *Q*-learning algorithm without modeling the environment [77]. A deep reinforcement learning-based methodology was proposed to address bidding problems for energy suppliers, which has significant advantages in contrast with the traditional *Q*-learning algorithm [78]. However, there is no game process between these strategic participants. In [79] and [80], the game problem was considered to update multi-agent bidding strategies for energy suppliers respectively in a large power system and regionally integrated energy system, in which historical bidding decisions of rivals are essential. Although this model has some advantages compared to that with perfect information of other rivals' cost functions and market clearing mechanism, it is still not practical as the real electricity market is more likely a market with incomplete information, i.e. each player knows about only its own cost function and bidding strategy without any knowledge of other competitors [81]. A combined multi-agent model-based and learning-based approach for generators' bidding decision problems with incomplete information was presented in [82], but the Nash equilibrium point is required which is time-consuming and hard to scale up. This is due to the complexity of the equilibrium calculation and storage pressure of state-action space. Further research shall therefore focus on exploring an optimal multi-agent approach without knowing the equilibrium point, suitable for the bidding strategy in a competitive market, which protects personal privacy with no bidding information communicated between agents and guarantees players could have right to make their own bids. So far, to the best of knowledge, there is little research considering the renewable WPPs and EV aggregators as oligopolists for developing a competitive multi-agent bidding strategy in a pool-based DA market without any information of opponents and calculating any equilibrium point, which stimulates the third incentive.

To satisfy the requirement of the bidding strategy described above, a recently

developed multi-agent decentralized *Win or Learn Fast Policy Hill Climbing* (*WoLF-PHC*) [83] learning method, based on an easy average policy instead of the equilibrium policy, is chosen to solve the bidding problem. It could not only meet the requirements of respecting individual privacy and the autonomy of WPPs and EV aggregators but also accommodate their complex bidding behaviors to maximize their respective revenues.

1.3 Primary Contributions

Firstly, based on the state-of-art bidding strategy of same-commodity cooperative arbitrage, potentials of cooperative WPPs and EVs are studied. A bi-level stochastic model of the offering strategy for the aggregated HPP consisting of the WPP an EV aggregator in the pool-based market is proposed. The model aims to maximize the HPP's revenues and manage expected revenues' risks with uncertainties of renewable energy productions and real market prices. In the proposed model, the aggregated EVs and elastic loads, as the price-maker and the price-taker in the market respectively, are implemented as flexible DR sources. Case studies are implemented to illustrate the large-scale renewable resources WPPs and EV aggregators could be aggregated for strategical bidding and setting electricity prices according to their and the grid's interests, in which EV aggregators cooperating with WPPs for satisfying high energy offered in V2G mode and using wind energy to meet EVs' charging requirement in G2V mode at moments of low energy offered.

Secondly, according to the cross-commodity cooperative arbitrage, the bidding strategy of synergies of electricity and natural gas in the multi-energy system is researched. A stochastic bi-level model is proposed to derive the optimal bidding strategy for the coordinated WPPs and NGG-P2G suppliers that maximizes VMP payoffs. The deviation of scheduled WPP output from its actual value in DA market is compensated by the coordinated suppliers participating as price-takers in RT market. The optimal bidding strategy of the coordinated WPPs and NGG-P2G suppliers is

considered in an integrated electricity and gas networks by strategically exploring multiple energy synergies in the electricity market and providing auxiliary services through NGG-P2G units, which consume excess wind energy to supply natural gas loads or storage natural gas in nature gas pipelines at hours of low offered power, and utilizes the energy of natural gas network to support electricity at hours of high offered power.

Lastly, research focuses on the competitive bidding strategy in the agent-based electricity market. A stochastic bi-level model, as compared to strategic participant WPPs in [6] and cooperate players including strategic WPPs and EV aggregators as previous mentions, for exploring a competitive bidding strategy for WPPs and EV aggregators in a pool-based oligopoly DA market based on a multi-agent game system, considering the uncertainty of power productions of WPPs and EV aggregators as well as bid prices for other participants. Compared with the centralized dispatch in [6, 84], WPPs and EV aggregators are neither controlled by an aggregator or central agent nor share any personal information with other rivals and make self-determined biddings to increase their respective profits in a competitive market. Comprehensively analyzed the proposed bidding problem of the market model as a multi-agent stochastic game with incomplete information, and applied a multi-agent decentralized *WoLF-PHC* to counterbalance their lack of information in this stochastic market environment for WPPs and EV aggregators and make their own bidding decisions by self-game. Compared with the existing methods in [79, 80] and [82], no rivals' information and time-consuming equilibrium calculation are needed. Simulation results demonstrate the *WoLF-PHC* method could be successfully applied to solve the multi-supplier bidding strategies problem in large systems.

1.4 Thesis Layout

The rest of this thesis consists of five Chapters. Chapter II introduces essentials on developing bidding strategy of DERs. Chapter III shows the development of a risk-

constrained offering strategy for a hybrid power plant consisting of the WPP and EV aggregator in DA energy market. Chapter IV proposes a bidding strategy for the cooperative WPP and NGG-P2G unit in multiple energy systems being a price-maker in DA market and price-taker in RT and regulation markets to enhance their common interests. Chapter V presents a multi-agent competitive bidding strategy in a pool-based electricity market with price-maker participants of WPPs and EV aggregators. Finally, the conclusions of the thesis are drawn in Chapter VI with suggestions on future work.

1.5 List of Publications

Journal paper

1. X. Gao, K. W. Chan, S. W. Xia, B. Zhou, X. Lu, D. Xu, "Risk-constrained offering strategy for a hybrid power plant consisting of wind power producer and electric vehicle aggregator," *Energy*, vol. 177, pp. 183-191, 15 Jun 2019. DOI: 10.1016/ j.energy.2019.04.048
2. X. Gao, K. W. Chan, S. W. Xia, X. S. Zhang, K. Zhang, J. H. Zhou, "A Multi-agent Competitive Bidding Strategy in a Pool-Based Electricity Market with Price-Maker Participants of WPPs and EV Aggregators," *IEEE Transactions on Industrial Informatics*, Early Access. DOI 10.1109/TII.2021.3055817
3. X. Gao, K. W. Chan, S. W. Xia, X. Zhang, G. B. Wang, "Bidding Strategy for the Coordinated Operation of Wind Power Plants and NGG-P2G Units in Electricity Market," *CSEE Journal of Power and Energy Systems*, JPES-2020-0610, Oct 2020. Under Review.
4. B. Zhou, K. Zhang, K. W. Chan, C. Li, X. Lu, S. Q. Bu, X. Gao, "Optimal Coordination of Electric Vehicles for Virtual Power Plants with Dynamic Communication Spectrum Allocation," *IEEE Transactions on Industrial Informatics*, vol. 17, no. 1, pp. 450-462, Jan. 2021. DOI: 10.1109/TII.2020.2986883

Conference paper

5. X. Gao, X. Lu, K.W. Chan, J. Hu, S. Xia, D. Xu. "Distributed Coordinated Management for Multiple Distributed Energy Resources Optimal Operation with Security Constrains", in *2019 IEEE Power & Energy Society Innovative Smart Grid Technologies Conference (ISGT)*, Feb 2019. DOI: 10.1109/ISGT.2019.8791673
6. S. W. Xia, S. Q. Bu, X. Gao, X. Lu and X. Zhang, "A hybrid fully distributed generation dispatch approach for distribution network integrating with multiple DGs", in *the 11th International Conference on Advances in Power System Control, Operation & Management (APSCOM)*, 2018.

Chapter II

Essentials on Developing Bidding Strategy of DERs

2.1 Approaches for solving optimization problems involving uncertainties of DERs

Optimization has been the most widely used approach to solve problems in power system, which usually explores the best solution for maximizing or minimizing an objective function [85]. As the bidding strategy of the electricity market highly depends on optimization, it is essential to explore efficient approaches to solve optimization problems of aggregated DERs with consideration of uncertainties and distinguished features of DERs.

For solving the optimization problem with uncertainties, stochastic optimization and robust optimization are two commonly used methods. The robust optimization takes the worst-case of uncertainties into account and there is no high demand for information on uncertainties. However, this approach is often over-conservative to handle the optimized operation in electricity market [86, 87]. The other one is stochastic optimization, which is the most widely used. One type of stochastic optimization is transforming the optimization problem with uncertainties into deterministic forms by assuming the uncertainty obeys a certain distribution. For example, [11] assumes the uncertain wind speed follows Weibull distribution, [46] assumes uncertain electricity price follows log-normal distribution, [88] assumes uncertain EV numbers follow the normal distribution. However, this type of stochastic optimization is often over-optimistic and has limited application [89]. Another type of stochastic optimization relies on selected scenarios and corresponding discrete probability distributions for realizations of uncertainties. In this way, the optimized objective function is represented by selected scenarios and relevant weights, and all constraints should satisfy for all scenarios.

There are several scenario generation strategies in literature [90-92], in which the Monte Carlo simulation is widely used. Different scenarios are defined according to the probability density function (PDF) of a random variable, whereas each scenario has an associated probability of occurrence. Generally, uncertain variables or forecast errors of uncertain variables are considered as a certain distribution. In the latter case, the forecasted values are derived from historical data. Thus, the value of uncertain variables for each scenario is determined by adding the error of each uncertain variable determined by the PDF to their forecasted value. Once the PDF of random variable is confirmed, the PDF of each random variable can be first discretized into seven different intervals using the Monte Carlo simulation. The intervals are centered on the zero mean, with a probability and a width equal to the standard deviation. The probability associated with each PDF interval is then normalized so that their summation is equal to one. A scenario which includes a matrix of binary parameters consisting of coefficient interval of each market participant is generated. Next, scenarios of each uncertain variable and a random number in the range (0,1) for each scenario are generated with the roulette wheel mechanism. The associated binary parameter is set to 1 when the generated random number is within the interval l. Otherwise, the binary parameters of other intervals equal to 0. Lastly, the probability of each generated scenario is calculated. With the consideration of correlations, the stochastic models can be unified and denoted by the uncertain variables $\boldsymbol{X}$ with the correlations $\boldsymbol{Rx}$, and the Monte Carlo sampling method incorporated with the Cholesky decomposition strategy is introduced to generate representative scenarios for correlated uncertain variables via the following steps; 1) For the given probabilistic distributions of uncertain variables $\boldsymbol{X}$ with the correlations $\boldsymbol{Rx}$, build a correlation coefficient matrix $\boldsymbol{Ry}$ using $\boldsymbol{Ry}=G(\boldsymbol{Rx})*\boldsymbol{Rx}$, where $G(\boldsymbol{Rx})$ is the correlation coefficient shift function associated with the specific type of probability distributions, which could be obtained by using Tables 4-8 in [93]; 2) Apply the Cholesky decomposition to $\boldsymbol{Ry}$ to obtain an orthogonal matrix $\boldsymbol{B}$, namely $\boldsymbol{Ry} = \boldsymbol{B}*\boldsymbol{B}^{\boldsymbol{T}}$ where $\boldsymbol{T}$ denotes the transpose of a matrix; 3) Generate a sample matrix $\boldsymbol{Z}$ of independent standard normal variables, for example using the statistical analysis

function normrnd () in MATLAB, and afterward obtain the correlated standard normal matrix $\boldsymbol{Y=B\text{-}1*Z}$; 4) Apply the transformation $\boldsymbol{S}=H\text{-}1(\varphi(\boldsymbol{Y}))$ to generate the final scenarios $\boldsymbol{S}$ for the original uncertain variables $\boldsymbol{X}$, where φ is the cumulative distribution function (CDF) of the standard normal distribution, and H is the CDF of the input variables $\boldsymbol{X}$.

The computation burden increases with the number of scenarios, which may result in the optimization problems becoming intractable. Thus, there are some techniques to decrease the number of scenarios for achieving the balance between accuracy and computational efficiency [94]. Scenario reduction methods often rely on probability distances which measure distances between probabilities distributions. Different probability distances such as Kantorovich distance in [95] and Fortet-Mourier metrics in [96] are used in different reduction technologies. Furthermore, no one reduction method is universally suitable and different techniques can be suitable for different problems, which results that it is essential to choose a proper one according to the specific condition. In Chapter IV and V, the forward selection method [95] is used to reduce the number of scenarios considered, while minimizing the inevitable dilution of stochastic information contained in the original set. By minimizing the Kantorovich distance between the initial scenario set and the reduced scenario set, the forward selection algorithm recursively adds scenarios from the initial set to the reduced set until the total number of constituent members of the reduced set reaches the required number.

2.2 Solutions for solving bi-level optimization problems

The model of the bi-level optimization problem in Chapters III and IV of this thesis can be expressed mathematically as:

Minimize

$$\left\{x^{U}\right\}\cup\left\{x_1^{L},\ldots,x_i^{L},\ldots,x_n^{L}\right\}\cup\left\{\lambda_1^{L},\ldots,\lambda_i^{L},\ldots,\lambda_n^{L},\mu_1^{L},\ldots,\mu_i^{L},\ldots,\mu_n^{L}\right\}$$

$$f^U\left(x^U, x_1^L, \ldots, x_i^L, \ldots, x_n^L, \lambda_1^L, \ldots, \lambda_i^L, \ldots, \lambda_n^L, \mu_1^L, \ldots, \mu_i^L, \ldots, \mu_n^L\right) \tag{2.1a}$$

Subject to

$$h^U\left(x^U, x_1^L, \ldots, x_i^L, \ldots, x_n^L, \lambda_1^L, \ldots, \lambda_i^L, \ldots, \lambda_n^L, \mu_1^L, \ldots, \mu_i^L, \ldots, \mu_n^L\right) = 0 \tag{2.1b}$$

$$g^U\left(x^U, x_1^L, \ldots, x_i^L, \ldots, x_n^L, \lambda_1^L, \ldots, \lambda_i^L, \ldots, \lambda_n^L, \mu_1^L, \ldots, \mu_i^L, \ldots, \mu_n^L\right) \leq 0 \tag{2.1c}$$

$$\begin{cases} \underset{x_i^L}{\textit{Minimize}} \\ \qquad {c_1^L}^T\left(x^U\right)x_1^L \\ \textit{subject to} \\ \qquad A_1^L\left(x^U\right)x_1^L = b_1^L\left(x^U\right) : \lambda_1^L \\ \qquad D_1^L\left(x^U\right)x_1^L = e_1^L\left(x^U\right) : \mu_1^L \end{cases} \tag{2.2a}$$

$$\begin{cases} \underset{x_i^L}{\textit{Minimize}} \\ \qquad {c_i^L}^T\left(x^U\right)x_i^L \\ \textit{subject to} \\ \qquad A_i^L\left(x^U\right)x_i^L = b_i^L\left(x^U\right) : \lambda_i^L \\ \qquad D_i^L\left(x^U\right)x_i^L = e_i^L\left(x^U\right) : \mu_i^L \end{cases} \tag{2.2b}$$

$$\begin{cases} \underset{x_n^L}{\textit{Minimize}} \\ \qquad {c_n^L}^T\left(x^U\right)x_n^L \\ \textit{subject to} \\ \qquad A_n^L\left(x^U\right)x_n^L = b_n^L\left(x^U\right) : \lambda_n^L \\ \qquad D_n^L\left(x^U\right)x_n^L = e_n^L\left(x^U\right) : \mu_n^L \end{cases} \tag{2.2c}$$

Bi-level model (2.1a)-(2.2c) include an upper-level problem (2.1) and a collection of lower-level problems (2.2). These lower-level problems constrain the upper-level one. In these formulations, symbols with superscript *U* and *L* represent the upper-level and lower-level problems respectively. In this thesis, the lower-level problem (2.2b) is convex as it is continuous and linear. λ_i^L and λ_i^U are dual variables, which are related to each equality and inequality constraint separately. x^U of the upper level is assumed as a constant value in the lower level, while the primal variables x_i^L and dual variables (λ_i^L, λ_i^U) of the lower level associated with the upper-level variable x^U are considered as optimization variables of the upper-level problem (2.1).

2.2.1 MPEC problem

The upper and lower layers of the bi-level model need to be solved together. To do this, the lower level of the optimization problem representing the DA market clearing can be replaced by their optimality constraints. There are two optimality conditions for the lower-level convex problem. The first one is its Karush-Kuhn-Tucker (KKT) optimality conditions. The other one is its primal constraints, its dual constraints, and its strong duality equality. These optimal conditions of the lower-level problem are then as constraints added to the upper-level problem for solving the upper-level objective function. The bi-level optimization problem is then transformed to a single mathematical program with equilibrium constraints (MPEC).

(1) KKT condition

The MPEC can be formulated as below, in which the lower-level problems (2.2) are replaced by its KKT conditions (2.3g)-(2.3i). Constraint (2.3i) is the complementary constraint, which can be replaced by a set of constraints (2.4a)-(2.4c).

Minimize

$$\left\{x^U\right\}\cup\left\{x_1^L,\ldots,x_i^L,\ldots,x_n^L\right\}\cup\left\{\lambda_1^L,\ldots,\lambda_i^L,\ldots,\lambda_n^L,\mu_1^L,\ldots,\mu_i^L,\ldots,\mu_n^L\right\}$$

$$f^U\left(x^U,x_1^L,\ldots,x_i^L,\ldots,x_n^L,\lambda_1^L,\ldots,\lambda_i^L,\ldots,\lambda_n^L,\mu_1^L,\ldots,\mu_i^L,\ldots,\mu_n^L\right) \tag{2.3a}$$

Subject to

$$h^U\left(x^U, x_1^L, \ldots, x_i^L, \ldots, x_n^L, \lambda_1^L, \ldots, \lambda_i^L, \ldots, \lambda_n^L, \mu_1^L, \ldots, \mu_i^L, \ldots, \mu_n^L\right) = 0 \tag{2.3b}$$

$$g^U\left(x^U, x_1^L, \ldots, x_i^L, \ldots, x_n^L, \lambda_1^L, \ldots, \lambda_i^L, \ldots, \lambda_n^L, \mu_1^L, \ldots, \mu_i^L, \ldots, \mu_n^L\right) \le 0 \tag{2.3c}$$

$$c_1^L\left(x^U\right) - A_1^{L^T}\left(x^U\right)\lambda_1^L + D_1^{L^T}\left(x^U\right)\mu_1^L = 0 \tag{2.3d}$$

$$A_1^L\left(x^U\right)x_1^L = b_1^L\left(x^U\right) \tag{2.3e}$$

$$0 \le \left[e_1^L\left(x^U\right) - D_1^L\left(x^U\right)x_1^L\right] \perp \mu_1^L \ge 0 \tag{2.3f}$$

$$c_i^L\left(x^U\right) - A_i^{L^T}\left(x^U\right)\lambda_i^L + D_i^{L^T}\left(x^U\right)\mu_i^L = 0 \tag{2.3g}$$

$$A_i^L\left(x^U\right)x_i^L = b_i^L\left(x^U\right) \tag{2.3h}$$

$$0 \le \left[e_i^L\left(x^U\right) - D_i^L\left(x^U\right)x_i^L\right] \perp \mu_i^L \ge 0 \tag{2.3i}$$

$$c_n^L\left(x^U\right) - A_n^{L^T}\left(x^U\right)\lambda_n^L + D_n^{L^T}\left(x^U\right)\mu_n^L = 0 \tag{2.3j}$$

$$A_n^L\left(x^U\right)x_n^L = b_n^L\left(x^U\right) \tag{2.3k}$$

$$0 \le \left[e_n^L\left(x^U\right) - D_n^L\left(x^U\right)x_n^L\right] \perp \mu_n^L \ge 0 \tag{2.3l}$$

$$diag\left[e_i^L\left(x^U\right) - D_i^L\left(x^U\right)x_i^L\right] \perp \mu_i^L \ge 0 \qquad \forall i \tag{2.4a}$$

$$e_i^L\left(x^U\right) - D_i^L\left(x^U\right)x_i^L \ge 0 \qquad \forall i \tag{2.4b}$$

$$\mu_i^L \ge 0 \qquad \forall i \tag{2.4c}$$

After the above transformation with the KKT condition, it is obvious that the constraint (2.4a) is non-linear, which is difficult to solve.

(2) Primal-dual formulation

The dual formulation of the lower level (1.2) can be written as (2.5). According to

the strong duality, the objective function of its primal and dual formulation has the same value for solving the optimization problem and can be expressed as (2.6).

$$\begin{cases} \underset{\left\{\lambda_i^L\right\}\cup\left\{\mu_i^L\right\}}{Maximize} \\ \qquad b_i^{L^T}\left(x^U\right)\lambda_i^L - e_i^{L^T}\left(x^U\right)\mu_i^L \\ subject\ \ to \\ \qquad A_i^L\left(x^U\right)\lambda_i^L - D_i^{L^T}\left(x^U\right)\mu_i^L = c_i^L\left(x^U\right) \\ \qquad \mu_i^L \geq 0 \end{cases} \tag{2.5}$$

$$c_i^{L^T}\left(x^U\right)x_i^L = b_i^{L^T}\left(x^U\right)\lambda_i^L - e_i^{L^T}\left(x^U\right)\mu_i^L \qquad \forall i \tag{2.6}$$

After the transformation with the primal-dual formulation, a MPEC problem with replacing the original bi-level optimization problem can be written as (2.7a)-(2.7o). Equation (2.7h) is the primary constraint, (2.7i)-(2.8j) are dual constraints, and (2.7k) is the strong duality equation of the lower level.

Minimize

$$\left\{x^U\right\}\cup\left\{x_1^L,\ldots,x_i^L,\ldots,x_n^L\right\}\cup\left\{\lambda_1^L,\ldots,\lambda_i^L,\ldots,\lambda_n^L,\mu_1^L,\ldots,\mu_i^L,\ldots,\mu_n^L\right\}$$

$$f^U\left(x^U,x_1^L,\ldots,x_i^L,\ldots,x_n^L,\lambda_1^L,\ldots,\lambda_i^L,\ldots,\lambda_n^L,\mu_1^L,\ldots,\mu_i^L,\ldots,\mu_n^L\right) \tag{2.7a}$$

Subject to

$$h^U\left(x^U,x_1^L,\ldots,x_i^L,\ldots,x_n^L,\lambda_1^L,\ldots,\lambda_i^L,\ldots,\lambda_n^L,\mu_1^L,\ldots,\mu_i^L,\ldots,\mu_n^L\right) = 0 \tag{2.7b}$$

$$g^U\left(x^U,x_1^L,\ldots,x_i^L,\ldots,x_n^L,\lambda_1^L,\ldots,\lambda_i^L,\ldots,\lambda_n^L,\mu_1^L,\ldots,\mu_i^L,\ldots,\mu_n^L\right) \leq 0 \tag{2.7c}$$

$$A_1^L\left(x^U\right)x_1^L = b_1^L\left(x^U\right) \tag{2.7d}$$

$$A_1^{L^T}\left(x^U\right)\lambda_1^L - D_1^{L^T}\left(x^U\right)\mu_1^L = c_1^L\left(x^U\right) \tag{2.7e}$$

$$\mu_1^L \geq 0 \tag{2.7f}$$

$$c_1^L\left(x^U\right)x_1^L = b_1^{L^T}\left(x^U\right)\lambda_1^L - e_1^{L^T}\left(x^U\right)\mu_1^L \tag{2.7g}$$

$$A_i^L\left(x^U\right)x_i^L = b_i^L\left(x^U\right) \tag{2.7h}$$

$$A_i^{L^T}\left(x^U\right)\lambda_i^L - D_i^{L^T}\left(x^U\right)\mu_i^L = c_i^L\left(x^U\right) \tag{2.7i}$$

$$\mu_i^L \geq 0 \tag{2.7j}$$

$$c_i^L\left(x^U\right)x_i^L = b_i^{L^T}\left(x^U\right)\lambda_i^L - e_i^{L^T}\left(x^U\right)\mu_i^L \tag{2.7k}$$

$$A_n^L\left(x^U\right)x_n^L = b_n^L\left(x^U\right) \tag{2.7l}$$

$$A_n^{L^T}\left(x^U\right)\lambda_n^L - D_n^{L^T}\left(x^U\right)\mu_n^L = c_n^L\left(x^U\right) \tag{2.7m}$$

$$\mu_n^L \geq 0 \tag{2.7n}$$

$$c_n^L\left(x^U\right)x_n^L = b_n^{L^T}\left(x^U\right)\lambda_n^L - e_n^{L^T}\left(x^U\right)\mu_n^L \tag{2.7o}$$

The MPECs formula based on the KKT optimality condition is equivalent to the primal-dual method. The bi-level model developed in Chapters III and IV includes an upper layer problem where the objective function is non-linear and the objective function can use some equation-based linearization with the strong duality theorem. Because the target function can be linearized by using lower-level strong duality equation, which thus cannot be used to reconstruct lower-level problems using primal-dual methods. As a result, the KKT condition is used in this thesis.

2.2.2 MILP problem

The resulting MPEC in Section 2.2.1 is single-level but generally nonlinear, especially when it is taken from (2.4a) under KKT optimality conditions. These nonlinearities are then usually linearized with precise mixed-integer linear equivalencies such as strong duality theorem (SDT) and the Fortuny-Amat transformation, and MPEC can ultimately be expressed as a mixed-integer linear programming (MILP) problem. The non-linear part of complementarity constraint (2.4a) can be represented as $0 \leq \alpha \perp \beta \gg 0,$ which is equal to the formulation (2.8a) and (2.8b) as below. Both α and β or either α or β must be equal to 0. These nonlinear

expressions can be transferred by the mixed-integer linear expressions as equivalent (2.9a)-(2.9d), in which M is a large enough constant. If $\alpha = 0$, then $u = 0$. Thus, constraints (2.9a) and (2.9c) form that $0 \ll \alpha \ll 0$, i.e., $\alpha = 0$; while constraints (2.9b) and (2.9c) establish $0 \ll \beta \ll M$. Otherwise, if $\beta = 0$, then $u = 1$. Thus, constraints (2.9b) and (2.9c) establish that $0 \ll \beta \ll 0$, i.e., $\beta = 0$; while constraints (2.9a) and (2.9c) establish $0 \ll \alpha \ll M$.

$$\alpha \cdot \beta = 0 \tag{2.8a}$$

$$\alpha, \beta \geq 0 \tag{2.8b}$$

$$\alpha \leq M \cdot u \tag{2.9a}$$

$$\beta \leq M \cdot (1-u) \tag{2.9b}$$

$$\alpha, \beta \geq 0 \tag{2.9c}$$

$$u \in \{0,1\} \tag{2.9d}$$

Finally, the stochastic complementarity model of DERs bidding is reconstructed into a MILP problem, which is effectively solved with branch-and-cut method.

2.2.3 Computational tool

After the transformation above, the transformed MILP model throughout this dissertation is solved by commercial software such as MOSEK through YALMIP interface in MATLAB and run on an Intel Core i5 CPU at 1.6 GHz with 8 GB RAM iMac computer. It is worth noting that the solvers work well only if the problem is convex. Simulation times are influenced by the number of nodes in the system and the number of scenarios. Besides, large numbers of binary variables are needed to linearize complementary constraints in the MEPC model, which may result in dramatically increasing the running time of the simulation.

2.3 Risk Modeling

As described in Section 2.1, the bidding problem of uncertain DERs is modeled as

stochastic optimization. However, this approach ignores the variability of profit distribution. In such a condition, it is important to introduce a risk metric to measure the profit variability, providing guiding information to bidding decision-makers.

In the existing literature, there are three widely used risk metrics are introduced: mean-variance in [97, 98], value at risk (*VaR*) in [99], and conditional value at risk (*CVaR*) in [100, 101]. The mean-variance risk function derives from the variance as a measure of dispersion and can be categorized into risk-averse and risk-seeking according to different design parameters. Whereas in the case of asymmetrical distribution, mean-variance risk measure cannot meet the second order stochastic advantage and monotonicity axiom [102]. Thus, the mean-variance risk approach is not a coherent measure of risk. The *VaR* focuses on the tail risk and is expressed as the extreme fractile of the loss distributions to limit projected losses at a given level of confidence α. However, *VaR* is also not a coherent risk measure as it lacks sub-additively when the underlying loss distribution is not normal [103]. Besides, the *VaR* cannot offer any information on possible losses in the $(1-\alpha)$ worst cases, thus it is hard to calculate the *VaR* optimization problem. The *CVaR* is a generalization of *VaR* and *CVaR* at a given confidence level α is computed as the expected profit of the $(1-\alpha) \times 100\%$ scenarios yielding the lowest profits [100]. The *CVaR* can overcome the drawbacks of *VaR* and thus is coherent and theoretically preferable. In addition, downside risk constraints (DRC) and second-order stochastic dominance constraints (SOSDCs) are newly introduced as the risk-evaluation method to control the stochastic resources in [104-106].

The risk metric can be categorized into risk-neutral and risk-averse. In Chapter III, the proposed bidding problem is modeled as risk-averse. In general, a risk-neutral energy decision-maker has more opportunities to dynamically adapt the bidding strategy to the information observed, and thus to increase the expected profit, than for a risk-averse decision-maker. This is because the risk-averse bidding strategy is generally more conservative [107]. Thus in chapters IV and V, bidding problems are considered risk-neutral.

Chapter III

Risk-Constrained Offering Strategy for a Hybrid Power Plant Consisting of Wind Power Producer and Electric Vehicle Aggregator

3.1 Introduction

Renewable wind energy resources involve a lot of uncertainties, which would cause fluctuations and lead to economic losses for renewable WPPs. Large-scaled EVs will be increasingly important to the power system, and the flexible charging and discharging characteristic of EVs motivates EV aggregators to cooperate with WPPs to form a hybrid power plant (HPP) [108]. So far little research has been done for the EV aggregator with both G2V and V2G services cooperating with WPPs as a price-maker in the electricity market to increase their overall profits. Therefore, a risk-constrained offering strategy for the aggregated HPP with consideration of WPP and EV aggregator in an oligopoly electricity market to be price-makers is proposed here.

This Chapter proposes a bi-level stochastic optimization model of offering strategy for an aggregated WPP-EV HPP as a price-maker in the day-ahead (DA) market while considering the uncertainties of the energy production and spot price in the real-time (RT) market. While the HPP's profits are maximized in the upper level of the proposed model with the use of conditional-value-at-risk (*CVaR)* to manage the risk of expected revenues, the social welfare from the perspective of the grid is maximized in the lower level. The formulated bi-level model is first transformed into a single-level mathematical program with equilibrium constraints (MPEC) and then further transformed into a mixed-integer linear programming (MILP) problem for solution.

Simulation results have demonstrated the effectiveness of the proposed HPP model with strategically bidding prices to increase profits and reduce the volatility of profits by considering the risk-metric.

The nomenclature of symbols used in this Chapter is given as follows.

Indices:

l	Loads
g	Traditional generation units
e	EV aggregator units
ω	WPP units
h	HPP units
n	Nodes
α	Real-time market scenarios
β	Scenarios of WPPs'/ EV aggregators' energy productions

Sets:

Ω_n^L	Loads at node *n*
Ω_n^G	Traditional generation units at node *n*
Ω_n^E	EV aggregator units at node *n*
Ω_n^ω	WPP units at node *n*
Ω_n^H	HPP units at node *n*
Ω_n^N	All nodes connected to the node *n*
T	Number of time periods
N_α	Number of scenarios for RT market price
N_β	Number of scenarios for WPPs'/ EV aggregators' energy productions

Parameters:

τ_α	Weight of RT market prices
τ_β	Weight of WPPs'/ EV aggregators' energy productions

φ_{α}^{BAL}	RT market price based on scenario α
$P_{e,t,\beta}^{EV,max}$	EV capacity for the *e*th EV aggregator at time *t* based on scenario β, in MW
$P_{\omega,\beta}^{Wind,max}$	Wind capacity for the ωth WPP based on scenario β, in MW
$P_{e}^{EV,BAL,max}$	Maximum energy bought or sold for the *e*th EV aggregator in the RT market, in MW
$P_{\omega}^{Wind,BAL,max}$	Maximum energy bought or sold for the ωth WPP in the RT market, in MW
SOC^{min}	Minimize state of charge for EVs, in %
SOC^{max}	Maximum state of charge for EVs, in %
E_{ev}^{max}	Maximum total charging energy of the aggregator *e* at time *t*, in MWh
γ_{charge}	Charging efficiency, in %
$\gamma_{discharge}$	Discharging efficiency, in %
γ^{max}	Maximum charging/discharging rate at time *t*, in %
λ_{g}^{DA}	Offer price for the *g*th traditional generation unit located at node *n* in the DA market
λ_{l}^{DA}	Bid price for the *l*th load unit located at node *n* in the DA market
$\lambda_{ch/disch}$	Charging/discharging price between EV aggregators and EV owners at time *t*
B_{ab}	Susceptance of the transmission line between nodes *a* and *b*
f_{ab}^{max}	Maximum capacity of the transmission line between nodes *a* and *b*
P_{g}^{max}	Maximum energy production for the *g*th traditional generation unit
P_{l}^{max}	Maximum consuming for the *l*th load unit
D_{factor}	Demand factor
$T_{battery}$	Battery lifetime
$C_{battery}$	Capital cost for battery
ξ	Parameter to weigh the expected revenue and *CVaR*

α_{CVaR}	Confidence level

Variables:

$\varphi_{n,t}$	Clearing LMP price at node *n* and time *t*
$P_{e,t}^{EV,DA}$	*e*th EV aggregator' energy production for the DA market at time *t*, in MW
$P_{\omega,t}^{Wind,DA}$	*ω*th WPP' energy production for the DA market at time *t*, in MW
$P_{h,t}^{HPP,DA}$	*h*th HPP' energy production for the DA market at time *t*, in MW
$P_{e,t,\beta}^{EV,BAL}$	*e*th EV aggregator' energy bought or sold for the RT market in scenario β at time *t*, in MW
$P_{\omega,t,\beta}^{Wind,BAL}$	*ω*th WPP' bought or sold for the RT market in scenario β at time *t*, in MW
$P_{h,t,\beta}^{HPP,BAL}$	*h*th HPP' energy bought or sold for the RT market in scenario β at time *t*, in MW
$P_{e,t,\beta}^{EV}$	*e*th EV aggregator' energy production in scenario β at time *t*, in MW
$P_{\omega,t,\beta}^{Wind}$	*ω*th WPP' energy production in scenario β at time *t*, in MW
$P_{h,t,\beta}^{HPP}$	*h*th HPP' energy production in scenario β at time *t*, in MW
$SOC_{e,t}$	State of charge for EVs connected to the aggregator *e* at time *t*, in %
$P_{e,t}^{V2G,DA}$	*e*th EV aggregator' energy from EVs to the grid for the DA market at time *t*, in MW
$P_{e,t}^{G2V,DA}$	*e*th EV aggregator' energy from the grid to EVs for the DA market at time *t*, in MW
$\lambda_{h,t}^{HPP,offer}$	Offer price for the *h*th HPP in the DA market at time *t*
$P_{g,t}^{G,DA}$	Energy scheduled to be produced in the DA market for traditional generation units located at node *g* and time *t*, in MW

$P_{l,t}^{L,DA}$	Energy scheduled to be consumed in the DA market for fixed and reduced loads located at node *l* and time *t*, in MW
$\theta_{n,t}^{DA}$	Voltage angle at node *n* and time *t* in the DA market
$P_{h,t}^{HPP,offer}$	Energy scheduled to be offered in the DA market for the *h*th HPP at time *t*, in MW
σ^{DA}	Value-at-risk in the DA market
$\rho_{\alpha,\beta}^{DA}$	Auxiliary variable to calculate the *CVaR* in the DA market
χ	Expected revenue of the HPP unit

3.2 Problem Description

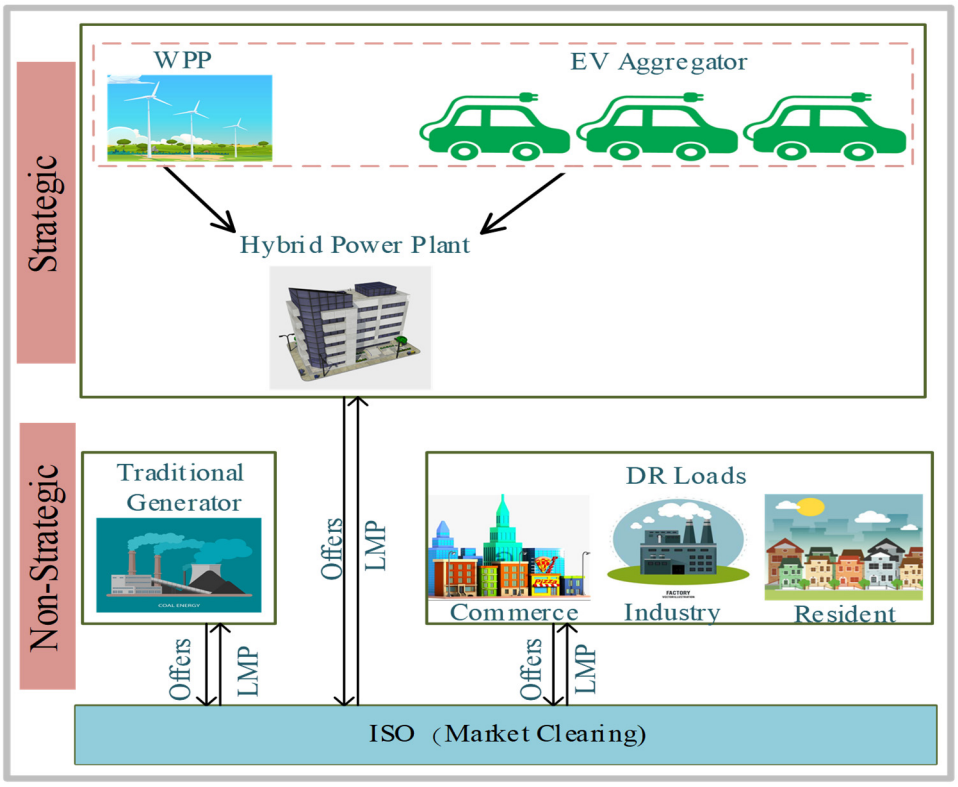

Fig. 3.1 Schematic representation of proposed HPP model

The electricity market consists of the offering stage and clearing stage in both DA and RT markets. Most of the energy trading is completed in the DA market, while the energy deviations are compensated in the RT market. In a pool-based electricity market shown as Fig. 3.1, all participants provide optimal offer prices and energy to the ISO in

the offering stage. Then ISO uses the collected data for market clearing to obtain locational marginal prices (LMP) paid to energy providers in the clearing stage [109]. This Chapter focuses on developing a stochastic offering strategy for the proposed HPP considering uncertainties of renewable energy in the offering stage of the DA market.

In a pool-based DA market, all participants have to submit their sales or purchases offer to the ISO for each hour of the next day and several hours in advance. Participants could be categorized into two different groups, which are energy sellers such as traditional generators and multiple renewable energy providers, and energy buyers such as various consumers. In a fully competitive market environment, all participants could participate in setting prices. However, the actual market is closer to an oligopoly market. It means energy providers with large-scale capacities are easier to alter electricity prices according to their interests, while other small-scale participants are just price-takers. The increasing installed capacities of WPPs and growing numbers of EVs connected to the grid results in these two distributed renewable resources to be aggregated to strategically affect the market prices [110]. It could be beneficial to cost and price reduction for EV aggregators and WPPs bidding separately in the electrical market. These EV aggregators may not be able to compete with WPPs for bidding prices as the battery capacity of aggregated EVs is much less than WPPs. As a result, the aggregated EVs are expected to cooperate with WPP to offer in the DA market. Meanwhile, interests of the gird should not be ignored with price-maker participants strategically offering to bring their economic benefits. Consequently, this Chapter focuses on the coordination of WPPs and EV resources as a HPP to develop the optimal offering strategy for improving their own interests. This would be solved by peak shaving as flexible charging or discharging characteristics of EVs. To be specific, EV owners may provide energy by V2G in due time to compensate the WPP for satisfying the high energy offered, then use the wind energy to meet charging demand for EV owners when the energy offered is relatively low. In this way, EV owners could help the WPP to sell more electricity and earn more money at the high energy offered time while the wind energy would not be wasted during periods of the low energy offered, which is

beneficial to both the HPP and the grid.

Therefore, capacities of cooperative EV aggregators and WPPs are assumed large enough. Thus, EV aggregators and WPPs can be collaborated as a price-maker HPP here. This central planner makes decisions based on collecting necessary information from WPPs and EV aggregators, and then uniformly schedules their individual energy. Other participants including traditional generators and DR loads are set as small-scale participants and just act as price-takers. They would offer productions at their marginal costs, and offer prices are known for strategic energy providers [3]. In this study, the transmission network is represented by a DC model without losses, and uncertainties of actual energy productions and real-time market prices are modeled by corresponding scenarios based on the stochastic approach [111]. As the approaches presented in Section 2.1 for solving optimization problems involving uncertainties of DERs, scenarios of actual energy productions for the WPP and EV aggregator are respectively represented by the maximum output energy derived from historical wind speeds and historical data for the number of EVs connected to the aggregator with τ_β and τ_α respectively represented their probabilities. The expected profit is finally characterized by corresponding probability distribution for these uncertainties. As uncertainties will take high volatility for energy providers' revenues, the risk management measure *CVaR* introduced in Section 2.3 is added to problem formulation to evaluate the expected profits according to offering decisions [112].

3.3 Mathematical Formulation

Aiming at the market described above, a stochastic optimization model of risk-constrained offering strategy for the aggregated HPP including the WPP and EV aggregator in the DA market is proposed. It is further developed as a bi-level model as shown in equations (3.1)-(3.2.8), in which the upper level is used to maximize profits of the strategical HPP while the lower level aims to maximize the social welfare from the perspective of ISO in the grid.

3.3.1 HPP Model

In this model, the HPP in the upper level first provides energy offered $P_{h,t}^{HPP,offer}$ and offer price $\lambda_{h,t}^{HPP,offer}$ to the ISO in the lower level. Then ISO clears market combining this information with offers and bids from non-strategical traditional generators and DR loads separately by using the optimal power flow (OPF). After that, scheduled energy production in the DA market $P_{h,t}^{HPP,DA}$ and LMP $\varphi_{n,t}$ are provided to the HPP in the upper level to maximize profits. Lastly, optimized offer results $P_{\omega,t}^{Wind,offer}$ and $\lambda_{h,t}^{HPP,offer}$ for the WPP, $P_{e,t}^{EV,offer}$ and $\lambda_{h,t}^{HPP,offer}$ for the EV aggregator could be obtained and provided to the DA market. These optimized price-energy production curves are the offering strategies in this research.

1) Upper level

By combining the WPP and EV aggregator to be a HPP, the offering strategy model corresponding to the expected profit function can be expressed as follows:

$$\chi = HPP_{revenue} - HPP_{cost} \tag{3.1}$$

Maximum

$$\begin{aligned}
&\sum_{n\in\Omega_n^N}\sum_{h\in\Omega_n^H}\Big(\sum_{t\in T}\varphi_{n,t}\cdot P_{h,t}^{HPP,DA}-\sum_{t\in T}\sum_{\beta\in N_\beta}\tau_\beta\cdot\lambda_{ch/disch}\cdot P_{e,t,\beta}^{EV}\\
&-\sum_{t\in T}\sum_{\beta\in N_\beta}\sum_{\alpha\in N_\alpha}\tau_\beta\cdot\tau_\alpha\cdot(\varphi_\alpha^{BAL}\cdot P_{e,t,\beta}^{EV,BAL})-\sum_{t\in T}(C_{battery}/T_{battery})\cdot P_{e,t}^{V2G,DA}\\
&-\sum_{t\in T}\sum_{\beta\in N_\beta}\sum_{\alpha\in N_\alpha}\tau_\beta\cdot\tau_\alpha\cdot(\varphi_\alpha^{BAL}\cdot P_{\omega,t,\beta}^{Wind,BAL})\\
&+\xi\cdot(\sigma^{DA}-\frac{1}{1-\alpha_{CVaR}}\cdot\sum_{\alpha\in N_\alpha}\sum_{\beta\in N_\beta}\tau_\beta\cdot\tau_\alpha\cdot\rho_{\alpha,\beta}^{DA})
\end{aligned} \tag{3.1.1}$$

Subject to

$$P_{h,t}^{HPP,DA}=P_{\omega,t}^{Wind,DA}+P_{e,t}^{EV,DA},\quad\forall t \tag{3.1.2}$$

$$P_{h,t,\beta}^{HPP}=P_{\omega,t,\beta}^{Wind}+P_{e,t,\beta}^{EV},\quad\forall t \tag{3.1.3}$$

$$P_{h,t,\beta}^{HPP}\le P_{\omega,t,\beta}^{Wind,\max}+P_{e,t,\beta}^{EV,\max},\quad\forall t \tag{3.1.4}$$

$$P_{h,t,\beta}^{HPP,BAL} = P_{\omega,t,\beta}^{Wind,BAL} + P_{e,t,\beta}^{EV,BAL}, \quad \forall t \tag{3.1.5}$$

$$\begin{aligned} &-P_{\omega}^{Wind,BAL,\max} - P_{e}^{EV,BAL,\max} \\ &\le P_{h,t,\beta}^{HPP,BAL} \le P_{\omega}^{Wind,BAL,\max} + P_{e}^{EV,BAL,\max}, \quad \forall t \end{aligned} \tag{3.1.6}$$

$$P_{e,t}^{EV,DA} - P_{e,t,\beta}^{EV,BAL} = P_{e,t,\beta}^{EV}, \forall e,\beta,t \tag{3.1.7}$$

$$P_{\omega,t}^{Wind,DA} - P_{\omega,t,\beta}^{Wind,BAL} = P_{\omega,t,\beta}^{Wind}, \forall \omega,\beta,t \tag{3.1.8}$$

$$SOC^{\min} \le SOC_{e,t} \le SOC^{\max}, \forall e,t \tag{3.1.9}$$

$$SOC_{e,t} = SOC_{e,t-1} - \frac{\frac{P_{e,t-1}^{G2V,DA}}{E_{ev}^{\max}}}{\gamma_{discharge}} + (\frac{P_{e,t-1}^{V2G,DA}}{E_{ev}^{\max}}) \cdot \gamma_{charge}, \forall e,t \tag{3.1.10}$$

$$\begin{aligned} &（SOC_{e,t}\text{-}SOC_{e,t-1}）/ \gamma_{charge} \\ &+(SOC_{e,t-1} - SOC_{e,t}) \cdot \gamma_{discharge} \le \gamma^{\max}, \forall e,t \end{aligned} \tag{3.1.11}$$

$$P_{e,t}^{EV,DA} = P_{e,t}^{V2G,DA} \cdot \gamma_{charge} - \frac{P_{e,t}^{G2V,DA}}{\gamma_{discharge}}, \forall e,t \tag{3.1.12}$$

$$U_{e,t} \cdot P_{e}^{EV,\min} \le P_{e,t}^{V2G,DA} \le U_{e,t} \cdot P_{e}^{EV,\max}, \forall e,t \tag{3.1.13}$$

$$V_{e,t} \cdot P_{e}^{EV,\min} \le P_{e,t}^{G2V,DA} \le V_{e,t} \cdot P_{e}^{EV,\max}, \forall e,t \tag{3.1.14}$$

$$U_{e,t} + V_{e,t} \le 1, \forall e,t \tag{3.1.15}$$

$$\begin{aligned} &\sigma^{DA} - (\sum_{h\in\Omega_n^H}\sum_{t\in T}\varphi_{n,t} \cdot P_{h,t}^{HPP,DA} - \sum_{e\in\Omega_n^E}\sum_{t\in T}\lambda_{ch/disch} \cdot P_{e,t,\beta}^{EV} \\ &- \sum_{e\in\Omega_n^E}\sum_{t\in T}\varphi_{\alpha}^{BAL} \cdot P_{e,t,\beta}^{EV,BAL} - \sum_{e\in\Omega_n^E}\sum_{t\in T}(C_{battery} / T_{battery}) \cdot P_{e,t}^{V2G,DA} \\ &- \sum_{\omega\in\Omega_n^{\omega}}\sum_{t\in T}\varphi_{\alpha}^{BAL} \cdot P_{\omega,t,\beta}^{Wind,BAL}) \le \rho_{\alpha,\ \beta}^{DA}, \forall \alpha,\beta \end{aligned} \tag{3.1.16}$$

$$\rho_{\alpha,\ \beta}^{DA} \ge 0, \forall \alpha,\beta \tag{3.1.17}$$

The optimization variables of the UL problem are the variables in the set

$\Delta^{UL}=\{\varphi_{n,t}, P_{h,t}^{HPP,DA}, P_{e,t,\beta}^{EV}, P_{e,t,\beta}^{EV,BAL}, P_{e,t}^{V2G,DA}, P_{\omega,t,\beta}^{Wind,BAL}, P_{\omega,t}^{Wind,DA}, P_{e,t}^{EV,DA}, P_{\omega,t,\beta}^{Wind,BAL}, SOC_{e,t}, P_{e,t}^{G2V,DA}, P_{\alpha,\beta}^{DA}\}$.

The objective function in the upper level is to maximize the HPP's profit. It should be noticed that an EV aggregator is unable to produce energy by itself. It takes part in the electricity market as an agent for buying electricity from individual EV owners and selling electricity to the grid. The payoff function (3.1.1) consists of six terms. The first term is the revenues of selling electricity in the DA market $\varphi_{n,t} \cdot P_{h,t}^{HPP,DA}$. The second term is EV aggregator's cost of energy production in DA and RT market $\tau_\beta \cdot \lambda_{ch/disch} \cdot P_{e,t,\beta}^{EV}$, which is followed by EV aggregator's incomes or expenses from selling or buying electricity in the RT market $\tau_\beta \cdot \tau_\alpha \cdot (\varphi_\alpha^{BAL} \cdot P_{e,t,\beta}^{EV,BAL})$. The next two terms are compensation cost for battery degradation $\sum_{t\in T}(C_{battery}/T_{battery}) \cdot P_{e,t}^{V2G,DA}$ and wind's incomes or expenses from selling or buying electricity in the RT market $\tau_\beta \cdot \tau_\alpha \cdot (\varphi_\alpha^{BAL} \cdot P_{\omega,t,\beta}^{Wind,BAL})$. $\varphi_{n,t}$ is the LMP calculated from the lower level as a dual variable in constraint (3.2.2) for energy balance, which is used to pay for the EV aggregator and the WPP. There are two kinds of uncertainties considered in this model, which are spot price in the RT market φ_α^{BAL} and actual energy production capacities $P_{\omega,\beta}^{Wind,max} + P_{e,t,\beta}^{EV,max}$. As actual energy productions $P_{h,t,\beta}^{HPP}$ may be more or less than energy scheduled in the DA market $P_{h,t}^{HPP,DA}$, HPP needs to buy deficit or sell surplus energy $P_{h,t,\beta}^{HPP,BAL}$ in the RT market to compensate the energy deviation in the DA market, and hence, $P_{h,t,\beta}^{HPP,BAL}$could be positive or negative. The last term is *CVaR*. Here, the weight parameter ξ is used to weigh expected profit and *CVaR*, and to show different offering strategy. If ξ is 0, the proposed model will consider the maximum profit and neglect the risk. As ξ becomes larger, the HPP considers not only its profit but also its risk. When ξ is close to 1, a risk-averse offering model is considered, in which a minimum revenue should be maintained for a confidence level α_{CVaR} [113].

(3.1.2)-(3.1.3) constrain the upper level objective function (3.1). Constraint (3.1.2) states the relationship between scheduled energy productions in the DA market by the WPP, the EV aggregator, and the HPP. Constraint (3.1.3) imposes the relationship between actual energy generated by the WPP, the EV aggregator, and the HPP.

Constraint (3.1.4) imposes the limit of available energy for the HPP according to each scenario. Then (3.1.5) gives the relationship between scheduled energy productions in the RT market by the WPP, the EV aggregator, and the HPP. (3.1.6) limits energy bought or sold for the HPP in the RT market. (3.1.7) and (3.1.8) state the relationship between scheduled energy productions in the DA market, RT market, and total energy productions for the EV aggregator and WPP separately. Constraint (3.1.9) is used to maintain EVs to avoid overcharging and over-discharging. Equation (3.1.10) gives state changes of charging/discharging for EVs connected to the EV aggregator. The charging / discharging rate in each hour is limited in (3.1.11). Equation (3.1.12) shows the *e*th EV aggregator's scheduled energy in the DA market, which is equal to the energy provided in V2G minus the energy consumed in G2V. Besides, $U_{e,t}$ and $V_{e,t}$ are binary variables as (3.1.15). So inequalities (3.1.13) and (3.1.14) are used to constrain $P_{e,t}^{V2G,DA}$ and $P_{e,t}^{G2V,DA}$ not to exist at the same time. Additionally, the lower limit for $P_{e,t}^{V2G,DA}$ and $P_{e,t}^{G2V,DA}$ is a nonzero value $P_{e,t}^{EV,min}$. It means that the EV aggregator may provide energy by V2G in due time with WPP to satisfy the high energy offered, and use wind energy to meet charging demand for EV owners when offered energy is relatively low. Finally, (3.1.16) and (3.1.17) are used to compute the *CVaR* [113].

2) Lower Level

In the pool-based electricity market, ISO collects all producers' offer prices and consumers' bid prices and finishes market clearing. Finally, ISO provides price signals and the scheduled energy to all participants in the upper level. This process is finished in the lower level model. As demands are considered as elastic, the objective function (3.2) in the lower level is to maximize social welfare from the perspective of the grid. Besides, traditional OPF is used to clear the market transaction.

Maximize

$$\sum_{t\in T}\Big(\sum_{l\in\Omega_n^L}\lambda_l^{DA}\cdot P_{l,t}^{L,DA}-\sum_{g\in\Omega_n^G}\lambda_g^{DA}\cdot P_{g,t}^{G,DA}-\sum_{h\in\Omega_n^H}\lambda_{h,t}^{HPP,offer}\cdot P_{h,t}^{HPP,DA}\Big) \qquad (3.2)$$

Subject to

$$\lambda_{h,t}^{HPP,offer} \geq 0, \forall h,t \tag{3.2.1}$$

$$\sum_{g\in\Omega_n^G} P_{g,t}^{G,DA} + \sum_{h\in\Omega_n^h} P_{h,t}^{HPP,DA} - \sum_{a\in\Omega_n^N} B_{na}\cdot(\theta_{n,t}^{DA} - \theta_{a,t}^{DA}) = \sum_{l\in\Omega_n^L} P_{l,t}^{L,DA} : \varphi_{n,t}, \forall n,t \tag{3.2.2}$$

$$-f_{na}^{\max} \leq B_{na}\cdot(\theta_{n,t}^{DA} - \theta_{a,t}^{DA}) \leq f_{na}^{\max} : \mu_{na,t}^{L,DA}, \mu_{na,t}^{U,DA}, \forall a,n \in \Omega_n^N, \forall t \tag{3.2.3}$$

$$P_g^{\min} \leq P_{g,t}^{G,DA} \leq P_g^{\max} : \mu_{g,t}^{L,DA}, \mu_{g,t}^{U,DA}, \forall g,t \tag{3.2.4}$$

$$P_l^{\min}\cdot D_{factor} \leq P_{l,t}^{L,DA} \leq P_l^{\max}\cdot D_{factor} : \mu_{l,t}^{L,DA}, \mu_{l,t}^{U,DA}, \forall l,t \tag{3.2.5}$$

$$0 \leq P_{h,t}^{HPP,DA} \leq P_{h,t}^{HPP,offer} : \mu_{h,t}^{L,DA}, \mu_{h,t}^{U,DA}, \forall h,t \tag{3.2.6}$$

$$\theta_{n,t}^{DA} = 0 : \mu_{\theta,t}^{DA}, n : ref, \forall t \tag{3.2.7}$$

$$-\pi \leq \theta_{n,t}^{DA} \leq \pi : \mu_{\theta,t}^{L,DA}, \ \ \mu_{\theta,t}^{U,DA}, \forall n \setminus n : ref, \forall t \tag{3.2.8}$$

The optimization variables of the LL problem are the variables in the set $\Delta^{LL}=\{P_{l,t}^{L,DA}, P_{g,t}^{G,DA}, \lambda_{h,t}^{HPP,offer}, P_{h,t}^{HPP,DA}, \lambda_{h,t}^{HPP,DA}, \theta_{n,t}^{DA}, P_{l,t}^{l,DA}\}$.

The first constraint (3.2.1) defines the offer price of HPP in the DA market which should be nonnegative. (3.2.2) enforces the energy balance between supply and demand, which is associated with a dual variable $\varphi_{n,t}$ to donate the LMP used in the upper-level. Inequality (3.2.3) limits the energy flow in each transmission line. Maximum and minimum productions of scheduled energy for traditional generation units, load consumptions and the HPP in the DA market are shown in (3.2.4), (3.2.5) and (3.2.6) individually. It shall be noted that load consumptions, including fixed load requirement represented by minimum load values and curtailed load as DR, are considered as variables in the model. Equation (3.2.7) sets the voltage angle at the reference node as zero and inequality (3.2.8) constrains voltage angles at nodes except the reference node.

Additionally, $\mu_{na,t}^{L,DA}, \mu_{na,t}^{U,DA}, \mu_{g,t}^{L,DA}, \mu_{g,t}^{U,DA}, \mu_{l,t}^{L,DA}, \mu_{l,t}^{U,DA}, \mu_{h,t}^{L,DA}, \mu_{h,t}^{U,DA}, \mu_{\theta,t}^{DA}, \mu_{\theta,t}^{L,DA}, \mu_{\theta,t}^{U,DA}$ are the corresponding dual variables for constraints from (3.2.2) to (3.2.8).

3.3.2 Solution methodology

To obtain the optimal value, the proposed bi-level model is first transformed into a single-level model by replacing the lower level model with KKT (Karush-Kuhn-Tucker) constraints, as (2.3a)-(2.4c) in Section 2.2.1 [6]. Then, transformed constraints are added to constraints in the upper level to limit the upper objective function. In this way, the original bi-level model could become a single-level MPEC problem. The MPEC model contains two terms of nonlinearities. Replacing these two non-linear terms using strong duality theorem (SDT) and the Fortuny-Amat transformation respectively as (2.8a)-(2.9d) in Section 2.2.2, this MPEC model could be further transformed into a MILP model [114]. Lastly, the transformed MILP model is well solved by the computational tool represented in Section 2.2.3.

3.4 Case Studies

The proposed model is tested in the IEEE six-bus and thirty-bus systems for a day divided into 24 hours.

While the traditional generation unit capacities are assumed constant throughout the day, the capacities of loads would change over time with the demand factor shown in Fig. 3.2 [6]. The uncertainties of the RT market price φ_{α}^{BAL} are represented by the same 10 scenarios in 24 hours with corresponding probabilities selected from [6]. Fig. 3.3 and Fig. 3.4 show respectively the uncertainties of maximized productions for the WPP and the number of EVs that can be aggregated by the EV aggregator over time [11, 115]. For the sake of simplicity, probabilities of all scenarios for energy productions are considered as (0.1). Additionally, the charging / discharging cost for the EV aggregator and the rated power for every EV are set to 20$/MWh and 10kW, respectively. Other parameters for the EV aggregator are listed in Table 3.1.

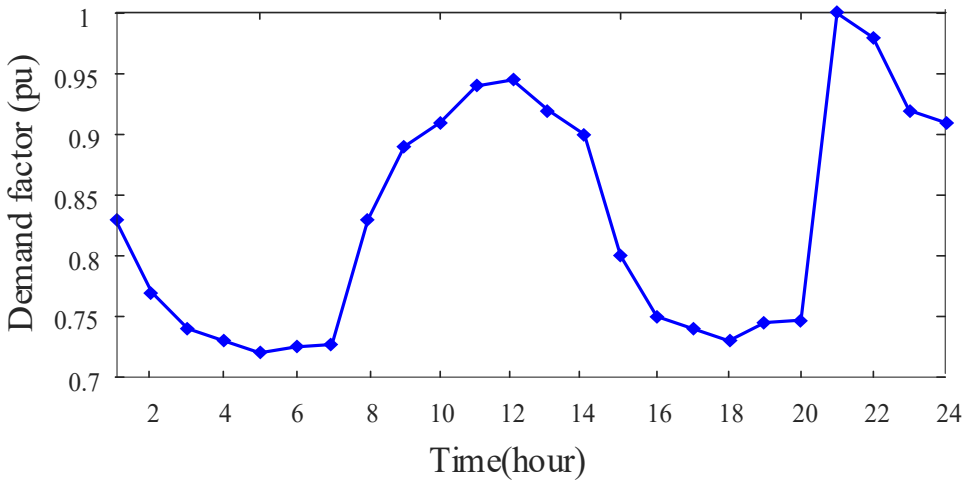

Fig. 3.2 Demand factors over time

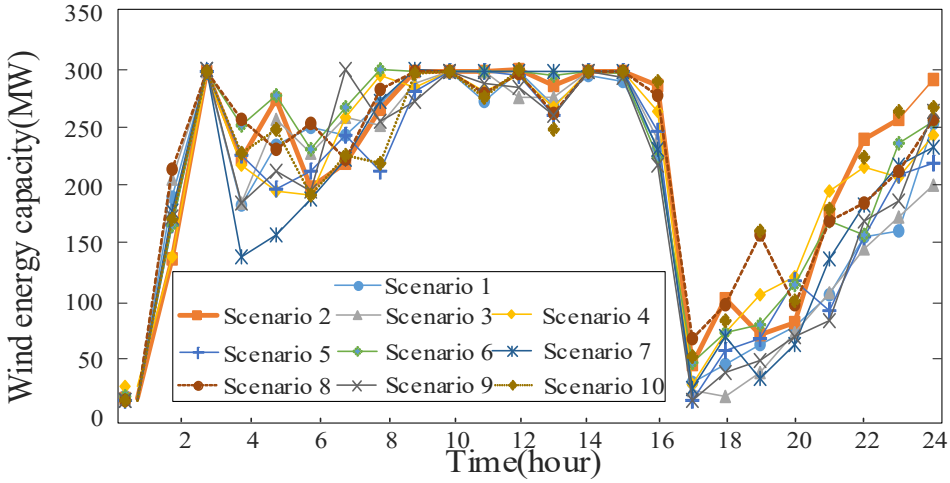

Fig. 3.3 Scenarios data for actual maximize output of the wind energy

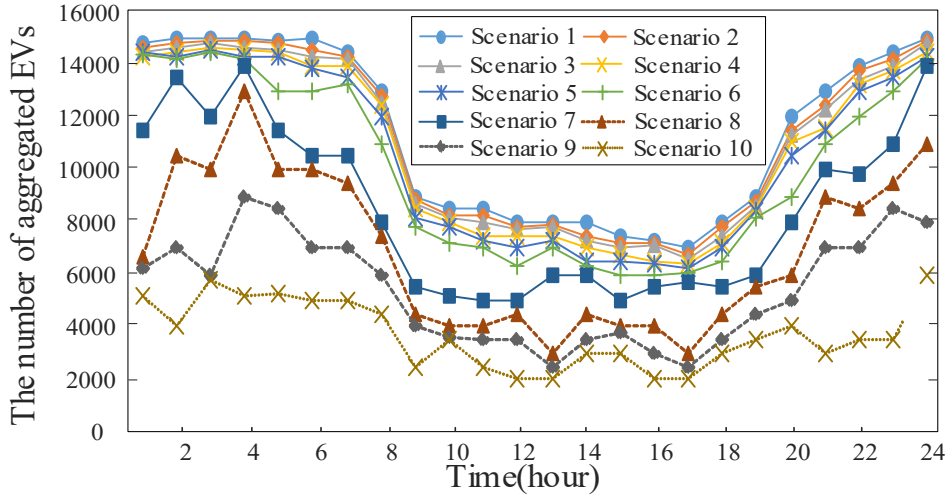

Fig. 3.4 Scenarios data for the number of aggregated EVs

Table 3.1 Data for the EV aggregator

EV Aggregator	SOC^{max} (pu)	SOC^{min} (pu)	γ_{charge}	$\gamma_{discharge}$	γ^{max}	E_{ev}^{max} (MWh)
Value	0.9	0.3	0.9	0.85	0.2	600

3.4.1 Six-Bus System

The IEEE six-bus system consists of 3 generators, 3 demands, and 11 transmission lines. A WPP and an EV aggregator are located at node 4 and node 5, respectively. Table 3.2 lists capacities, offer prices and bid prices for traditional generation units and load units [6].

Table 3.2 Offer and bid data for generators and loads

	Traditional generators			Loads		
Bus	1	2	3	4	5	6
Offer price($/MWh)	49	50	44	0	0	0
Bid price ($/MWh)	0	0	0	59	50	40

1) Offering curve of the HPP model

With system settings described above, Fig.3.5 presents optimized offering results of the aggregated HPP. The blue curve and the green curve refer to energy offered and offer prices, respectively, in 24 hours for the DA market. As uncertainties of actual energy productions and RT market prices, the energy offered would vary throughout the day. Besides, the curve of offer prices would change with the curve of the energy offered. The energy offered in Fig. 3.5 is relatively high in the first few hours 9-15 and last three hours while corresponding prices are comparatively low. This is because it will take an economic risk for the HPP with offer prices being relatively high at these moments. Specifically, if the actual energy production is lower than the energy offered, the HPP will have to buy the energy at a high price in the RT market for meeting the energy offered in the DA market. As a result, the HPP offers relatively low prices at moments of comparatively high energy offered, in which it could sell the surplus to the

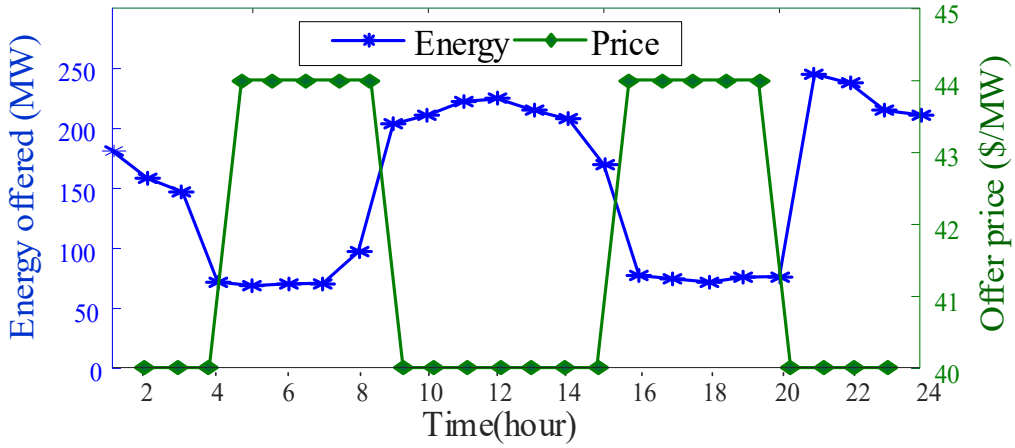

Fig. 3.5 Offer results for aggregated HPP in six-bus system

RT market with the actual production exceeding the energy offered. Similarly, the HPP offers a relatively high price when the energy offered is comparatively low. In this way, the HPP may only need to buy a small amount of deficiency at a high price in the RT market once the actual production is lower than the energy offered. Conversely, the HPP could sell the surplus at a high price when the actual production exceeds the energy offered, which makes sense for the HPP's profits. In general, the HPP adjusts the offer price and set the electricity price according to the energy offered. After the clearing process in the DA market, the LMP is equal to the offer price at the same node. Then energy providers at each node will be paid at the corresponding LMP in the RT market. Besides, all clearing LMPs are equal at all nodes in a six-bus system with no congestion occur. To sum up, the influence of energy quantities offered on cleared market prices shows how large-scale renewable resources strategically affect electricity prices in the electricity market.

2) Optimal offering energy quantity of the HPP model

Optimal quantities of energy offered for the HPP model in the six-bus system is shown in Fig.3.6. Offering quantities of the aggregated HPP increase at hours 9-15 and 20-24. At these moments, the cooperated EV aggregator calls for EV owners to discharge and provides energy to the WPP for the energy offered in Fig. 3.6. Besides, the EV aggregator may use redundant wind energy to satisfy the charging demand for EV owners when the energy offered is relatively low.

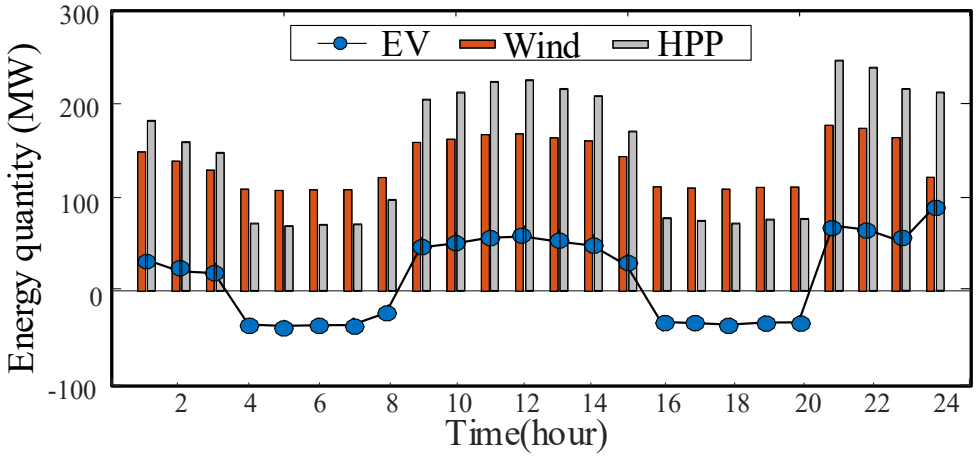

Fig. 3.6 Energy quantity of HPP for the DA market in six-bus system

3) Comparison and Discussion

Here, the proposed HPP model is compared to three other models. The first one has only a WPP strategically offering price to be price-makers and the clearing process consists of the WPP, traditional units and loads. The second model is similar to the first one but has only an EV aggregator strategically offering price instead. The third is the sum model in which a HPP and an EV aggregator offer price together but without cooperating. In the proposed model, EVs are required to compensate the WPP to provide energy to satisfy the high energy offered and the WPP is used to meet charging demand for EV owners when the offered energy is relatively low.

Fig. 3.7 shows the comparison of revenues from these three models with the proposed one. According to revenue graphs in 24 hours, the HPP model takes more profits. This is due to the EV aggregator mitigates uncertainties of the WPP and the change of demand sides by controlling V2G and G2V flexibility, which further improves the profits by selling energy during high energy offered time and increasing EV owners' consumption for storing more energy at moments of low energy offered.

4) Impact of Incorporating Risk on the HPP model

Table 3.3 compares the expected revenues and the *CVaR* for different weighting parameter ξ in the sum model and the HPP model. The confidential level α_{CVaR} is set to 0.95. As the parameter ξ increases from 0.01 to 1, the expected profit decreases

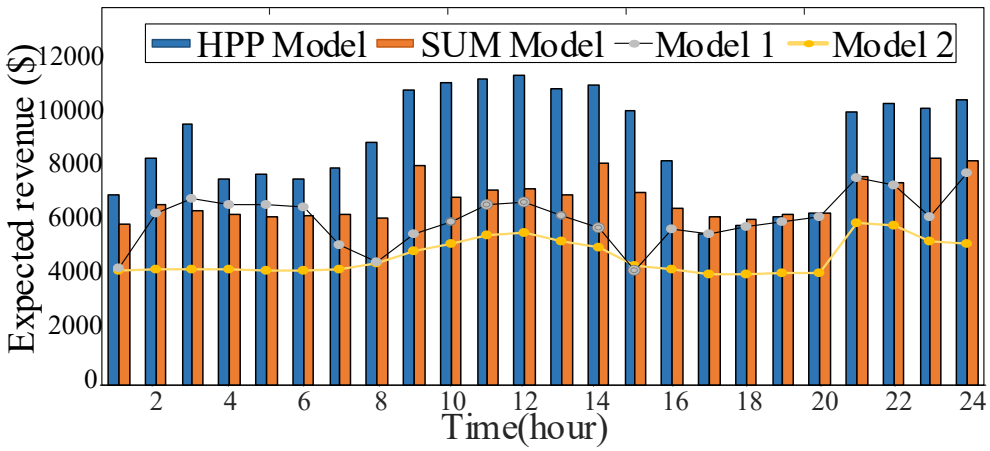

Fig. 3.7 Comparison of revenues with other three models

Table 3.3 Comparison of revenues and *CVaR* for different weighting parameter ξ

ξ	Sum		HPP	
	Revenue ($)	*CVaR* ($)	Revenue ($)	*CVaR* ($)
0.01	137955.70	72.29	179632.29	76.30
0.1	137933.30	681.22	179622.87	749.25
0.2	137730.75	1115.71	179585.16	1451.05
0.5	137165.48	1906.29	179294.70	3160.38
0.8	136497.45	2278.35	178877.82	3673.69
1	136430.83	2771.84	178487.78	4514.93
$-\frac{\Delta(CVaR)}{\Delta(\chi)}$	1.77		3.88	

while the *CVaR* increases. Specifically, the revenue decreases by 1.1% and 0.64% for the sum model and the combined HPP model respectively, while the *CVaR* increases by 2.7% and 1.7% respectively. Therefore, just a small decrease in revenues could diminish the risk. Besides, $-\Delta(CVaR)/\Delta(\chi)$ means the changing rate of *CVaR* relating to the change of revenue. The higher $-\Delta(CVaR)/\Delta(\chi)$ implies less decrease in revenue and more increase in *CVaR*, which also means the profit volatility is better controlled. Table 3.3 shows this ratio is higher for the HPP model. Meanwhile, offering curves would change with different risk weighing parameters. The HPP reduces its profit's volatility caused by uncertainties with introducing the *CVaR* to offer strategically.

3.4.2 Thirty-Bus System

The IEEE thirty-bus system consists of 6 generators, 20 demands, and 41 transmission lines. A strategic WPP and an EV aggregator are located at node 17 and node 26, respectively.

Offer results for the HPP model are plotted in Fig. 3.8. Due to the uncertainties of actual energy productions and RT market prices, the energy scheduled to offer would vary throughout the day. Besides, the curve of offer prices would change as the curve of the energy offered. In Fig. 3.8, the energy scheduled to offer are relatively high in the first few hours 13-19 and last two hours. During these periods, corresponding prices are comparatively low. The analysis for this case is similar to the IEEE six-bus system. Optimal energy quantities of the HPP model offered in this case system is shown in Fig. 3.9, in which offering quantities increase at hours 13-14 and 23-24. At these moments, the cooperated EV aggregator calls for EV owners to discharge for the energy offered in Fig. 3.8. Then the EV aggregator could use the wind energy to satisfy the charging demands from EV owners during periods of low energy offered such as hours 11-12 and 21-22. Fig. 3.10 shows the comparison of combined HPP revenues with the sum model, in which the EV aggregator and the WPP participates in the electricity market offer separately. It can be seen the HPP model takes more profits.

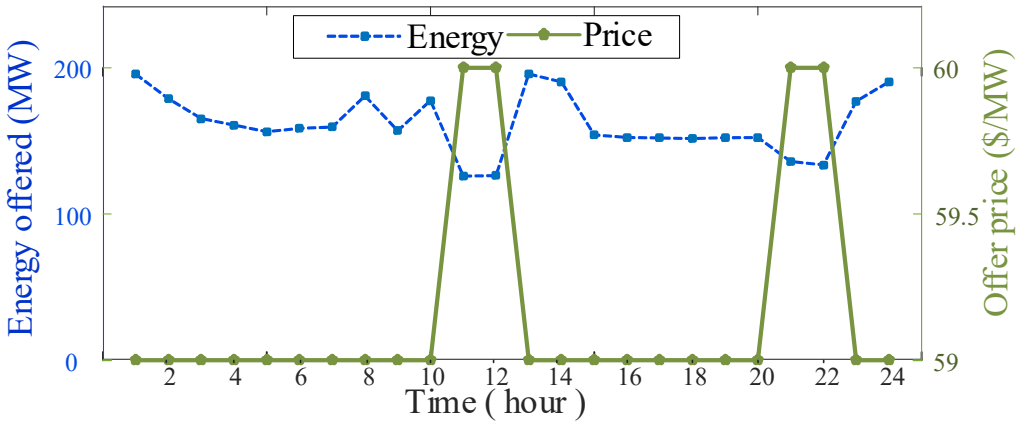

Fig. 3.8 Offer results for aggregated HPP in thirty-bus system

Remark: The proposed model is developed from the perspective of the aggregated large scale DERs, thus they affect electricity prices by strategically bidding. It is critical

to avoid market power from the market designer's point of view. In general, there are two approaches. One is reducing the percentage of each participant, the other one is setting price cap of the bidding. This can be done as a future work.

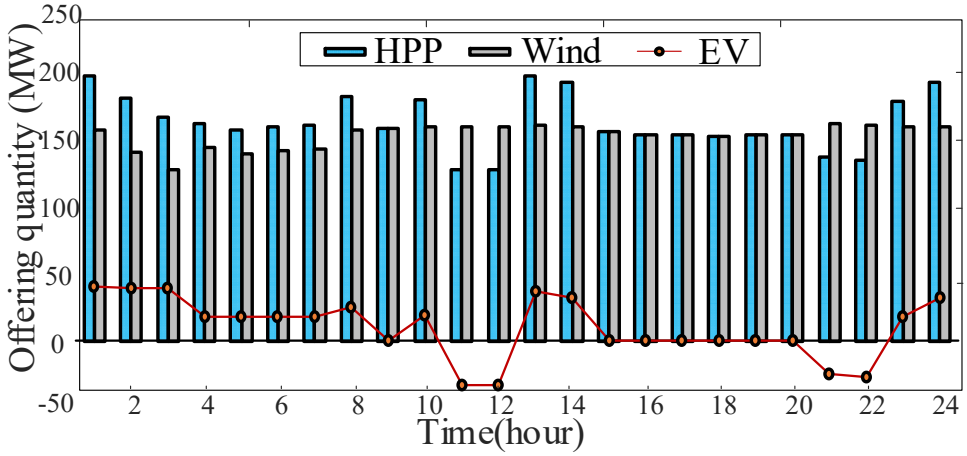

Fig. 3.9 Energy quantity of HPP for the DA market in thirty-bus system

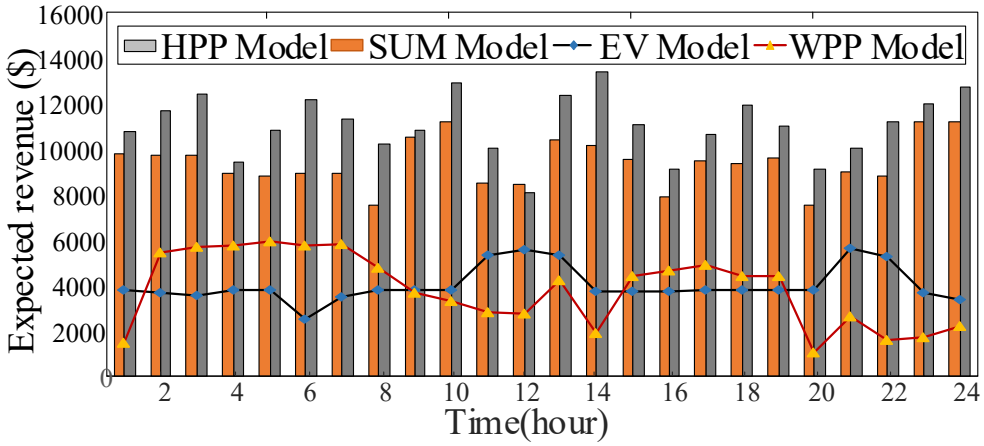

Fig. 3.10 Comparison of revenues from other models

3.5 Summary

A stochastic optimization model is proposed in this Chapter to derive the offering strategy for the aggregated HPP to be a price-maker in the DA pool-based market. The model consists of two levels, with offering decisions to make to maximize the HPP's profits in the upper level and market clearing to complete to maximize revenues of the grid in the lower level. This bi-level problem is then transformed into a MPEC problem by KKT conditions and further solved as a MILP problem with Strong Duality theory

and the Fortuny-Amat transformation. By combining WPPs and EVs, several promising results have demonstrated the validity of the proposed HPP model: 1) Large-scale renewable resources could be aggregated for strategical bidding and setting electricity prices according to their and the grid's interests. 2) The proposed model shows cooperative energy provided by the WPP and the EV aggregator during different time slots. In this way, the total cost of energy consumptions and the waste of wind resources are reduced, which is cost-effective and more environmentally friendly. 3) The proposed HPP model has been demonstrated that it could take more profits by comparing with three other models. 4) With the consideration of risk in the HPP model, the profit volatility caused by uncertainties could be coped with more effective.

Chapter IV

Bidding Strategy for the Coordinated Operation of Wind Power Plants and NGG-P2G Units in Electricity Market

4.1 Introduction

Extending virtual power plant (VPP) to a virtual multi-energy plant (VMP) and exploring multiple energy synergies could help balance fluctuations of renewable DERs [116, 117]. The proliferation of NGGs and the emerging P2G technology have enabled bidirectional energy flows between electric power network and natural gas systems. As a result, the integrated NGG-P2G with high operation flexibility is promising to coordinate with the WPP. The coordinated model is expected to bring more profits as NGG-P2Gs could counterbalance wind energy fluctuations and provide large capacities for ancillary services in a VMP. So far, to the best of knowledge, there are few studies considering the coordinated NGG-P2G unit and WPPs as a price-maker in electricity market to increase their overall profits. Therefore, considering uncertainties of wind output capacities and RT prices, a bidding strategy model of coordinated suppliers consisting of WPP and NGG-P2G unit is proposed here, where the coordinated supplier is considered as a price-maker in DA market and a price-taker in RT market as well as providing ancillary services employed in real-time through the NGG-P2G unit to enhance their common interests.

In this Chapter, a bi-level stochastic optimization model is proposed for a coordinated WPP and NGG- P2G supplier participating in DA market and RT market as well as providing auxiliary services in real-time. The coordinated supplier's profit is maximized in the upper level with consideration of the uncertainties of WPP's output

capacities and RT electricity prices, while the social welfare of the grid is maximized in the lower level. Simulation results have demonstrated the effectiveness of the proposed bidding model of the coordinated WPP and NGG-P2G unit by examining its bidding behaviors and benefits with comparisons of four other bidding models.

The nomenclature of symbols used in this Chapter is given as follows.

Indices:

le/lg/let/lgt	Index of interruptible electricity loads (IELs) /natural gas loads (NGLs)/electric thermal loads (ETLs)/ gas thermal loads (GTLs)
*s/b/*ω	Index of PV units/battery energy storage systems (BESSs)/ wind power plants (WPPs)
i	Index of integrated natural gas generating (NGG) and power-to-gas (P2G) units
c	Index of coordinated WPPs and NGG-P2G suppliers
g	Index of natural gas wells
n/q	Index of nodes in electricity/natural gas network
α/β	Index of scenarios of real-time (RT) market prices/WPP output

Sets:

$\Omega_n^{Le}/\Omega_n^{Let}$ $/\Omega_n^S/\Omega_n^B$	Set of nodes with IELs / ETLs /PV units/BESSs in electricity network
Ω_q^{Lgt}	Set of nodes with GTLs in natural gas network
Ω_n^N/Ω_q^Q	Set of nodes connected to node *n*/*q* in electricity/natural gas network
Ω^T	Set of natural gas pipelines
T	Total time periods
N_α/N_β	Set of scenarios for RT market prices/WPP output

Parameters:

τ_α/τ_β	Probability of scenario α of RT market prices/ scenario β of WPP output
φ_α^{RT}	RT market price in scenario α, in \$/MW
λ_{gas}	Natural gas price for NGG units, in \$/MW
$P_{limit}^{CO,RT}$	Maximum traded power of coordinated suppliers in RT market
$P_{\beta,w,t}^{Wind,max}$	WPP capacity in scenario β at time t, in MW
$P_i^{IN,max}$	Integrated NGG-P2G capacity, in MW
$P_i^{NGG,max}$ /$P_i^{P2G,max}$	Maximum operation power of NGG/P2G facility, in MW
$\lambda_{reg,i,t}^{IN,up}/\lambda_{reg,i,t}^{IN,dn}$	Up/down regulation price of NGG-P2G unit, in \$/MW
$\lambda_{le}^{Int,DA}/\lambda_{let}^{et,DA}$ /$\lambda_s^{S,DA}/\lambda_b^{B,DA}$	Offer price of IEL/ETL/PV/BESS at node *n* in DA market, in \$/MW
f_{nm}^{max}	Capacity of power line *nm*, in MW
B_{nm}	Susceptance of power line *nm*
$\gamma_{P2G}/\gamma_{NGG}$	Power-to-gas/Gas-to-power conversion efficiency, in %
$S^{STR,min}$ /$S^{STR,max}$	Minimum/maximum gas storage in natural gas network, in MW
$P^{The,min}$	Minimum thermal consumption of all GTLs, in MW
P^{The}	Thermal consumption of all ETLs and GTLs, in MW
$P_g^{Gw,max}$/ $P_{pq}^{gasflow,max}$	Capacity of natural gas well *g*/ gas pipeline *pq*, in MW
P_s^{max}/P_b^{max}	Maximum power output of PV/BESS in MW
$P_{le}^{Int,max}$	Maximum power consumption of IEL *le*, in MW
$P_{lg,t}^{Gas}$	Power consumption of NGL *lg* at time *t*, in MW
σ_{qp}	Gas pipeline constant

Variables:

$\varphi_{n,t}$	Locational marginal price (LMP) at node *n* and time *t*, in \$/MW
$P_{c,t}^{CO,DA}$	Scheduled power output of coordinated supplier in DA market at time *t*, in MW
$P_{c,t}^{CO,bid}$	Offered power of coordinated supplier in DA market at time *t*, in MW
$P_{\alpha,\beta,c,t}^{CO,RT}$	Traded power in RT market for coordinated supplier in scenario α and β at time *t*, in MW
$P_{\alpha,\beta,i,t}^{IN,up}/P_{\alpha,\beta,i,t}^{IN,dn}$	Up/down regulation power of integrated NGG-P2G unit in scenario α and β at time *t*, in MW
$P_{\omega,t}^{Wind,DA}$ $/P_{i,t}^{IN,DA}$	Scheduled power output of WPP/ NGG-P2G unit in DA market at time *t*, in MW
$P_{\alpha,\beta,\omega,t}^{Wind,RT}$ $/P_{\alpha,\beta,i,t}^{IN,RT}$	Traded power in RT market by WPP/ NGG-P2G unit in scenarios α and β at time *t*, in MW
$P_{i,t}^{NGG,DA}$ $/P_{i,t}^{P2G,DA}$	Scheduled power output of NGG/ P2G unit in DA market at time *t*, in MW
$P_{\alpha,\beta,i,t}^{P2G}/P_{\alpha,\beta,i,t}^{NGG}$	P2G output/ NGG consumption in scenario α and β at time *t* in DA and RT market, in MW
$P_{\alpha,\beta,i,t}^{NGG,up}$ $/P_{\alpha,\beta,i,t}^{P2G,up}$	Up regulation power provided by NGG/P2G unit in scenario α and β at time *t*, in MW
$P_{\alpha,\beta,i,t}^{NGG,dn}$ $/P_{\alpha,\beta,i,t}^{P2G,dn}$	Down regulation power provided by NGG/ P2G unit in scenario α and β at time *t*, in MW
$P_{le,t}^{Int,DA}$ $/P_{let,t}^{et,DA}$	Scheduled power consumption of IEL/ ETL at time *t* in DA market, in MW
$P_{s,t}^{S,DA}$ $/P_{b,t}^{B,DA}$	Scheduled power output of PV unit/BESS in DA market at time *t*, in MW
$\lambda_{c,t}^{CO,bid}$	Offer price of coordinated supplier in DA market at time *t*, in \$/MW
$\theta_{n,t}^{DA}$	Voltage angle at node *n* and time *t* in DA market

$P^{IN}_{\alpha,\beta,i,t}/P^{IN,gas}_{\alpha,\beta,i,t}$	Electricity/Gas output of NGG-P2G unit in scenario α and β at time t, in MW
$S^{STR}_{\alpha,\beta,t}$	Gas storage in gas pipelines in scenario α and β at time t, in MW
$P^{Gaswell}_{g,t}$	Gas supplied by gas well g at time t, in MW
$\pi_{q,t}/\pi_{p,t}$	Gas pressure of node q/p at time t
$P^{Gasflow}_{qp,t}$	Gas flow in pipeline qp at time t, in MW, positive for gas flow from node q to p, otherwise negative
Γ_{qp}	Compressor pressure ratio between pipeline nodes q and p
$P^{GTL}_{lgt,t}$	Gas consumed by GTL lgt at time t, in MW

4.2 Problem Description

For a VMP as shown in Fig. 4.1, the electricity network includes WPPs, NGG-P2G and PV units, BESS, and IELs, and the natural gas network comprises gas wells and compressors, and NGLs. The thermal load can be jointly supplied by electricity and natural gas resources.

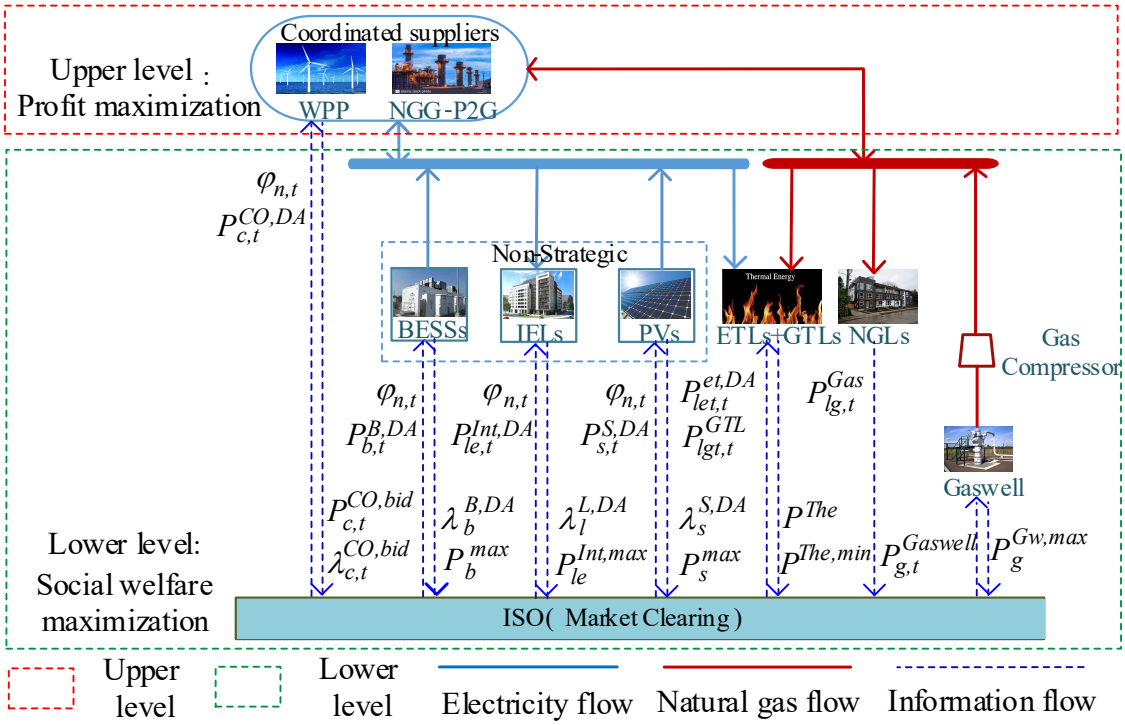

Fig. 4.1 Coordinated WPPs and NGG-P2G units

A stochastic bi-level model is proposed, as illustrated in Fig. 4.1, to obtain the optimal bidding strategy of coordinated WPPs and NGG-P2G suppliers. At the lower level (LL), the ISO in DA market completes market clearing with offers collected from all participants to maximize the social welfare. The large-scale WPPs and NGG-P2G suppliers are coordinated as price-makers to provide offers to ISO while the small-scale PV units, BESSs and DR loads are non-strategic participants with given offer prices and provide their supply limits to ISO [6]. The ISO in LL provides Locational Marginal Prices (LMPs) and scheduled power output to participants at the upper level (UL). At UL, a two-stage complementarity model is presented to maximize the payoff of coordinated WPPs and NGG-P2G suppliers. At the first stage, they decide the offer price and quantity strategically as well as the synergies between WPPs and NGG-P2G units in DA market. At the second stage, WPPs and NGG-P2G units would optimize electricity trading and provide auxiliary services in RT market. Note that the coordinated supplier behaves as a price maker only in DA market, while it buys/sells its production deviations as a price taker in RT market. This assumption relies on the fact that the highest volume of energy trading generally occurs in DA market. Nevertheless, it is feasible to consider the coordinated supplier as a price-maker in RT market.

In the proposed stochastic bi-level model, uncertainties of RT electricity prices and WPP outputs are considered by scenarios. As described in Section 2.1, scenarios are derived from a scenario generation process by the roulette wheel mechanism and an efficient scenario-reduction algorithm based on the fast-forward selection method. The electricity transmission network is represented by a DC model, and the components in the natural gas network including linepacks, gas flows and gas compressors are linearized in steady-state operating conditions [118].

4.3 Mathematical Formulation

In this Section, a stochastic bi-level bidding strategy model is proposed. The

coordinated WPP and NGG-P2G supplier model is introduced at the upper level, while the lower level represents the integrated electricity and gas system.

4.3.1 Upper-level model

In DA market, coordinated WPPs and NGG-P2G suppliers in UL first provides the offer power $P_{c,t}^{CO,\mathrm{bid}}$ and price $\lambda_{c,t}^{CO,\mathrm{bid}}$ to ISO at LL, then the scheduled power output $P_{c,t}^{CO,DA}$ and LMP $\varphi_{n,t}$ in LL are feedbacked to the coordinated WPPs and NGG-P2G suppliers to maximize their payoffs in UL in (4.1).

Maximum

$$\sum_{t\in T}(\varphi_{n,t}\cdot P_{c,t}^{CO,DA}+\sum_{\beta\in N_\beta}\sum_{\alpha\in N_\alpha}\tau_\beta\cdot\tau_\alpha\cdot(\varphi_\alpha^{RT}\cdot P_{\alpha,\beta,c,t}^{CO,RT}-\lambda_{gas}\cdot P_{\alpha,\beta,i,t}^{IN} + \lambda_{reg,i,t}^{IN,up}\cdot P_{\alpha,\beta,i,t}^{IN,up}+\lambda_{reg,i,t}^{IN,dn}\cdot P_{\alpha,\beta,i,t}^{IN,dn}) \tag{4.1}$$

The first term $\varphi_{n,t}\cdot P_{c,t}^{CO,DA}$ in (4.1) is the revenues for selling power in DA market, followed by incomes of selling or expenses of buying power in RT market $\varphi_\alpha^{RT}\cdot P_{\alpha,\beta,c,t}^{CO,RT}$ and power production cost $\lambda_{gas}\cdot P_{\alpha,\beta,i,t}^{IN}$ of natural gas by NGG-P2G units in DA and RT markets. Because the actual power $P_{\alpha,\beta,c,t}^{CO}$ is usually deviated from the scheduled power output $P_{c,t}^{CO,DA}$ in DA market, the coordinated WPPs and NGG-P2G supplier needs to buy deficit or sell surplus power $P_{\alpha,\beta,c,t}^{CO,RT}$ in RT market to compensate the power deviation in DA market, and hence $P_{\alpha,\beta,c,t}^{CO,RT}$ could be positive or negative. The third term $(\lambda_{reg,i,t}^{IN,up}\cdot P_{reg,i,t}^{IN,up}+\lambda_{reg,i,t}^{IN,dn}\cdot P_{reg,i,t}^{IN,dn})$ is the revenue of NGG-P2G units for providing auxiliary services in RT market. The model uncertainties pertain to φ_α^{RT} in (4.1) and $P_{\beta,\omega,t}^{Wind,max}$ in (4.1.4), in which α and β are indexes of scenarios for RT market prices and WPP output separately. The upper-level constraints include (4.1.1)-(4.1.20) as listed below.

(1) Generation constraints for the coordinated WPPs and NGG-P2G units

$$P_{c,t}^{CO,DA}=P_{\omega,t}^{Wind,DA}+P_{i,t}^{IN,DA},\ \ \forall t \tag{4.1.1}$$

$$P_{\alpha,\beta,c,t}^{CO,RT}=P_{\alpha,\beta,\omega,t}^{Wind,RT}+P_{\alpha,\beta,i,t}^{IN,RT},\ \ \forall\alpha,\beta,t \tag{4.1.2}$$

$$-P_{limit}^{CO,RT} \le P_{\alpha,\beta,c,t}^{CO,RT} \le P_{limit}^{CO,RT}, \forall c, t \tag{4.1.3}$$

Constraints (4.1.1)-(4.1.2) state the power relationship among coordinated WPPs, NGG-P2G suppliers in DA and RT markets, respectively. Constraint (4.1.3) constrains coordinated supplier trading in RT market.

(2) WPP constraints

$$P_{\omega,t}^{Wind,DA} + P_{\alpha,\beta,\omega,t}^{Wind,RT} \le P_{\beta,\omega,t}^{Wind,max}, \forall \alpha, \beta, \omega, t \tag{4.1.4}$$

$$P_{\omega,t}^{Wind,DA} \ge 0, \quad \forall \omega, t \tag{4.1.5}$$

Constraint (4.1.4) limits the sum of the scheduled WPP output in DA market and the power output in RT market. (4.1.5) defines the nonnegativity of the scheduled WPP output in DA market.

(3) Constraints of the integrated NGG-P2G unit

$$P_{i,t}^{IN,DA} + P_{\alpha,\beta,i,t}^{IN,RT} = P_{\alpha,\beta,i,t}^{IN}, \forall \alpha, \beta, i, t \tag{4.1.6}$$

$$P_{\alpha,\beta,i,t}^{IN} \le P_i^{IN,max}, \forall \alpha, \beta, i, t \tag{4.1.7}$$

$$P_{i,t}^{IN,DA} = P_{i,t}^{NGG,DA} - P_{i,t}^{P2G,DA}, \forall i, t \tag{4.1.8}$$

$$U_{i,t} + V_{i,t} \le 1, \forall i, t \tag{4.1.9}$$

$$V_{i,t} \cdot P_i^{P2G,min} \le P_{i,t}^{P2G,DA} \le V_{i,t} \cdot P_i^{P2G,max}, \forall i, t \tag{4.1.10}$$

$$U_{i,t} \cdot P_i^{NGG,min} \le P_{i,t}^{NGG,DA} \le U_{i,t} \cdot P_i^{NGG,max}, \forall i, t \tag{4.1.11}$$

$$P_{\alpha,\beta,i,t}^{IN,RT} = P_{\alpha,\beta,i,t}^{IN,up} - P_{\alpha,\beta,i,t}^{IN,dn}, \forall \alpha, \beta, i, t \tag{4.1.12}$$

$$P_{\alpha,\beta,i,t}^{IN,up} = P_{\alpha,\beta,i,t}^{NGG,up} + P_{\alpha,\beta,i,t}^{P2G,up}, \forall \alpha, \beta, i, t \tag{4.1.13}$$

$$P_{\alpha,\beta,i,t}^{IN,dn} = P_{\alpha,\beta,i,t}^{NGG,dn} + P_{\alpha,\beta,i,t}^{P2G,dn}, \forall \alpha, \beta, i, t \tag{4.1.14}$$

$$P_{\alpha,\beta,i,t}^{P2G} = P_{i,t}^{P2G,DA} - P_{\alpha,\beta,i,t}^{P2G,up} + P_{\alpha,\beta,i,t}^{P2G,dn}, \forall \alpha, \beta, i, t \tag{4.1.15}$$

$$P_{\alpha,\beta,i,t}^{NGG} = P_{i,t}^{NGG,DA} + P_{\alpha,\beta,i,t}^{NGG,up} - P_{\alpha,\beta,i,t}^{NGG,dn}, \forall \alpha, \beta, i, t \tag{4.1.16}$$

$$0 \le P_{\alpha,\beta,i,t}^{P2G,dn} \le V_{i,t} \cdot P_i^{P2G,max} - P_{i,t}^{P2G,DA}, \forall \alpha, \beta, i, t \tag{4.1.17}$$

$$0 \le P_{\alpha,\beta,i,t}^{P2G,up} \le P_{i,t}^{P2G,DA} - V_{i,t} \cdot P_i^{P2G,min}, \forall \alpha, \beta, i, t \tag{4.1.18}$$

$$0 \le P_{\alpha,\beta,i,t}^{NGG,up} \le U_{i,t} \cdot P_i^{NGG,max} - P_{i,t}^{NGG,DA}, \forall \alpha, \beta, i, t \quad (4.1.19)$$

$$0 \le P_{\alpha,\beta,i,t}^{NGG,dn} \le P_{i,t}^{NGG,DA} - U_{i,t} \cdot P_i^{NGG,min}, \forall \alpha, \beta, i, t \quad (4.1.20)$$

Constraints (4.1.6)-(4.1.7) state bounds of total power output of the integrated NGG-P2G in DA and RT markets. Equation (4.1.8) shows the NGG-P2G scheduled power output in DA market is equal to the power provided by NGG minus power consumed by P2G. Besides, $U_{i,t}$ and $V_{i,t}$ are binary variables as in (4.1.9) and inequalities (4.1.10)-(4.1.11) are used to constrain $P_{i,t}^{P2G,DA}$, $P_{i,t}^{NGG,DA}$ respectively. Note that the lower limits of $P_{i,t}^{P2G,DA}$ and $P_{i,t}^{NGG,DA}$ are nonzero. This is because the integrated NGG-P2G facility is coordinated with WPP to provide power in due time, while using surplus wind energy to supply NGLs or be stored as storage natural gas when power offer is relatively low. Equation (4.1.12) shows the relationship between power production or consumption in RT market and the up and down auxiliary power of the integrated NGG-P2G. Constraints (4.1.13) and (4.1.14) calculate the power up and down auxiliary services of the integrated NGG-P2G, respectively. The total NGG and P2G power generation in DA and RT markets is calculated in (4.1.15) and (4.1.16), respectively, which are used in the LL to constrain natural gas network. The limits for the auxiliary power of NGG-P2G are shown in (4.1.17)-(4.1.20). The optimization variables of the UL problem are the variables in the set Δ^{UL} ={ $\varphi_{n,t}$, $P_{c,t}^{CO,DA}$, $P_{\omega,t}^{Wind,DA}$, $P_{i,t}^{IN,DA}$, $P_{\alpha,\beta,c,t}^{CO,RT}$, $P_{\alpha,\beta,\omega,t}^{Wind,RT}$, $P_{\alpha,\beta,i,t}^{IN,RT}$, $P_{\alpha,\beta,i,t}^{IN}$, $P_{reg,i,t}^{IN,up}$, $P_{reg,i,t}^{IN,dn}$, $P_{i,t}^{NGG,DA}$, $P_{i,t}^{P2G,DA}$, $P_{\alpha,\beta,i,t}^{NGG,up}$, $P_{\alpha,\beta,i,t}^{P2G,up}$, $P_{\alpha,\beta,i,t}^{NGG,dn}$, $P_{\alpha,\beta,i,t}^{P2G,dn}$}.

4.3.2. Lower-Level model

At the lower level, the ISO collects offers from all market participants and then completes market clearing with the traditional optimal power flow to maximize the overall social welfare. As a result, the objective in the lower level could be described by the revenues of selling power to loads $\lambda_{le}^{Int,DA} \cdot P_{le,t}^{Int,DA} + \lambda_{let}^{et,\mathrm{DA}} \cdot P_{let,t}^{et,\mathrm{DA}}$ minus costs of buying power from suppliers $\lambda_s^{S,DA} \cdot P_{s,t}^{S,DA}$, $\lambda_b^{B,DA} \cdot P_{b,t}^{B,DA}$ and $\lambda_{c,t}^{CO,\mathrm{bid}} \cdot$

$P_{c,t}^{CO,\mathrm{DA}}$, and the constraints include (4.2.1)-(4.2.20).

Maximize

$$\sum_{t\in T}\Big(\sum_{le\in\Omega_n^{Le}}\lambda_{le}^{Int,DA}\cdot P_{le,t}^{Int,DA}+\sum_{let\in\Omega_n^{Let}}\lambda_{let}^{et,DA}\cdot P_{let,t}^{et,\mathrm{DA}}- \tag{4.2}$$

$$\sum_{s\in\Omega_n^{S}}\lambda_{s}^{S,DA}\cdot P_{s,t}^{S,DA}-\sum_{b\in\Omega_n^{B}}\lambda_{b}^{B,DA}\cdot P_{b,t}^{B,DA}-\sum_{c\in\Omega_n^{C}}\lambda_{c,t}^{CO,\mathrm{bid}}\cdot P_{c,t}^{CO,\mathrm{DA}}\Big)$$

(1) Generation constraints for the coordinated WPPs and NGG-P2G supplier, PV, BESS and loads

$$\lambda_{c,t}^{CO,bid}\geq 0,\forall c,t \tag{4.2.1}$$

$$0\leq P_{c,t}^{CO,DA}\leq P_{c,t}^{CO,bid}:\mu_{c,t}^{L},\mu_{c,t}^{U},\forall c,t \tag{4.2.2}$$

$$0\leq P_{s,t}^{S,DA}\leq P_{s}^{max}:\mu_{s,t}^{L,DA},\mu_{s,t}^{U,DA},\forall s,t \tag{4.2.3}$$

$$0\leq P_{b,t}^{B,DA}\leq P_{b}^{max}:\mu_{b,t}^{L,DA},\mu_{b,t}^{U,DA},\forall b,t \tag{4.2.4}$$

$$0\leq P_{le,t}^{Int,DA}\leq P_{le}^{Int,max}:\mu_{le,t}^{int,L,DA},\mu_{le,t}^{int,U,DA},\forall le,t \tag{4.2.5}$$

The first constraint (4.2.1) defines the offer price of the coordinated supplier in DA market is nonnegative. Maximum and minimum production constraints of the coordinated WPPs and NGG-P2G supplier, PV unit, BESS unit, and the IEL are shown in (4.2.2)-(4.2.5) individually.

(2) Electricity network constraints

$$\begin{aligned}P_{s,t}^{S,DA}+P_{b,t}^{B,DA}+P_{c,t}^{CO,DA}-\sum_{m\in\Omega_n^{N}}B_{nm}\cdot(\theta_{n,t}^{DA}-\theta_{m,t}^{DA})\\ =P_{le,t}^{Int,DA}+P_{let,t}^{et,\mathrm{DA}}:\varphi_{n,t},\forall n,t\end{aligned} \tag{4.2.6}$$

$$\begin{aligned}-f_{nm}^{max}\leq B_{nm}\cdot\left(\theta_{n,t}^{DA}-\theta_{m,t}^{DA}\right)\\ \leq f_{nm}^{max}:\mu_{nm,t}^{L,DA},\mu_{nm,t}^{U,DA},\forall m,n\in\Omega_n^{N},t\end{aligned} \tag{4.2.7}$$

$$\theta_{n,t}^{DA}=0:\mu_{\theta,t}^{DA},n:ref,\forall t \tag{4.2.8}$$

$$-\pi\leq\theta_{n,t}^{DA}\leq\pi:\mu_{\theta,t}^{L,DA},\mu_{\theta,t}^{U,DA},\forall n\backslash n:ref,\forall t \tag{4.2.9}$$

Equation (4.2.6) enforces the power balance between nodal supply and demand,

which is associated with a dual variable $\varphi_{n,t}$ to donate the LMP used in the upper-level. Inequality (4.2.7) limits the power flow in each transmission line. Equation (4.2.8) sets the voltage angle at the reference bus and inequality (4.2.9) is voltage angle limit. Additionally, $\mu_{c,t}^{L}, \mu_{c,t}^{U}, \mu_{s,t}^{L,DA}, \mu_{s,t}^{U,DA}, \mu_{b,t}^{L,DA}, \mu_{b,t}^{U,DA}, \mu_{le,t}^{int,L,DA}, \mu_{le,t}^{int,U,DA}, \varphi_{n,t}, \mu_{nm,t}^{L,DA}$, $\mu_{nm,t}^{U,DA}, \mu_{\theta,t}^{DA}, \mu_{\theta,t}^{L,DA}, \mu_{\theta,t}^{U,DA}$ are dual variables for (4.2.2) to (4.2.9).

(3) Natural gas network constraints

$$S_{\alpha,\beta,t}^{STR} = S_{\alpha,\beta,t-1}^{STR} + \sum_{qp\in\Omega^{T}} P_{qp,t}^{Gasflow}, \quad \forall\alpha,\beta,t \tag{4.2.10}$$

$$S^{STR,min} \le S_{\alpha,\beta,t}^{STR} \le S^{STR,max}, \quad \forall\alpha,\beta,t \tag{4.2.11}$$

$$P_{\alpha,\beta,i,t}^{IN,gas} + P_{g,t}^{Gaswell} - \sum_{p\in\Omega_q^{Q}} P_{qp,t}^{Gasflow} = P_{lg,t}^{Gas} + P_{lgt,t}^{GTL}, \quad \forall q,t \tag{4.2.12}$$

$$P_{\alpha,\beta,i,t}^{IN,gas} = P_{\alpha,\beta,i,t}^{P2G} \cdot \gamma_{P2G} - P_{\alpha,\beta,i,t}^{NGG}/\gamma_{NGG}, \forall\alpha,\beta,i,t \tag{4.2.13}$$

$$0 \le P_{g,t}^{Gaswell} \le P_{g}^{Gw,max}, \forall g,t \tag{4.2.14}$$

$$P_{qp,t}^{Gasflow} = sgn(\pi_{q,t},\pi_{p,t}) \cdot \sigma_{qp} \cdot \sqrt{\left|\pi_{q,t}^{2} - \pi_{p,t}^{2}\right|}, \forall p,q \in \Omega_q^{Q}, t \tag{4.2.15}$$

$$sgn(\pi_{q,t},\pi_{p,t}) = \begin{cases} 1; if \pi_{q,t} \gg \pi_{p,t} \\ -1; if \pi_{q,t} < \pi_{p,t} \end{cases}, \forall p \in \Omega_q^{Q}, t \tag{4.2.16}$$

$$P_{qp,t}^{Gasflow} \le P_{qp}^{gasflow,max}, \forall qp \in \Omega^{T}, dt \tag{4.2.17}$$

$$\pi_{q,t} \le \Gamma_{qp} * \pi_{p,t}, \quad \Gamma_{qp} > 1 \tag{4.2.18}$$

$$\sum_{lgt\in\Omega_q^{Lgt}} P_{lgt,t}^{GTL} + \sum_{let\in\Omega_n^{Let}} P_{let,t}^{et,DA} = P^{The}, \forall t \tag{4.2.19}$$

$$\sum_{lgt\in\Omega_q^{Lgt}} P_{lgt,t}^{GTL} \ge P^{The,min}, \forall lgt,t \tag{4.2.20}$$

Equation (4.2.10) defines the pressurized gas stored in natural gas pipelines which is constrained in (4.2.11). Equation (4.2.12) is the gas balance between supply and demand in the natural gas network for node q. Equation (4.2.13) shows that the integrated NGG-P2G scheduled natural gas output is equal to the energy provided by

P2G minus the energy consumed in NGG. Inequality (4.2.14) limits the gas well quantity. The steady state gas flow is modeled by the Weymouth's formula and represented as (4.2.15)-(4.2.16), in which the gas flow direction $sgn(\pi_{q,t}, \pi_{p,t})$ depends on nodal pressure differences [119]. It is noted that these nonlinear constraints (4.2.15)-(4.2.16) are linearized by the first-order Taylor series approximation [120] to make the proposed model computationally tractable. Inequality (4.2.17) represents the pipeline flow limit in natural gas network. The natural gas compressor is modeled as (4.2.18) [119]. Equation (4.2.19) shows thermal loads supplied by electricity or natural gas. Constraint (4.2.20) is the gas quantity limit for the gas thermal unit. The optimization variables of the LL problem are the variables in the set $\Delta^{LL} = \{ P_{le,t}^{Int,DA}, P_{let,t}^{et,\mathrm{DA}}, P_{s,t}^{S,DA}, P_{b,t}^{B,DA}, P_{c,t}^{CO,\mathrm{DA}}, \lambda_{c,t}^{CO,bid}, \theta_{n,t}^{DA}, S_{\alpha,\beta,t}^{STR}, P_{g,t}^{Gaswell}, P_{qp,t}^{Gasflow}, P_{lgt,t}^{GTL}, P_{\alpha,\beta,i,t}^{P2G}, P_{\alpha,\beta,i,t}^{NGG}, P_{g,t}^{Gas\mathrm{well}} \}$. The optimal bidding strategy can be obtained through solving the proposed bi-level model with the approaches (2.1a)-(2.9d) in Section 2.2, which is the same as the solution methodology in Chapter III. The specific formula transformations from a bi-level problem to a single-level MILP are listed in the Appendix.

4.4 Case Studies

Experiment Setting

The proposed model is tested on an IEEE 6-bus electric system with a 7-node natural gas network and an IEEE 30-bus electric system with a 14-node natural gas network for 24 hours with a 1 hour resolution. 1000 scenarios are first generated [121] respectively for RT market electricity prices and WPP outputs, which are separately derived from the price data in [94] and wind data in [115]. The scenarios are then reduced to 10 through the scenario-reduction algorithm as in Figs. 4.2 and 4.3, with scenario probabilities listed in Table 4.1. The gas price is 8.37$/MWh for 24 hours. Parameters of the integrated NGG-P2G unit are listed in Table 4.2. The rated power of PV unit and BESS is 100MW and 140MW respectively, while NGLs, maximum IELs,

and maximum thermal loads would change over time as shown in Tables 4.3 to 4.5. Offer prices for non-strategic participants including the PV unit, BESS, IEL and ETL, and prices of up/down power regulations are presented in Fig. 4.4.

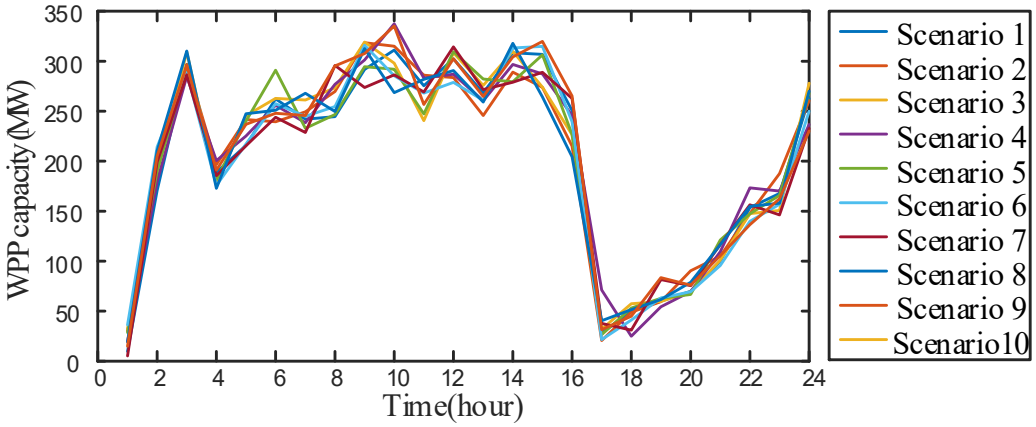

Fig. 4.2 Scenarios for WPP output

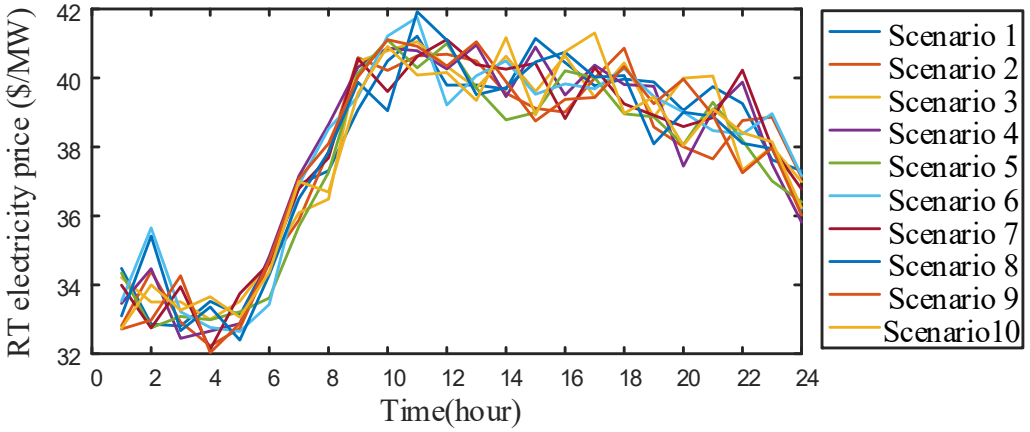

Fig. 4.3 Scenarios for RT electricity prices

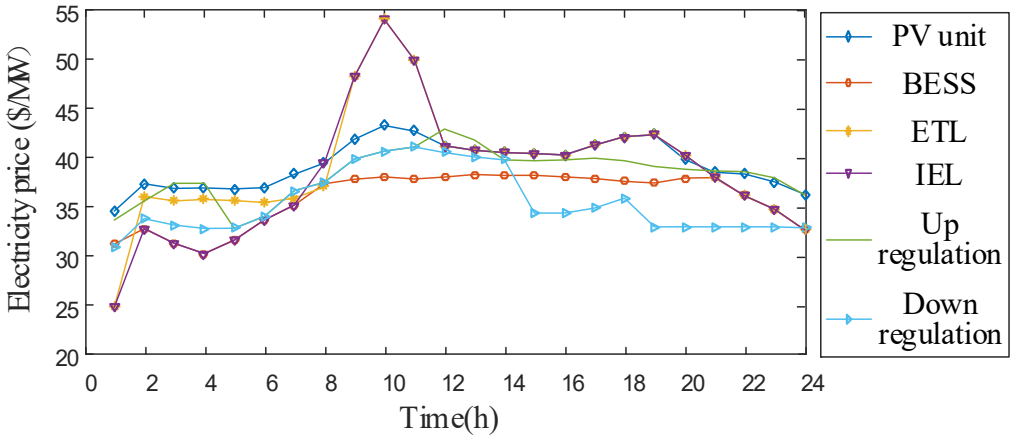

Fig. 4.4 Bid prices of non-strategic participants of DA market and prices of up and down regulation

Table 4.1 Probabilities for scenarios of the WPP output and RT market prices

Sce	1	2	3	4	5	6	7	8	9	10
τ_β	0.167	0.153	0.121	0.068	0.105	0.082	0.080	0.072	0.062	0.089
τ_α	0.122	0.132	0.096	0.105	0.109	0.082	0.094	0.077	0.119	0.064

Table 4.2 Parameters of the integrated NGG-P2G unit

λ_{gas} ($/MWh)	$\gamma_{NGG}/\gamma_{P2G}$	$P_i^{IN,max}$ (MW)	$P_i^{NGG,max}$ (MW)	$P_i^{P2G,max}$ (MW)	$P_l^{Int,max}$ (MW)
8.37	0.8/0.5	100	100	100	100
$P_g^{Gaswell,max}$ (MW)	$S_i^{STR,ini}$ (MWh)	$S_i^{STR,min}$ (MWh)	$S_i^{STR,max}$ (MWh)	$P_{pq}^{gasflow,max}$ (MW)	$P_{gl}^{Thermal,min}$ (MW)
100	25	0	100	150	10

Table 4.3 Maximum power consumption of each IEL in 24 hours

Hour	load (MW)	Hour	load (MW)	Hour	load (MW)	Hour	load (MW)
1	87.60	7	86.70	13	121.09	19	122.99
2	82.58	8	95.20	14	121.80	20	118.68
3	79.34	9	102.78	15	124.43	21	118.66
4	77.37	10	108.60	16	127.90	22	113.57
5	77.53	11	114.31	17	128.00	23	100.53
6	80.24	12	118.05	18	123.37	24	98.38

Table 4.4 Power consumption of each NGL in 24 hours

Hour	Load (MW)	Hour	Load (MW)	Hour	Load (MW)	Hour	Load (MW)
1	73.92	7	79.02	13	84.96	19	92.61
2	69.67	8	85.81	14	80.71	20	96.00
3	66.27	9	87.51	15	81.56	21	94.31
4	67.12	10	89.78	16	83.26	22	92.61
5	58.06	11	86.66	17	85.81	23	85.81
6	79.85	12	86.66	18	88.36	24	78.17

Table 4.5 Hourly total thermal consumption of EILs and GTLs

Hour	Load (MW)	Hour	Load (MW)	Hour	Load (MW)	Hour	Load (MW)
1	24.90	7	21.81	13	27.60	19	22.35
2	23.10	8	24.90	14	27.00	20	22.41
3	22.20	9	26.70	15	24.00	21	30.00
4	21.90	10	27.30	16	22.50	22	29.40
5	21.60	11	28.20	17	22.20	23	27.60
6	21.75	12	28.35	18	21.90	24	27.30

4.4.1 Six-Bus System

The proposed model is first tested on an IEEE 6-bus electric power system coupled with a 7-node natural gas network by the integrated NGG-P2G unit as shown in Fig. 4.5. In the electric power network, PV unit and BESS are located at buses 1 and 6, respectively, while two IELs are connected at buses 3-4 and an ETL is connected at bus 5. The coordinated WPP and NGG-P2G supplier as strategic partners are deployed at bus 5. In the natural gas network, the connections include an integrated NGG-P2G at node 1, a gas well at node 7, a compressor between nodes 2 and 4, and a NGL and a GTL at nodes 3 and 5, respectively.

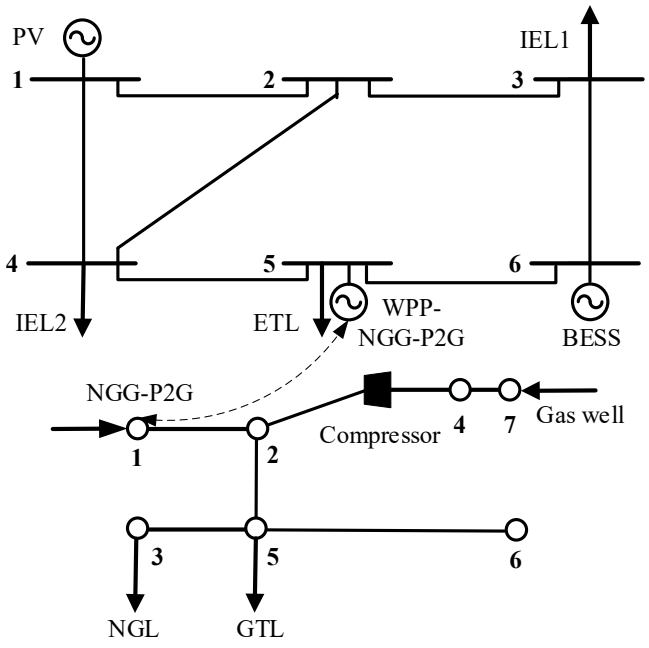

Fig. 4.5 The 6-bus power system with a 7-node gas network

Fig. 4.6 shows scheduled power of all market participants in VMP. The scheduled power output of the coordinated WPP and NGG-P2G supplier $P_{c,t}^{CO,DA}$ is equal to its offered power $P_{c,t}^{CO,\text{bid}}$ during 24 hours. In addition, the offered power of the coordinated WPP and NGG-P2G supplier can cover all loads including IELs and ETL in the first 16 hours and last three hours. While the offered power of the coordinated WPP and NGG-P2G supplier is significantly smaller than the total load during the remaining hours 17-21, where the deficient power is supplied by non-strategic BESS and PV unit. The schedule is optimized to avoid buying power at a high price in RT market for supplementing the coordinated WPP and NGG-P2G supplier. In this case, the WPP output which accounts for a large proportion in the total capacity of the coordinated WPP and NGG-P2G supplier is dramatically low while RT electricity price is relatively high during hours 17 and 21 as depicted in Figs. 4.2 and 4.3, respectively.

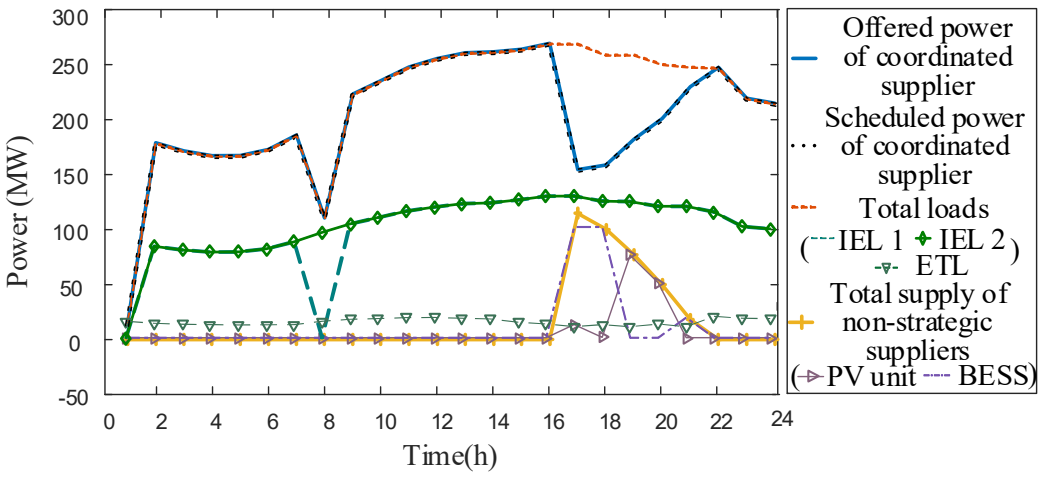

Fig. 4.6 Scheduled power of market participants in 6-bus system

The proposed schedule satisfies the coordinated WPP and NGG-P2G supplier constraints. In addition, the offered power of the coordinated WPP and NGG-P2G supplier $P_{c,t}^{CO,\text{bid}}$ is less than the scheduled WPP output $P_{\omega,t}^{Wind,DA}$ and the total generating capacity $P_{\beta,\omega,t}^{Wind,max} + P_i^{IN,max}$ (indicated by scenarios 1 to 10) at hours 1-15 and 24 in Fig. 4.7. During this period, offered power can satisfy load requirements as shown in Fig. 4.6. Thus, the surplus wind energy between $P_{\omega,t}^{Wind,DA}$ and $P_{c,t}^{CO,\text{bid}}$ would be used by the P2G facility for storage in the natural gas network to avoid wind

energy curtailments. From hours 16-23, the offered power of the coordinated WPP and NGG-P2G supplier is approximately equal to the total power generating capacity, which is slightly larger than the scheduled WPP output as shown in Fig. 4.7. Here, NGG unit is coordinated with WPP and utilizes the energy in the natural gas network to satisfy the offered power of the coordinated WPP and NGG-P2G supplier $P_{c,t}^{CO,\text{bid}}$. Based on these distinguished behaviors of P2G and NGG during hours 16-23 and the rest hours, it is noted that P2G and NGG are coordinated with WPP to well explore the synergy between WPP and NGG-P2G unit.

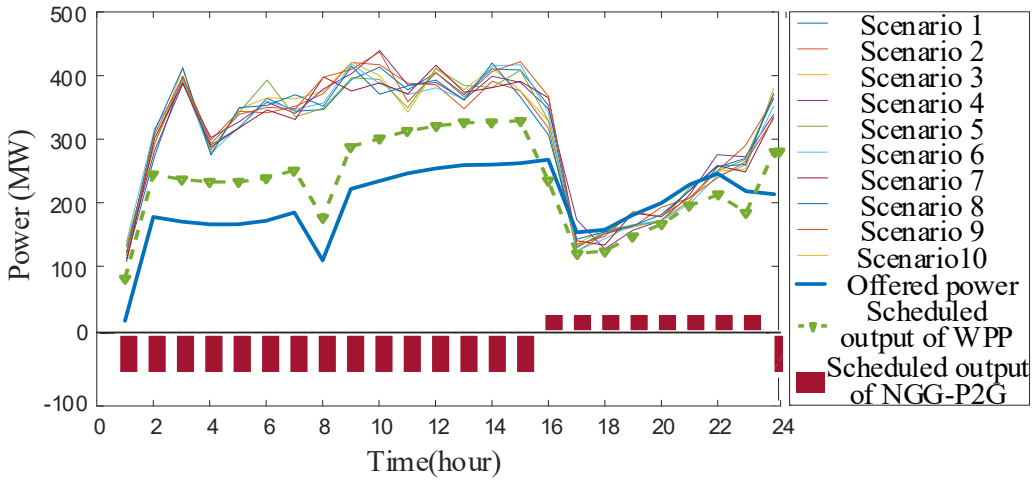

Fig. 4.7 Total power output scenarios, offered power of the coordinated WPP and NGG-P2G supplier, scheduled output of WPP and NGG-P2G unit in 6-bus system

Additionally, the clearing LMP is kept lower than the RT electricity price throughout the 24 hours in Fig. 4.8. As the total power generating capacity of the coordinated supplier is larger than its offered power before hours 16 and 23-24 in Fig. 4.7, the coordinated supplier can sell its surplus in RT market at higher prices for making payoff. The offered power by the coordinated supplier is approximately equal to the total power generating capacity during hours 16 and 22 as depicted in Fig. 4.7. Hence, the coordinated supplier would only buy a small amount of deficiency at a higher price in RT market when the actual output of the coordinated supplier is lower than its scheduled outputs, which helps improve the coordinated supplier's payoff. These results indicate that the large-scale coordinated supplier can strategically affect

LMPs in DA market, in which the NGG is coordinated with WPP to provide more electricity by consuming natural gas at hours with high offered power, while the P2G unit is coordinated with WPP to store surplus wind energy in the natural gas network at hours with low offered power. Table 4.6 shows payoffs of the coordinated supplier,

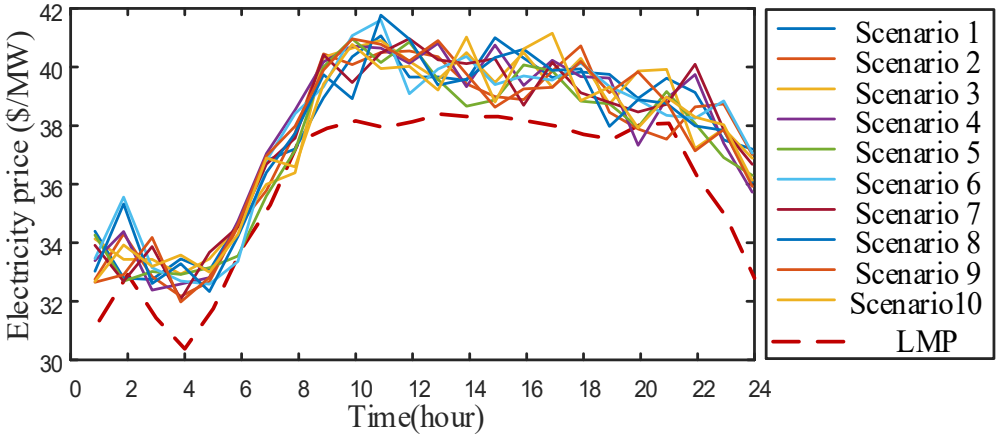

Fig. 4.8 LMPs and RT electricity price scenarios in 6-bus system

WPP, and NGG-P2G unit obtained in DA market, RT market and auxiliary services. Most of the payoff is provided by the WPP in DA market, which is due to the strategic bidding of the coordinated supplier in DA market. The WPP accounts for a large proportion in the total capacity of the coordinated WPP and NGG-P2G supplier. The payoff is also obtained in RT market because a small difference between scheduled and actual power output of the coordinated WPP and NGG-P2G supplier is traded in this market. In addition, the energy arbitrage for the provision of auxiliary services is attributed to the integrated NGG-P2G unit.

Table 4.6 Payoff ($) of the coordinated WPP and NGG-P2G supplier in 6-bus system

Market	WPP	NGG-P2G	Coordinated WPP and NGG-P2G supplier
DA	2.01×10^5	-2.10×10^4	1.80×10^5
RT	-2.84×10^3	3.64×10^3	0.8×10^3
Auxiliary	0	8.77×10^4	$8.77e\times10^4$
Total	1.99×10^5	7.03×10^4	2.69×10^5

Comparison: The proposed model is compared to other models with strategic

suppliers represented by WPP, coordinated WPP-NGG unit, coordinated WPP-P2G unit, and coordinated WPP-EV aggregator in Chapter III [84]. In Table 4.7, the payoff of the proposed model is higher than those of WPP, coordinated WPP-NGG unit, or coordinated WPP-P2G unit. The proposed model offers a higher payoff because the NGG-P2G unit mitigates WPP variations using a flexible energy flow between power and gas systems. The proposed solution stores natural gas with P2G at low bid hours, generates electricity by the stored gas via NGG during high bid hours, and provides energy arbitrage for auxiliary services of NGG-P2G. Compared to the coordinated WPP-EV aggregator presented in Chapter III, which considered the power generation cost of EV aggregator and battery degradation cost, the proposed model also earns more payoffs as the generation per unit cost of natural gas is lower than that of EV aggregator, and the former is not involved with the battery degradation cost either.

Table 4.7 Payoff ($) of the proposed model and four other models in 6-bus system

Market	Proposed model	WPP	WPP-P2G	WPP-NGG	WPP-EV
DA	$1.80e\times10^5$	$1.79e\times10^5$	1.64×10^5	1.69×10^5	1.69×10^5
RT	799.00	-537.47	-2.69×10^3	3.42×10^3	3.94×10^4
Auxiliary	8.77×10^4	0	8.89×10^4	5.35×10^4	0
Total	2.69×10^5	1.78×10^5	2.51×10^5	2.26×10^5	2.08×10^5

4.4.2 Thirty-Bus System

The merits of the proposed model are further demonstrated by a modified IEEE 30-bus power system with 14-node gas network as shown in Fig. 4.9.

The electric power network includes a coordinated WPPs and NGG-P2G supplier located at bus 21, 41 branches, 5 PV units, 5 BESSs, 10 IELs and 3 ETLs. The natural gas network includes 2 gas wells, 2 compressors, 14 pipelines, 5 NGLs and 3 GTLs. The capacities of PV unit, BESS, IEL and NGL are 1/5 of those in Case 1, while the total thermal load is the same as in Case 1.

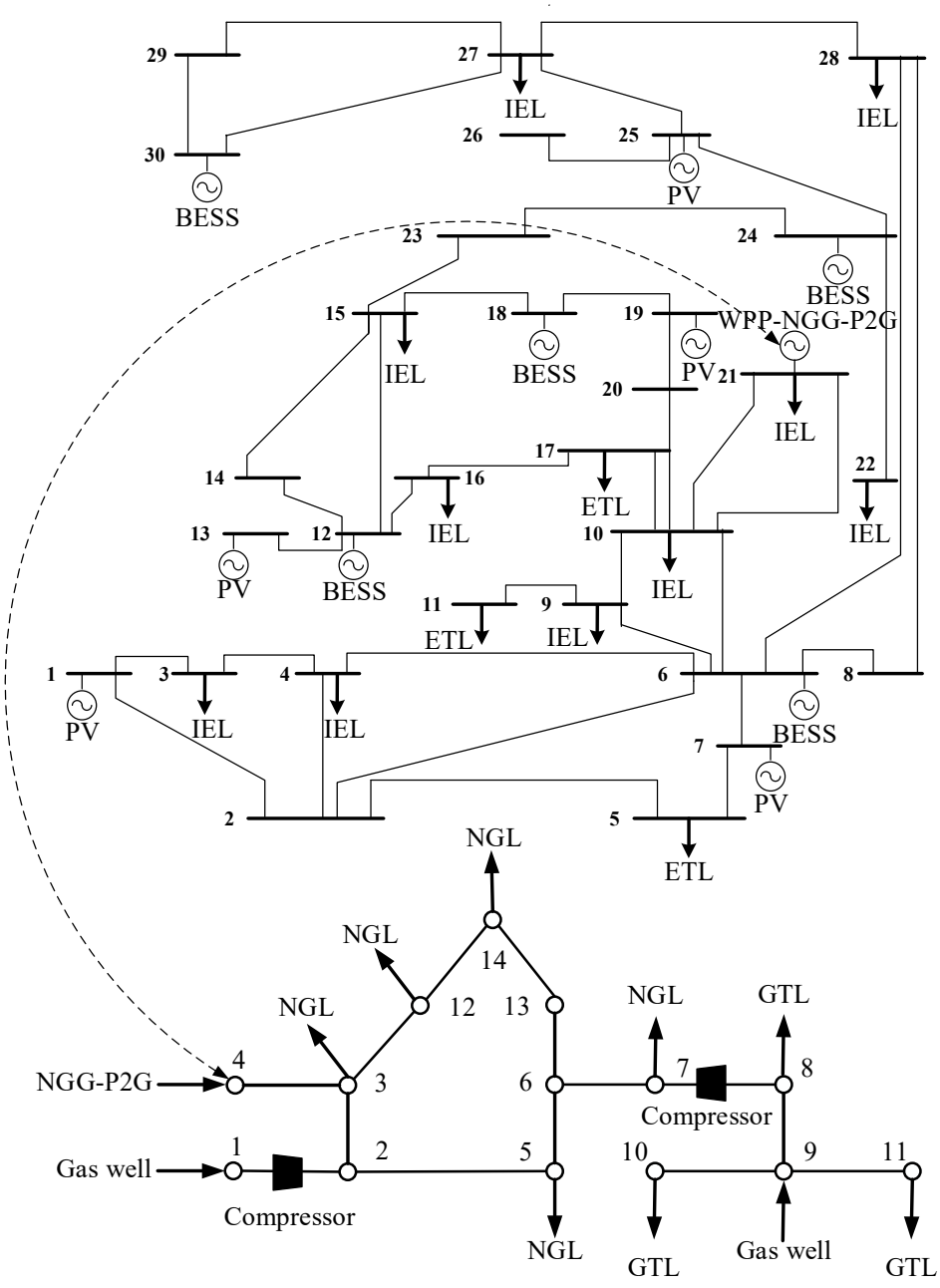

Fig. 4.9 The 30-bus power system with a 14-node gas network

Fig. 4.10 shows the offered power of the coordinated WPP and NGG-P2G supplier (i.e., strategic participants), total load and total power generation of non-strategic participants. The coordinated WPP and NGG-P2G supplier can fully supply the total load during hours 1-16 and 22-24, whereas partial load is supplied during hours 17-21. The WPP output is very low and RT prices are relatively high during hours 17-21 as shown in Figs. 4.2 and 4.3. Accordingly, if the coordinated WPP and NGG-P2G supplier tries to support all loads during hours 17- 21, it would have to buy power at

high prices in RT market which would lower its payoff. As a result, the offered power of the coordinated supplier is relatively low during hours 17-21.

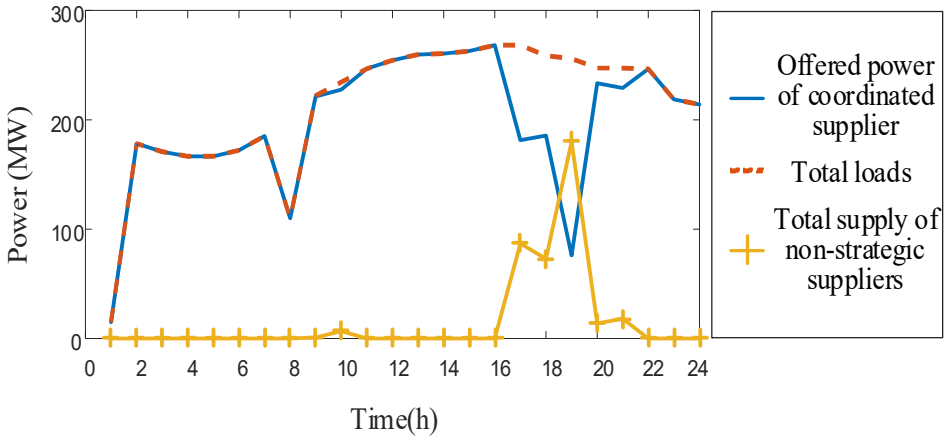

Fig. 4.10 Scheduled power of market participants in 30-bus system

The scheduled output of WPP and NGG-P2G, offered power of the coordinated WPP and NGG-P2G supplier in DA market, and 10 scenarios of total power generating capacity of WPP and NGG-P2G are represented in Fig. 4.11. The integrated NGG-P2G unit is coordinated with WPP to provide power when the offered power of the coordinated WPP and NGG-P2G supplier is high. The coordination consumes the surplus WPP energy to supply NGLs when offered power of the coordinated supplier is low.

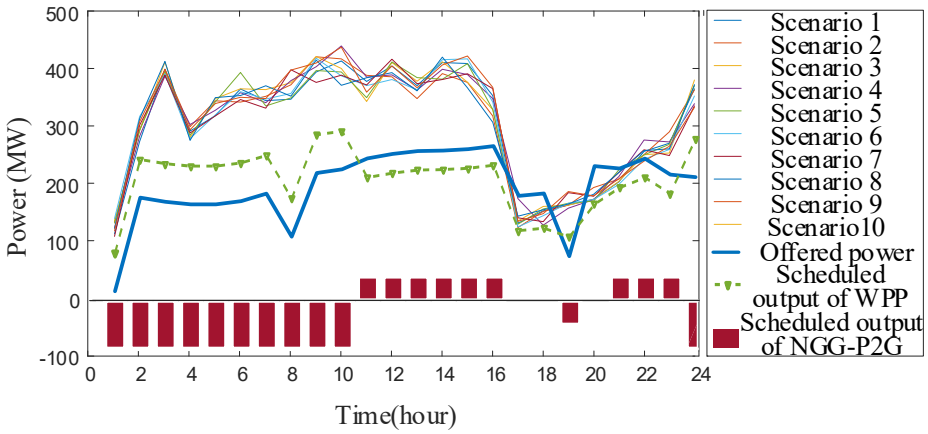

Fig. 4.11 Total power output capacity scenarios, offered power of the coordinated supplier, scheduled output of WPP and NGG-P2G unit in 30-bus system

Fig. 4.12 represents LMPs and the scenarios of RT electricity prices. During the hours 1-15 and 24, the total power generation of WPP and NGG-P2G unit is large enough to satisfy the offered power of the coordinated WPP and NGG-P2G supplier as depicted in Fig. 4.11. Here, LMPs are lower than RT electricity prices in Fig. 4.12, in which the coordinated WPP and NGG-P2G supplier could sell its surplus power at a higher price in RT market for earning higher payoffs. In addition, the NGG-P2G unit increases the offered power of the coordinated WPP and NGG-P2G supplier, which is approximately equal to the total power generation and increases payoffs during the hours 16-23 as shown in Fig. 4.11. In this case, a small amount of power is purchased at higher RT prices (see Fig. 4.12) once the actual power production of the coordinated supplier is less than its offered power. The effect of bidding behavior of the coordinated WPP and NGG-P2G supplier on LMPs shows that the large-scale WPP can be coordinated with the integrated NGG-P2G unit to be a price-maker in DA market.

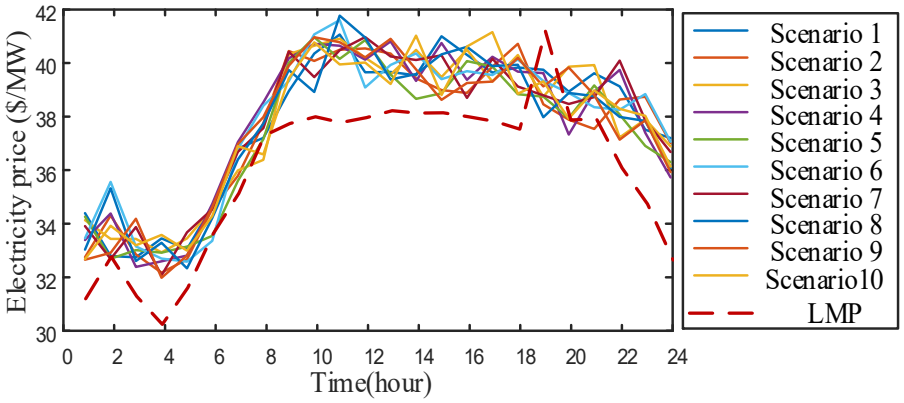

Fig. 4.12 Clearing LMPs and RT electricity price scenarios in 30-bus system

Table 4.8 shows payoffs of WPP, NGG-P2G and the coordinated supplier in DA and RT markets and auxiliary services, in which WPP gets most of payoff for the coordinated WPP and NGG-P2G supplier, and the NGG-P2G unit provides payoff by providing auxiliary services. Table 4.9 lists the payoff of the proposed coordinated WPP and NGG-P2G model and other four models, which shows the proposed model gains a higher payoff than the others because of the flexibility offered by the coordination of NGG-P2G and WPP

Table 4.8 Payoff ($) of the coordinated WPP and NGG-P2G supplier in 30-bus System

Market	WPP	P2G-G2P	Coordinated supplier
DA	1.72×10^5	-3.88×10^3	1.68×10^5
RT	-541.72	2.42×10^3	1.88×10^3
Auxiliary	0	8.49×10^4	8.49×10^4
Total	1.72×10^5	8.34×10^4	2.55×10^5

Table 4.9 Payoff ($) of the proposed model and four other models in 30-bus System

Market	Proposed model	WPP	WPP-P2G	WPP-NGG	WPP-EV
DA	1.68×10^5	1.98×10^5	1.63×10^5	1.58×10^5	1.98×10^5
RT	916.65	-2.53×10^3	-2.28×10^3	4.71×10^3	3.63×10^4
Auxiliary	8.49×10^4	0	8.97×10^4	8.69×10^4	0
Total	2.55×10^5	1.95×10^5	2.50×10^5	2.49×10^5	2.35×10^5

4.5 Summary

A bi-level stochastic optimization model is proposed for the coordinated operation of WPPs and NGG-P2G suppliers, which are modeled as price-makers in DA market and price-takers in RT market. At the upper level, the payoff of coordinated WPP and NGG-P2G suppliers is maximized with the consideration of uncertainties of WPP power output and RT electricity price, while the social welfare of the overall system is maximized at the lower level. The promising results of the proposed model are validated in the following respects: 1) The large-scale WPP can cooperate with the integrated NGG-P2G unit in VMP for strategically bidding in DA market. 2) The proposed model provides an effective and coordinated operation of WPP and the NGG-P2G unit for earning higher payoffs. The uncertainties of WPP output are mitigated and wind power curtailments are reduced with flexible operations of NGG-P2G unit. 3) The payoff in the proposed model is mostly provided by the WPP in DA market, where the

integrated P2G-G2P unit enhances payoffs further by providing auxiliary services. 4) The proposed model provides higher payoffs compared with the other four models because of the flexible operation and auxiliary services offered by the NGG-P2G unit.

Chapter V

A Multi-agent Competitive Bidding Strategy in a Pool-Based Electricity Market with Price-Maker Participants of WPPs and EV Aggregators

5.1 Introduction

Although the cooperated model in Chapter III has improved the common interests of EVs and WPPs on account of their energy coordination during different time slots, it depends highly on the centralized control and scheduling of a central aggregator who owns lots of bidding information of EVs and WPPs. The communication requirement between the central agent with EVs and WPPs is high, the privacy of EVs and WPPs cannot be guaranteed, and WPPs and EV aggregators have little flexibility to cope with any self-decisions. So far, to the best of knowledge, there is little research considering the renewable WPPs and EV aggregators as oligopolists for developing a competitive multi-agent bidding strategy in a pool-based DA market without any information of opponents. Therefore, a new competitive DA market model for oligopoly players WPPs and EV aggregators making their own bidding decisions to increase their respective profits without sharing any personal data with each other is first proposed in this Chapter.

A bi-level multi-agent based model is proposed to study their bidding behaviors, with market clearing completion in the lower level and revenue maximization in the upper level. A stochastic framework is developed to incorporate the uncertainties in power production of WPPs and EV aggregators and bid prices of other participants. The process of bidding decision is formulated as a stochastic game with incomplete

information, in which electricity suppliers including WPPs and EV aggregators are considered as players of the game, their lack of information in this stochastic market environment is counterbalanced by a multi-agent reinforcement learning (MARL) algorithm named win or learn fast policy hill climbing (*WoLF-PHC*) with their own profits maximized by self-game. The feasibility and effectiveness of the proposed model and the *WoLF-PHC* solution approach are successfully illustrated using a modified IEEE 6-bus system and a modified 118-bus system with different numbers of market players.

The nomenclature of symbols used in this Chapter is given as follows.

Indices:

l	Index of loads
g	Index of traditional generators
e	Index of EV aggregators
ω	Index of WPPs
n	Index of nodes
$ă$	Index of scenarios
k	Index of iterations

Sets:

Ω_n^L	Set of all nodes with loads
Ω_n^G	Set of all nodes with traditional generators
Ω_n^E	Set of all nodes with EV aggregators
Ω_n^W	Set of all nodes with WPPs
$N_{ă}$	Set of all scenarios for stochastic optimization (including bid prices of traditional generators and loads as well as power production capacities of WPPs and EV aggregators)

Parameters:

P_g^{max}	Max power output of traditional generator g, in MW
$P_{\omega,ă,t}^{W,max}$	Max power production of WPP ω at time t in scenario $ă$, in MW
$P_{e,ă}^{E,max}$	Max power production of EV aggregator e in scenario $ă$, in MW

$P_{l,t}^{max}$	Max power consumption for load *l* at time *t*, in MW
E_e^{max}	Max energy capacity of EV aggregator *e*, in MWh
$SOC_{e,ă,end}$	Desired SOC of EV aggregator *e* in scenario *ă* , in %
SOC^{max}	Upper limit of SOC for EV aggregators, in %
SOC^{min}	Lower limit of SOC for EV aggregators, in %
$\lambda_{gn,ă,t}^{DA}$	Bid price of traditional generator *g* at node *n* and time *t* in scenario *ă*, in \$/MW
$\lambda_{ln,ă,t}^{DA}$	Bid price of load *l* at node *n* and time *t* in scenario *ă*, in \$/MW
υ_c / υ_{dis}	Charging/discharging efficiency, in %
B_{nm}	Susceptance of the line connecting nodes *n* and *m*, in Siemens
f_{nm}^{max}	Thermal capacity of the line connecting nodes *n* and *m*, in MW
λ_{ev}	Price for EV aggregators traded with EV owners, in \$/MW
$\tau_{ă}$	Weighting factor (probability) of scenario *ă*, and the sum of probabilities for all scenarios is equal to 1, e.g., $\sum_{ă \epsilon N_{ă}} \tau_{ă} = 1$.
L_b	Battery lifetime, in MWh
C_b	Battery capital cost, in \$
μ	Learning rate of *WoLF-PHC*
η	Discount factor of *WoLF-PHC*
δ_w	Win learning parameters for updating the policy of the algorithm
δ_l	Lose learning parameters for updating the policy of the algorithm

Variables：

$\varphi_{n,ă,t}^{DA}$	Locational Marginal Pricing (LMP) at node *n* and time *t* in scenario *ă*, in \$/MW
$P_{e,ă,t}^{E,DA}$	Power dispatched for EV aggregator *e* at time *t* in scenario *ă*, in MW
$P_{\omega,ă,t}^{W,DA}$	Power dispatched for WPP ω at time *t* in scenario *ă*, in MW
$P_{g,ă,t}^{G,DA}$	Power dispatched for traditional generator *g* at time *t* in scenario *ă*, in MW
$P_{l,ă,t}^{L,DA}$	Power dispatched for load *l* at time *t* in scenario *ă*, in MW

$SOC_{e,ă,t}$	State of charge for EV aggregator *e* at time *t* in scenario *ă*, in %
$\lambda^{bid}_{\omega n,t}$	Bid price of WPP ω at node *n* and time *t*, in \$/MW
$\lambda^{bid}_{en,t}$	Bid price of EV aggregator *e* at node *n* and time *t*, in \$/MW
$\theta^{DA}_{n,ă,t}$	Voltage angle at node *n* and time *t* in scenario *ă*

5.2 Multi-agent Electricity Market Model

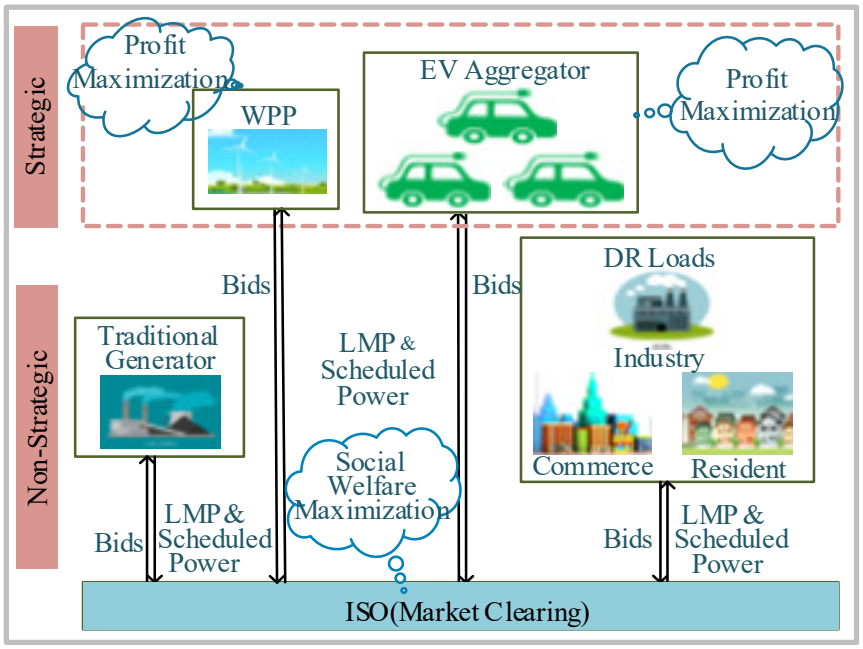

Fig. 5.1 Schematic representation of the proposed market model

In a pool-based DA market, all market participants are required to provide their sale or purchase offers to the ISO in each hour day-ahead [122]. Here, the market is modeled as a bi-level structure as shown in Fig 5.1. WPPs and EV aggregators are considered as two strategic oligopolies aimed to improve their respective revenues by solving bidding problems in the upper level. In the lower level, ISO collects bids from traditional generators, loads, and strategic WPPs and EV aggregators, and completes market clearing with maximizing the social welfare. Then ISO returns signals of Locational Marginal Pricing (LMP) and scheduled power to all participants. All the industrial, small residential and commercial loads are considered as a whole participant, i.e. a load aggregator. Loads dispatched by the load aggregator consist of fixed and curtailed parts. The latter is considered as the elastic load and satisfied with the requirement of DR. In

this model, traditional generators and loads are assumed as non-strategic participants. Their bid prices are their marginal cost prices and open to strategic suppliers [6]. Besides, the transmission network is represented by a DC model without losses. Three sources of uncertainties including the maximal power productions of WPPs and EV aggregators, and bid prices for non-strategic participants are considered. Besides, the correlations of uncertain variables are also taken into consideration in this Chapter.

1) Stochastic model of WPP maximal power production

Weibull distribution is popularly used for modeling the probabilistic wind speed v_ω as (5.1).

$$f(v_\omega, \lambda, k) = \frac{k}{\lambda}(\frac{v_\omega}{\lambda})^{k-1} e^{-(\frac{v_\omega}{\lambda})^k} \tag{5.1}$$

where λ and k are the shape and scale parameters. As wind power at nearby locations may have related patterns due to the similar meteorological conditions, wind speed correlations of multiple wind farms should be generally considered for a stochastic optimization problem. The correlation coefficient denoted as CWPP with the range (-1, 1) is introduced to quantify how well wind speeds at two sites follow each other. With the probabilistic wind speed model in (5.1), the maximal power production of a WPP is determined from the speed-power curve by (5.2) [122].

$$P_\omega^{W,max} = \begin{cases} 0, & (v_\omega < v_{ci},\ v_\omega > v_{ct}) \\ P_{rated} \cdot (\frac{v_\omega - v_{ci}}{v_{rd} - v_{ci}}), & (v_{ci} \le v_\omega \le v_{rd}) \\ P_{rated}, & (v_{rd} < v_\omega < v_{ct}) \end{cases} \tag{5.2}$$

where P_{rated} is the rated power; $v_{ci,}$ v_{rd} and v_{ct} are the cut-in, rated and cut-out wind speed, respectively.

2) Stochastic model of EV maximal power production

The maximal charging/discharging power of an aggregator is calculated by multiplying the number of EVs with the EV average rated power. According to [88, 123], the number of EVs connected at an aggregator could be described by Gaussian distribution, and therefore the stochastic maximal power production of an EV aggregator could be modeled as (5.3).

$$f(P_e^{E,\max}) = \frac{1}{\sqrt{2\pi}\sigma_p} e^{-(P_e^{E,\max}-\mu_p)^2/2\sigma_p^2} \tag{5.3}$$

where μ_p and σ_p are the mean and standard deviation of Gaussian distribution. In a general form, the maximal power production correlations of multiple EV aggregators are also represented by the correlation coefficients.

3) Stochastic model of bid prices for non-strategic participants

The bid price of non-strategic participants at each hour is characterized by the log-normal distribution as (5.4) [124].

$$f(\lambda_n^{DA}, \mu_q, \sigma_q) = \frac{1}{\lambda_n^{DA}\sigma_q\sqrt{2\pi}} e^{-(\ln\lambda_n^{DA}-\mu_q)^2/2\sigma_q^2} \tag{5.4}$$

where μ_q and σ_q are the mean and standard deviation of log-normal distribution, respectively. $\lambda_{\mathrm{n}}^{\mathrm{DA}}$ is the bid price of the non-strategic participant. Similarly, the correlation coefficients is used to represent the correlated bid price of multiple non-strategic participants.

Scenario generation and reduction strategies with the consideration of correlation introduced in Section 2.1 is used in this Chapter. The stochastic features of the maximal power production of WPPs and EV aggregators, and the bid prices of non-strategic participants modeled in (5.1)-(5.2) would be represented by a proper set of scenarios. In specific, the maximal power production of the WPP and EV aggregator, the bid price of the traditional generator and load are respectively denoted by $P_{\omega,ă,t}^{W,max}$, $P_{e,ă}^{E,max}$, $\lambda_{gn,ă,t}^{DA}$ and $\lambda_{ln,ă,t}^{DA}$. And the expected profits of WPPs and EV aggregators and the social welfare from the perspective of ISO can also be expressed by these scenarios and their probabilities. The analysis results are dependent on these assumptions, which have been generally accepted for such uncertainties. If historical data is used to model the uncertainties instead, the result will be similar.

5.2.1 Clearing model (Lower level)

In the lower level, the ISO first collects bids from all market participants and then completes market clearing. The ISO aims to ensure the efficiency of electricity market,

which is characterized by maximized social welfare. As a result, the objective function in the lower level should be maximizing social welfare. With the help of traditional optimal power flow (OPF) method to clear the market, the dispatched power production $P_{\omega,ă,t}^{W,DA}$ and $P_{e,ă,t}^{E,DA}$ for WPPs and EV aggregators respectively and LMP $\varphi_{n,ă,t}^{DA}$ will be returned to the upper level for maximizing the revenues of strategic WPPs and EV aggregators. The bid prices $\lambda_{\omega n,t}^{bid}$ and $\lambda_{en,t}^{bid}$ are bidding strategy for the WPP ω and the EV aggregator e at node n and time t respectively.

Maximize

$$\sum_{ă\in N_ă} \tau_ă \cdot \Big(\sum_{l\in\Omega_n^L} \lambda_{ln,ă,t}^{DA} \cdot P_{l,ă,t}^{L,DA} - \sum_{g\in\Omega_n^G} \lambda_{gn,ă,t}^{DA} \cdot P_{g,ă,t}^{G,DA} - \sum_{\omega\in\Omega_n^W} \lambda_{\omega n,t}^{bid} \cdot P_{\omega,ă,t}^{W,DA} - \sum_{e\in\Omega_n^E} \lambda_{en,t}^{bid} \cdot P_{e,ă,t}^{E,DA} \Big) \tag{5.5}$$

Subject to

$$P_{g,ă,t}^{G,DA} + P_{\omega,ă,t}^{W,DA} + P_{e,ă,t}^{E,DA} - \sum_{m\in\Omega_n^N} B_{nm} \cdot (\theta_{n,ă,t}^{DA} - \theta_{m,ă,t}^{DA}) = P_{l,ă,t}^{L,DA} : \varphi_{n,ă,t}^{DA},\ \forall n,t,ă \tag{5.5.1}$$

$$-f_{nm}^{\max} \le B_{nm} \cdot (\theta_{n,ă,t}^{DA} - \theta_{m,ă,t}^{DA}) \le f_{nm}^{\max},\ \forall n,m \in \Omega_n^N, t, ă \tag{5.5.2}$$

$$0 \le P_{g,ă,t}^{G,DA} \le P_g^{\max},\ \forall g,t,ă \tag{5.5.3}$$

$$P_{l,t}^{\min} \le P_{l,ă,t}^{L,DA} \le P_{l,t}^{\max},\ \forall l,t,ă \tag{5.5.4}$$

$$0 \le P_{\omega,ă,t}^{W,DA} \le P_{\omega,ă,t}^{W,\max},\ \forall \omega,t,ă \tag{5.5.5}$$

$$T_{urgent} = \left\lceil (SOC_{e,ă,end} - SOC_{e,ă,t-1}) E_e^{\max} / P_{e,ă}^{E,\max} \right\rceil,\ \forall e,t,ă \tag{5.5.6}$$

$$-P_{e,ă}^{E,\max} \le P_{e,ă,t}^{E,DA} \le P_{e,ă}^{E,\max},\ \forall e,ă,t < 24 - T_{urgent} \tag{5.5.7a}$$

$$P_{e,ă,t}^{E,DA} = -P_{e,ă}^{E,\max},\ \forall e,ă,t \ge 24 - T_{urgent} \tag{5.5.7b}$$

$$\theta_{n,ă,t}^{DA} = 0,\ \forall t,ă,n:ref \tag{5.5.8}$$

$$-\pi \le \theta_{n,ă,t}^{DA} \le \pi,\ \forall t,ă,n \backslash n:ref \tag{5.5.9}$$

$$SOC^{\min} \le SOC_{e,ă,t} \le SOC^{\max},\ \forall e,t,ă \tag{5.5.10}$$

$$SOC_{e,ă,t}=SOC_{e,ă,t\text{-}1}-(P^{E,DA}_{e,ă,t}/\upsilon_{dis}\cdot\Delta t/E^{\max}_{e}),\ \forall e,t,ă,P^{E,DA}_{e,ă,t}\geq 0 \tag{5.5.11a}$$

$$SOC_{e,ă,t}=SOC_{e,ă,t\text{-}1}-(P^{E,DA}_{e,ă,t}\cdot\upsilon_{c}\cdot\Delta t/E^{\max}_{e}),\ \forall e,t,ă,P^{E,DA}_{e,ă,t}<0 \tag{5.5.11b}$$

where $\lceil a \rceil$ is the round-up calculation of a. The optimization variables of the LL problem are the variables in the set $\Delta^{LL}=\{P^{L,DA}_{l,ă,t}, P^{G,DA}_{g,ă,t}, \lambda^{bid}_{\omega,n,t}, P^{W,DA}_{\omega,ă,t}, P^{E,DA}_{e,ă,t}, \theta^{DA}_{n,ă,t}, SOC_{e,ă,t}\}$.

The objective function (5.5) is to maximize social welfare. The first term is the revenues of selling electricity to load demands, while the other three terms represent the costs of purchasing electricity from traditional generators, WPPs and EV aggregators. The constraint (5.5.1) is the power production and consumption balance for node n with a dual variable $\varphi^{DA}_{n,ă,t}$ donating the LMP that would be provided to the upper-level. Inequality (5.5.2) limits the thermal capacity of the transmission line. Maximum and minimum energy dispatched for traditional units, load demand and WPPs are constrained in (5.5.3), (5.5.4) and (5.5.5) respectively. It is noted that a load demand consists of the fixed and curtailed parts represented by the minimum load $P^{min}_{l,t}$ and variable load $P^{L,DA}_{l,ă,t}$ respectively in (5.5.4). Equation (5.5.6) calculates the threshold hour of fully charging EV aggregator by the maximum charging power. Constraint (5.5.7a) applies when the EV aggregator is not in urgent charging period and could participate in the power market, while constraint (5.5.7b) applies when the EV aggregator is in urgent charging period so that EV aggregator is charged at the maximum power to satisfy the daily driving utilization. Equation (5.5.8) and inequality (5.5.9) set voltage angle limits at the slack bus and other buses respectively. Equation (5.5.10) represents the SOC range of an EV aggregator at the present hour, while constraints (5.5.11a) and (5.5.11b) indicate time-series SOC formulation of an EV aggregator at present and the previous hours.

5.2.2 The suppliers' bidding problem (Upper level)

The proposed strategic bidding problem considers the output capacity uncertainties of WPPs and EV aggregators as a set of scenarios. Strategic oligopolists' revenues for

the ωth WPP and the eth EV aggregator are expressed by these scenarios with corresponding probabilities and represented in the upper level by (5.6) and (5.7) respectively, where LMP $\varphi_{n,ă,t}^{DA}$, scheduled WPP power $P_{\omega,ă,t}^{W,DA}$ and EV aggregator output $P_{e,ă,t}^{E,DA}$ are obtained from the market clearing in the lower level. While the revenue of WPP is presented in (5.6), the revenue of an EV aggregator as presented in (5.7) includes the income of selling electricity to power market in the first term, the cost of buying electricity from EV owners in the second term and the battery degradation cost in the third term. Absolute-value function in (5.7) could be handled by a linear programming simplex method in [125].

$$R_{\omega} = \sum_{ă \in N_{ă}} \tau_{ă} \cdot (\varphi_{n,ă,t}^{DA} \cdot P_{\omega,ă,t}^{W,DA}) \tag{5.6}$$

$$R_{e} = \sum_{ă \in N_{ă}} \tau_{ă} \cdot (\varphi_{n,ă,t}^{DA} \cdot P_{e,ă,t}^{E,DA} - \lambda_{ev} \cdot P_{e,ă,t}^{E,DA} - (C_b / L_b) \cdot \left| P_{e,ă,t}^{E,DA} \right|) \tag{5.7}$$

The optimization variables of the UL problem are the variables in the set Δ^{uL}= $\{P_{\omega,ă,t}^{W,DA},\ P_{e,ă,t}^{E,DA}\}$. The game problem Ψ among strategic suppliers including WPPs and EV aggregators is defined here by a set of nodes with strategic players, bid prices and revenues as (5.8).

$$\psi = \begin{Bmatrix} \Omega_n^W, \{\lambda_{\omega}^{bid}\}_{\omega \in \Omega_n^W}, \{R_{\omega}\}_{\omega \in \Omega_n^W}, \\ \Omega_n^E, \{\lambda_{e}^{bid}\}_{e \in \Omega_n^E}, \{R_{e}\}_{e \in \Omega_n^E} \end{Bmatrix} \tag{5.8}$$

It is obvious that the revenues of other rivals are influenced by every strategic supplier's bid price through the clearing process as (5.5)-(5.5.11b). As there is no information on other strategic suppliers' profit functions and historical bidding decisions, the decision process of bidding strategies is a game problem rather than an optimization. As a result, these strategic players are required to learn for their optimal bids by repeated interaction with the market. In next Section, strategic bidding behaviors of WPPs and EV aggregators in a competitive market with incomplete information are modeled as stochastic games, where the market environment is

stochastic and determined by both bid prices and characteristics of all players. Electricity suppliers including WPPs and EV aggregators are considered as players of the game. Then the bidding strategy is explored using a multi-agent reinforcement learning (MARL) algorithm *WoLF-PHC* as a decision support tool.

5.3 Methodology

A brief summary of the RL theory and MARL is first introduced here, and then followed by a stochastic game framework for a DA electricity market. Afterward, a MARL method *WoFL-PHC* and the utilization of *WoLF-PHC* for multi-agent bidding strategies are described in detail.

5.3.1 Description of RL theory and the MARL

RL is an area of machine learning developed to analyze animal and artificial behavioral systems [126]. The agent updates its decision relying on instant feedbacks and gradual learning through repetitive interaction with the external environment, which is quite similar to the relationship between strategic energy suppliers and the market. Firstly, the agent perceives a state and a reward based on its past action from the environment. Then, its learning is reinforced by comparing the returned scalar reward signal every time with the one in the last round for evaluating the quality of its environment-based behavior. Specifically, the probability of this potential action will be increased if the compared result is better and decreased if conversely. Lastly, the highest probability action would be chosen through learning by itself.

There are three main classes of methods making use of RL principles, namely dynamic programming methods, Monte Carlo techniques and temporal difference learning methods [127]. The premise of using dynamic programming is the complete availability of system information. Although Monte Carlo techniques could cope with the unknown environment, the solution process is very time consuming and a long time would be needed to wait for the final outcome of learning. Temporal difference learning methods used to learn from an unknown environment after every step without the final

result is more suitable for the problem presented here, and *Q-learning* is one of such most frequently used RL approaches.

MARL is developed based on the single-agent RL to decide the optimal action of every agent in multi-agent domains. It combines the single-agent RL, game theory and policy research techniques, and hence is more suitable for solving bidding problems of multi-supplier in electricity market. However, due to the alterability and unpredictability of multi-agent dynamic environments, it would be more difficult and challenging for each agent to learn with other agents as moving targets. Next, a stochastic game framework is introduced to describe this complicated problem of multi-agent bidding decisions in electricity market.

5.3.2 The stochastic game framework of the proposed DA electricity market

The stochastic game framework is an extension and combination of the Markov Decision processes [79] and the Matrix games [128], presenting a single-agent multiple state framework and a multiple agent single state framework respectively, which includes multiple decision makers and multiple states. A multi-agent stochastic game could be described as a tuple (*M, X, A, T, R*) where *M* = {*1, 2, … , m*} denotes a set of agents, *X* is a set of game states $\{x_i\}$, *A*=$\{a_1, \dots, a_j, \dots, a_m\}$, in which a_j=$\{aa_{min}, \dots, aa_{max}\}$ represents the sects of actions available to any player a_j, *T* is the transition function represented by $X \times A \times X \to (0,1)$, and *R*=$\{R_1, \dots, R_j \dots, R_m\}$ shows the set of reward functions for all agents in which R_j: $(x_i, a_j) \to \mathcal{R}$ is the reward function of the *j*th agent in the state x_i with executing the action a_j. At each step, all agents observe the state $x_i \in X$ and choose to perform the action a_j according to an optimal action selection policy of learning algorithm, then go to the next state $x_i \in X$.

The proposed multi-agent market model is expressed as a stochastic game framework. There exist two types of agents, which are the WPP $\omega \in \Omega_n^W$ and the EV aggregator $e \in \Omega_n^E$. M =$\{\omega \in \Omega_n^W, e \in \Omega_n^E\}$ in the proposed model. States of the stochastic game consider different levels of WPP and EV aggregator suppliers' capacities represented as two sets $\{x_\omega\}_{\omega \in \Omega_n^W}$ and $\{x_e\}_{ej \in \Omega_n^E}$ respectively. The market

clearing process, representing the interactive environment, would provide the signal of scheduled power production $P_{\omega,ă}^{W,DA}$ and $P_{e,ă}^{E,DA}$ to every agent for WPPs and EV aggregators respectively. In this way, a state would be chosen for each agent after every market clearing. Next, admissible actions A=$\{a_j\}$ are defined for agents of WPPs and EV aggregators to update bid prices $\{\lambda_{\omega j}^{bid}\}_{\omega j\in\{a_j\}}$ and $\{\lambda_{ej}^{bid}\}_{ej\in\{a_j\}}$ respectively. As to the returned reward functions in (5.6) and (5.7), they could be expressed by $\{R_{\omega j}\}_{\omega j\in\{a_j\}}$ and $\{R_{ej}\}_{ej\in\{a_j\}}$ where $R_{\omega j}$: $(x_\omega,\ a_{\omega j})\to\mathcal{R}$ is the payoff of the ωth agent after clearing the market with bidding $\lambda_{\omega j}^{bid}$ in the WPP' capacity level x_ω, and R_{ej}: $(x_e,\ a_{ej})\to\mathcal{R}$ is the *e*th agent' profit after providing bid price λ_{ej}^{bid} in the EV aggregators' capacity level x_e to the clearing market. The decision process involves the choice of bidding actions for each player can be defined as B = $\{\{\lambda_{\omega j}^{bid}\}_{\omega j\in\{a_j\}}$, $\{\lambda_{ej}^{bid}\}_{ej\in\{a_j\}}\}$. Then their own perception of states would be reinforced through executing corresponding bidding decisions in the stochastic market, in which the set of states is described as X= $\{\{x_\omega\}_{\omega\in\Omega_n^W},\ \{x_e\}_{ej\in\Omega_n^E}\}$. Consider the property of stochastic game and the decision vectors B of players are in a competitive environment, the combined process given by B and M is a competitive stochastic game with incomplete information.

In order to determine an action to update the bid price for every player in the market environment, a policy, p: $X\times A\to[0,1]$, is introduced, which states the probability of the algorithm choosing an available action a_j, based on the game is in the state x_i. As a result, the target in this multi-agent stochastic game framework is to find a suitable algorithm that every agent could learn a policy along with others learning simultaneously. Here, the *WoLF-PHC* would be introduced to model the learning process in stochastic games.

5.3.3 The MARL method WoLF-PHC

An adaptive *Q-learning* algorithm for short term electricity market [129] and *Minmax-Q learning* in [130] have been used for analyzing bidding strategies in electricity market, but some restrictive assumptions are required to ensure their

convergence [131]. *Policy Hill Climbing (PHC)* is a simple extension of *Q-learning*, the policy of which is evolved by increasing the probability of selecting the action with the highest value with a learning rate $\delta \in (0,1]$ and performs hill-climbing in the space of mixed policies. However, its convergence is unclear [83]. *PHC* is then further developed to have a variable learning rate, consisting of two learning parameters δ_w and δ_l standing for the win and lose, respectively. The variable learning rate introduced aids in the convergence, with leaving more time for rivals to adjust when the player is gainful or compelling the player to adapt more quickly to rivals' strategy changes once its interest is damaged [83]. The unknown equilibrium policy can further be replaced by a more general average strategy to asymptotically approximate to the equilibrium, such that the agent could determine its win or lose by comparing the expected and average payoff. Specifically, δ_l should be greater than δ_w. The larger learning rate δ_l means agents could learn quickly to adjust their strategies after losing, while the smaller learning rate δ_w is used to remain caution if it wins. This is called the win or learn fast (*WoLF*) principle. The final algorithm is named as *WoLF-PHC* and described as follows. The transition from the last state to the current state comes as a result of the market clearance. For a given agent i, *Q-function* after the kth market clearance based on an exploration action a_{jk} under the past state $x_{i(k-1)}$ and the current state x_{ik} with a reward function R_{jk} is updated as (5.9).

$$\begin{aligned} &Q_i(x_{i(k\text{-}1)}, a_{jk}) \leftarrow (1-\mu) Q_i(x_{i(k\text{-}1)}, a_{jk}) \\ &+\mu\left(R_{jk} + \eta \max_{a'_{jk}} Q_i(x_{ik}, a'_{jk})\right) \end{aligned} \tag{5.9}$$

The corresponding policy p_i is updated as (5.10)-(5.13). δ_{ik} is kept within (0,1] in (5.12), policy for the last state is updated in (5.10)-(5.11) by increasing the probability of the action with the maximum Q-value or decrease probabilities of other actions in the last state. The maximized Q-value is used to determine the probability distribution of actions for the last state, which is prepared for the next visit in this state. δ_{ik} refers to the variable learning rate for the agent *i* at the *k*th iteration, in which δ_ω is chosen and the agent is winning if the past expected Q-value is larger than the

expected Q-value with the average policy $\overline{p_i}$, otherwise δ_l is selected.

$$p_i(x_{i(k-1)}, a_{jk}) \leftarrow p_i(x_{i(k-1)}, a_{jk}) + \Delta_{x_{i(k-1)}a_{jk}} \tag{5.10}$$

$$\Delta_{x_{i(k-1)}a_j} = \begin{cases} -\delta_{x_{i(k-1)}a_{jk}}, if a_{jk} \neq \arg\max_{a'_{jk}} Q_i(x_{i(k-1)}, a'_{jk}) \\ \sum_{a'_{jk} \neq a_{jk}} \delta_{x_{i(k-1)}a'_{jk}}, otherwise \end{cases} \tag{5.11}$$

$$\delta_{x_{i(k-1)}a_{jk}} = \min(p_i(x_{i(k-1)}, a_{jk}), \frac{\delta_{ik}}{|A|-1}) \tag{5.12}$$

$$\delta_{ik} = \begin{cases} \delta_\omega, if \sum_{a'_{jk}} p_i(x_{i(k-1)}, a'_{jk}) Q_i(x_{i(k-1)}, a'_{jk}) \\ > \sum_{a'_{jk}} \overline{p_i}(x_{i(k-1)}, a'_{jk}) Q_i(x_{i(k-1)}, a'_{jk}) \\ \delta_l, otherwise \end{cases} \tag{5.13}$$

where $\overline{p_i}$ in (5.13) is the average policy updated as in (5.14)-(5.15), $c(x_i)$ is the total number of the state x_i from the initial state to the current state, and the Q-value, policy and average policy are required to be updated based on the previous state.

$$c(x_i) \leftarrow c(x_i) + 1 \tag{5.14}$$

$$\overline{p}_i(x_{i(k-1)}, a'_{jk}) \leftarrow \overline{p}_i(x_{i(k-1)}, a'_{jk}) + \frac{1}{c(x_i)}(p_i(x_{i(k-1)}, a'_{jk}) - \overline{p}_i(x_{i(k-1)}, a'_{jk})), \forall a'_{jk} \in A_i \tag{5.15}$$

5.3.4 Implementation of WoLF-PHC for Suppliers' Bidding Strategies

In the proposed model, WPPs and EV aggregators would not share any private information with other rivals and make self-determined biddings to increase their respective profits. The proposed model thereby is a multi-agent stochastic game problem with incomplete information. Considering that *WoLF-PHC* is a decentralized self-game algorithm which could well counterbalance the lack of information, a multi-agent decentralized *WoLF-PHC* is therefore applied in this stochastic market environment for WPPs and EV aggregators to make bidding decisions. The specific learning procedures for the ωth WPP and eth EV aggregator strategically bidding through *WoLF-PHC* could be described as follows. Each agent would repeat steps in (2) until the count is met.

(1) Set learning rate $\mu \in(0,1]$, discount factor $\eta \in(0,1]$ and learning parameters used to update the policy $\delta_l > \delta_w \in(0,1]$. Initialize Q-value Q_ω and Q_e, policy p_ω and p_e, and the count of states $c(x_\omega)$ and $c(x_\omega)$ as (5.16) and (5.17).

$$Q_\omega(x,a) \leftarrow 0,\ p_\omega(x,a) \leftarrow \frac{1}{|A|},\ c(x_\omega) \leftarrow 0 \tag{5.16}$$

$$Q_e(x,a) \leftarrow 0,\ p_e(x,a) \leftarrow \frac{1}{|A|},\ c(x_e) \leftarrow 0 \tag{5.17}$$

(2) Repeat, in the *k*th episode,

(a) According to policy $p_\omega\left(x_{\omega(k-1),}a_{\omega jk}\right)$ and $p_e\left(x_{e(k-1),}a_{ejk}\right)$, choose corresponding actions $a_{\omega jk}$ and a_{ejk} respectively.

(b) The ωth WPP and *e*th EV aggregator' bid prices $\lambda_{\omega j}^{bid}$ and λ_{ej}^{bid} are updated in terms of actions $a_{\omega jk}$ and a_{ejk} selected in step (a).

(c) Bid prices $\lambda_{\omega j}^{bid}$ and λ_{ej}^{bid} updated in step (b) are sent to the ISO in the lower level of the proposed market model, with LMPs and scheduled WPP's and EV aggregator's productions are obtained from the clearing process (5.5)-(5.5.11b) and are provided to the upper level. Then reward functions $R_{\omega jk}$ and R_{ejk} are calculated based on (5.6) and (5.7).

(d) Q-functions $Q_\omega\left(x_{\omega(k-1),}a_{\omega jk}\right)$, $Q_e\left(x_{e(k-1),}a_{ejk}\right)$ are updated by observing scalar rewards $R_{\omega jk}$, R_{ejk} in step (c), and the current state $x_{\omega k}$, x_{ek} as (5.9).

(e) Observe every action $a'_{\omega jk}$ and a'_{ejk} for states $x_{\omega(k-1)}$ and $x_{e(k-1)}$ respectively, Q_ω and Q_e related to each pair $\left(x_{\omega(k-1),}a'_{\omega jk}\right)$ and $\left(x_{e(k-1),}a'_{ejk}\right)$.

(f) Update average polices $\bar{p}_\omega\left(x_{\omega(k-1),}a'_{\omega jk}\right)$ and $\bar{p}_e\left(x_{e(k-1),}a'_{ejk}\right)$ as (5.14) and (5.15).

(g) Update the variable learning rate $\delta_{\omega k}$ and δ_{ek} relied on $Q_\omega\left(x_{\omega(k-1),}a'_{\omega jk}\right)andQ_e\left(x_{e(k-1),}a'_{ejk}\right)$ in step (e) and $\bar{p}_\omega\left(x_{\omega(k-1),}a'_{\omega jk}\right)$ and $\bar{p}_e\left(x_{e(k-1),}a'_{ejk}\right)$ in step (f) as (5.13). Then policies $p_\omega\left(x_{\omega(k-1),}a_{\omega jk}\right)$, $p_e\left(x_{e(k-1),}a_{ejk}\right)$ are updated according to as (5.10)-(5.12).

(h) Set *k=k+1*, return to step (a).

The above learning process for a WPP and an EV aggregator developing respective bidding strategies through their interactions with the market is shown in Fig. 5.2, and it could be extended and scaled to have more strategic players. The *WoLF-PHC* to solve the proposed bidding problem for the agent *i* is represented as Fig.5.3.

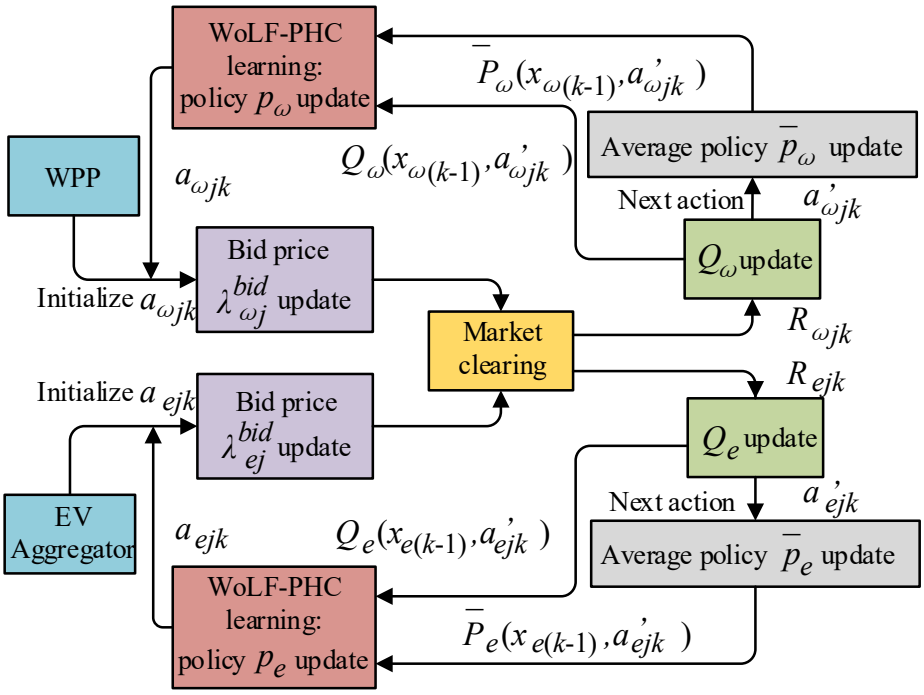

Fig. 5.2 The specific learning process for a WPP and an EV aggregator strategically bidding through *WoLF-PHC*

Remarks:

The proposed model is for a single hour of the DA market and can be considered as an offline approach. Since the model involves a large number of scenarios, the calculation process could be time-consuming. The *WoLF-PHC* pre-learning process [132] could therefore be firstly introduced to boost the computation efficiency, which uses the optimized Q-value and bid price in the previous hour as the initial point of the current *WoLF-PHC* computation such that the convergence rate can be accelerated. In addition, there are numerous scenarios in solving the DA market clearing, scenario-parallel computing could further be used to reduce the computation time.

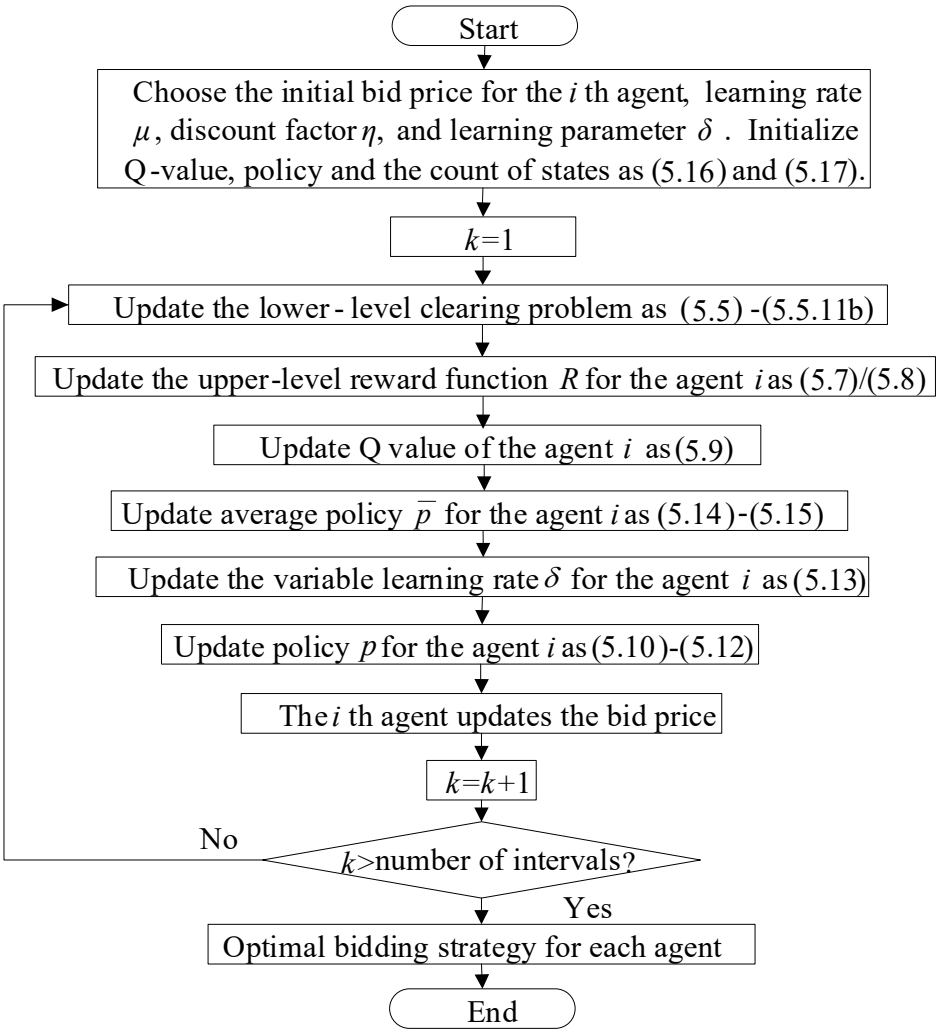

Fig. 5.3 Algorithm to solve the proposed bidding problem

5.4 Case Studies

Parameters of the three sources of uncertainties are configured as below. The shape and scale parameters of wind speed are set as λ=2 and k=12 with correlations of 0.3, while the cut-in, cut-out and rated wind speed are v_{ci}=3m/s, v_{ct}=25m/s and v_{rd}=12 m/s, respectively [133]. The parameters for the normal distribution of the EV aggregator are set as μ_p=120MW and σ_p =0.1μ_p with correlations of 0.1. The parameters of the log-normal distribution for the stochastic bid prices of non-strategic participants are set as μ_q=40\$/MW and σ_q=0.1μ_q with correlations of 0.2. Besides, the cost price for the EV aggregator buying electricity from EV owners is set as 20\$/MW [11]. The lower limit of bid price is the cost price of each energy supplier. Other EV aggregator

parameters are shown in Table 5.1 and parameters for the *WoLF-PHC* are listed in Table 5.2.

Table 5.1 EV aggregator parameters

EV aggregator	SOC^{max} (pu)	SOC^{min} (pu)	υ_c	υ_{dis}	E_{ev}^{max} (MWh)
Value	0.9	0.1	0.9	0.85	1000

Table 5.2 Data for the *WOLF-PHC*

Parameter	μ	η	δ_w	δ_l
Value	0.1	0.5	0.01	0.02

Four different cases are studied. Case 1 would first simulate the model proposed in Section 5.2, in which a WPP and an EV aggregator represent two strategic players, and then the proposed model is compared with the cooperated model in Chapter III [84]. In Case 2, the number of strategic players increases to three to allow a traditional generator to strategically bid and compete with the WPP and EV aggregator. Loads are changed to inelastic. Bidding results would be analyzed according to the relationship between generation supply and load demand. In Case 3, strategic players of the proposed model are expanded to cover loads as well. Four strategic players including a load, a traditional generator, a WPP and an EV aggregator are simulated in the model. In Case 4, the four players model in Case 3 is applied to a modified IEEE 118-bus system with the number of strategic players tripled to twelve, and their bidding results will be fully studied and analyzed. While Case 1 would provide the solutions for both a single hour 20:00 and the successive 24-hour operations to show the time-series performance of the proposed model, Cases 2-4 would only present the results of a single hour 20 for illustrating the convergence of bi-level model. All the cases are modeled and simulated in MATLAB running on a 1.6 GHz Intel Core i5 -5250U computer for Case 1-3 and a 3.2 GHz Intel Core i7-8700 computer for Case 4 with 8 GB of RAM.

5.4.1 Case 1

The proposed model is first tested on the IEEE 6-bus system. There are three

traditional generators locating in buses 1-3 and three loads connecting to buses 4-6. A WPP and an EV aggregator representing two strategic participants are set in bus 4 and bus 5, respectively. In order to generate the appropriate number of scenarios for the stochastic maximized power outputs of WPPs/EV aggregators and bid prices of non-strategic participants, the convergence theory in [133, 134] is used to determine the number of scenarios by formulas (5.18)-(5.20).

$$\varepsilon_{\mu} = 100(|\mu_{MC} - \mu_{*}|)/\mu_{*}[\%] \tag{5.18}$$

$$\varepsilon_{\sigma} = 100(|\sigma_{MC} - \sigma_{*}|)/\sigma_{*}[\%] \tag{5.19}$$

$$\varepsilon_{\lambda} = 100(|\lambda_{MC} - \lambda_{*}|)/\lambda_{*}[\%] \tag{5.20}$$

where μ_{MC}, σ_{MC} and λ_{MC} are the mean value, standard deviation and skewness calculated based on the generated scenarios; μ_{*}, σ_{*} and $\lambda_{*}$are the mean value, standard deviation and skewness derived theoretically from the proposed model in Section 5.2; $\varepsilon_{\mu}, \varepsilon_{\sigma}$ and ε_{λ} are the preset accuracy threshold. The number of generated scenarios is increased from 100 by a step of 100, and the number of scenarios with $\varepsilon_{\mu}, \varepsilon_{\sigma}$ and ε_{λ} just smaller than the settled accuracy 1% is deemed as the finally determined numbers. By using this strategy, the uncertainties of the maximized power outputs of WPPs/EV aggregators, and bid prices of non-strategic participants are respectively represented by 1000, 1000, and 500 scenarios.

In order to reduce the computational burden, the aforementioned forward selection method is used to curtail the number of scenarios and thus a set of the reduced number of scenarios is obtained. In the following, for investigating the impacts of the number of reduced scenarios on the accuracy of the scenario-based market model, comparative studies with different numbers of reduced scenarios are performed. Table 5.3 shows the profits of the WPP/EV aggregator, social welfare and the solution time for different numbers of reduced scenarios at hour 20. It can be found that, with the number of reduced scenarios increasing from 125 to 500, profits of the WPP and the EV aggregator as well as the social welfare would be slightly enhanced; whereas as the number of reduced scenarios further increasing beyond 500, there will be very little further

improvement. Regarding to the solution time, it would monotonically increase with the growing number of reduced scenarios. Consequently, to make a trade-off between the profits of the WPP/EV aggregator, social welfare and time consumption, 500 reduced scenarios are adopted as an appropriate choice for the following case study.

Table 5.3 Profits of the WPP/EV aggregator/social welfare and solution time under different numbers of reduced scenarios at hour 20

Number of reduced scenarios	Profit ($)		Social welfare ($)	Solution time(s)
	WPP	EV aggregator		
125	7630.9	2934.1	7352.5	105.68
250	7651.3	2949.6	7529.3	196.87
500	**7688.1**	**2961.2**	**7830.7**	**365.72**
1000	7686.7	2962.7	7832.9	1165.59
2000	7688.5	2961.5	7830.9	2508.94

Based on the parameter set above, the optimized revenues of EV aggregator and WPP in all scenarios are used to display the randomness of the stochastic model. Fig. 5.4 shows the relationship of revenues of the EV aggregator or WPP, as formulated in (5.6) and (5.7) respectively, LMPs and power output of the EV aggregator or WPP. The relationship of social welfare as represented in (5.5) and the EV aggregator/WPP power output is illustrated in Fig. 5.5. The revenues of WPP or EV aggregator and the social welfare are calculated based on a set of typical scenarios with probabilities derived by the scenario-generation and scenario-reduction algorithm.

In the model, WPP and EV aggregator develop respective bidding strategies through the learning process of *WoLF-PHC* and interact with the market, while their revenues and the social welfare are influenced by constraints of the market clearing model, i.e. the power output limits of WPP and EV aggregator in (5.5.5)-(5.5.7a) and the SOC limit of EV aggregator in (5.5.10)-(5.5.11b). As shown in Fig.5.6, bidding results converge nicely to equilibrium after 50 iterations. The computation time is 365.72s.

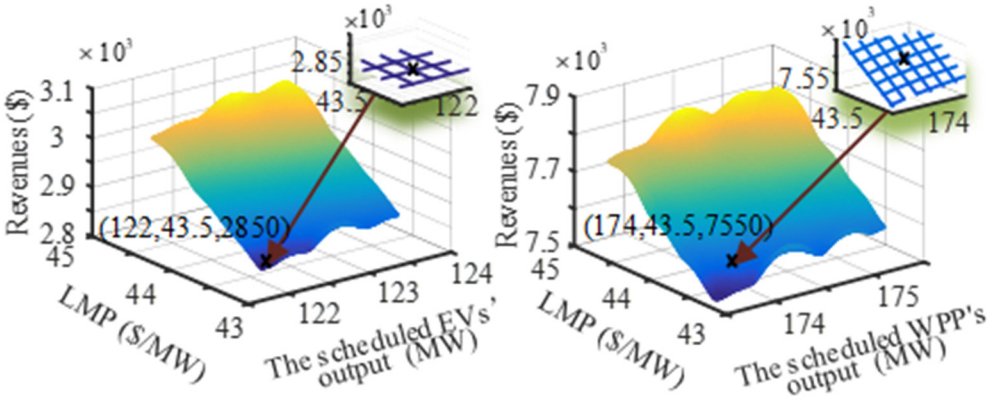

Fig. 5.4 Revenues of EV aggregator and WPP for all scenarios

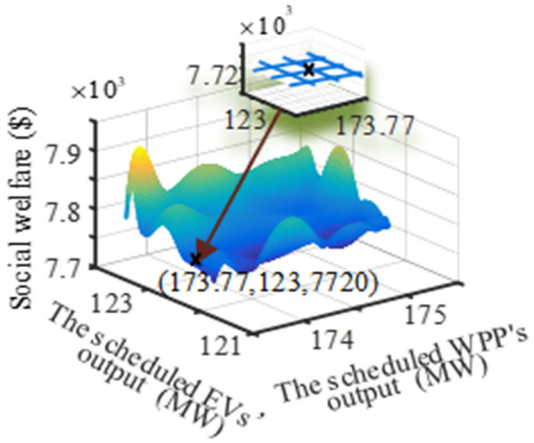

Fig. 5.5 Social welfare for all scenarios

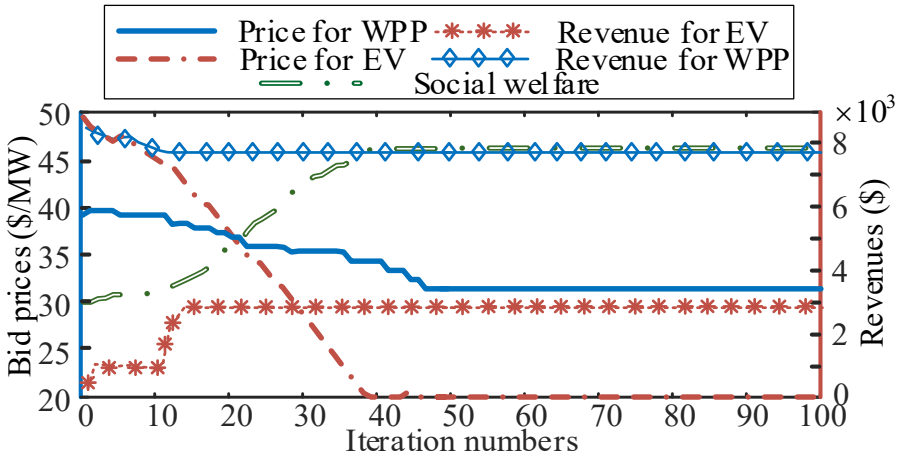

Fig. 5.6 Market clearing results for the WPP and EV aggregator

In this process, there is no complex KKT transformation nor complex calculations for

exploring the Nash equilibrium point, which demonstrates that flexible and concise *WoLF-PHC* could be used in the oligopoly electricity market to respectively optimize bid prices for the competitive WPP and the EV aggregator. Besides, each agent makes self-decision on bidding for maximizing its own interest only through the bidding information obtained from the ISO in the market without the cost functions or bidding data from the competitor. In this way, the privacy of personal data is protected.

Comparison with the cooperative model in Chapter III :

In the cooperative model in Chapter III [84], the WPP and the EV aggregator as a strategic Hybrid Power Plant (HPP) and the objective is to maximize the overall benefit of the HPP model. In order to improve the WPP and EV aggregator's common interests, the HPP owns their bidding information and cost function to strategically bid and dispatch their power as a central market player. The WPP and EV aggregator are fully controlled by the HPP and do not have any self-determination on bidding. Besides, the cooperative model would break if the WPP and EV aggregator do not provide their personal data to the HPP. Whereas, the proposed competitive model could adapt to a more flexible market environment and allows for self-bidding to increase individual revenue of the WPP and EV aggregator separately, which ensures better privacy of strategic players.

Table 5.4 shows comparative results of the cooperative and competitive models for the two strategic participants in hour 20. Compared with the cooperative model, both revenues of the EV aggregator and social welfare are increased while the profit of the WPP is slightly declined. This is due to the WPP's profits are increased by the EV aggregator with the help of the HPP's centralized dispatching in the cooperative model. In the competitive market, the EV aggregator could make self-decision on bidding and reduce its bid price to lower than the WPP to sell more and earn more in return. As a result, the EV aggregator's profit has an increase and the WPP' interest is reduced. Meanwhile, social revenue is improved as competition brings the reduction of bid prices.

In addition, the bidding strategy of the proposed model is also simulated for 24 hours. Scenarios of maximum power production of the WPP and bid prices of non-strategic participants are generated on an hourly basis as in [6, 54]. While the number of EVs connected to the EV aggregator is a normal distribution for 24 hours, and the initial and desired SOC are set as 0.6 and 0.8, respectively [135]. Comparative results of the cooperative and competitive models for 24 hours are provided in Table 5.5. The revenues of the WPP and EV aggregator in the proposed model outperformance those of the cooperative model, while the social welfare is also higher.

Table 5.4 Revenues comparison of cooperative and competitive models at hour 20

Market Type	WPP Revenues ($)	EV Aggregator Revenues ($)	Social Welfare ($)
Cooperate Model	7724.9	2489.8	4157.6
Competitive Model	7688.1	2961.2	7830.7

Table 5.5 Revenues Comparison of Cooperative and Competitive Models for 24 hours

Market Type	WPP Revenues ($)	EV Aggregator Revenues ($)	Social Welfare ($)
Cooperate Model	131943.8	44519.2	79943.1
Competitive Model	133720.3	45664.8	133674.2

Among the 500 reduced scenarios, Fig. 5.6 shows the SOC curve and scheduled output of the EV aggregator for 24 hours for scenario 1 as an example. As shown in Fig. 5.7, the EV aggregator is not in urgent charging period before 23:00 and its power output could be scheduled in the power market (refer to the constraint (5.5.7a)); whereas for the last several hours, the EV aggregator is fixed at the maximum charging power for preparing the daytime driving utilization (refer to the constraint (5.5.7b)). In this way, the EV aggregator strategically participates in the pool-based electricity market as well as satisfy the traffic energy demand.

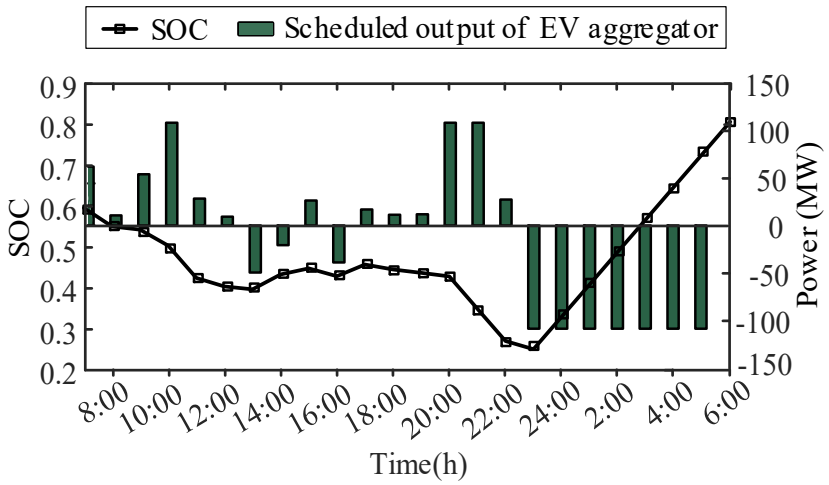

Fig. 5.7 SOC and scheduled output of the EV aggregator for scenario 1 during 24 hours

5.4.2 Case 2

In this case, the number of strategic players increases to three suppliers, with a traditional generation unit, a WPP and an EV aggregator located at bus 1, bus 4 and bus 6, respectively. The total generation capacity is 497.1MW consisting of 174.6MW, 122.5MW and 200MW for the traditional generator, WPP and EV aggregator respectively. The cost price of the traditional unit is set as 40$/MW. Loads are inelastic and set by the following four levels with bidding results analyzed as below.

(1) The total load demand is set equal to the total capacity of three suppliers. Fig.5.8 shows the market clearing bid prices, revenues of the three suppliers and the overall social welfare. The computation time is 250.87s. It is observed that the game for these three strategic players converges to its equilibrium, in which their bid prices are much higher than their cost prices. This is because there is no competitive relationship among players in this case, they have no incentive to decrease the bid prices and every supplier raises its bid price to gain more profits.

(2) The total load demand is reduced and set to 420 MW, and in this condition the total power supply is higher than the total load demand. Hence, the relationship between these three suppliers becomes competitive. Fig. 5.9 shows curves of bid prices and revenues as well as the social welfare obtained in 100 iterations of *WoLF-PHC* with the

computation time of 238.08s. The curves converge towards the equilibrium with ever decreasing amplitude. It is obvious that three players' bid prices are reduced compared to those in Fig. 5.8, which shows the competition forces every player to cut down its prices for selling more product.

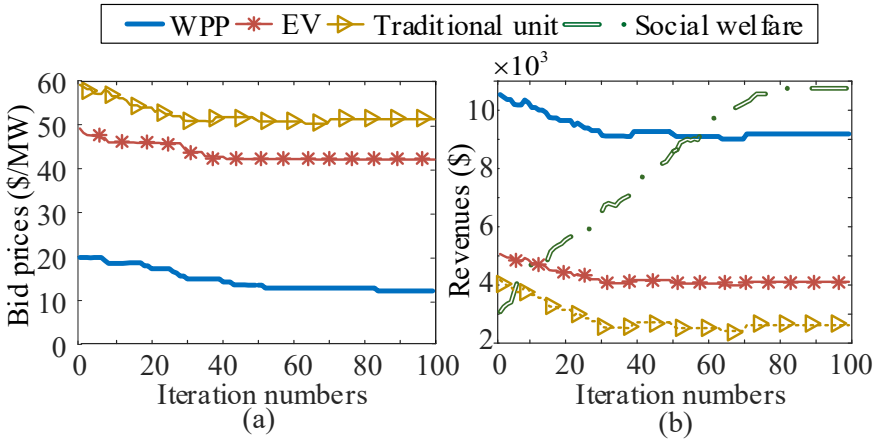

Fig. 5.8 Market clearing results of 3 players for total demand equal to total generation capacity in 6-bus system

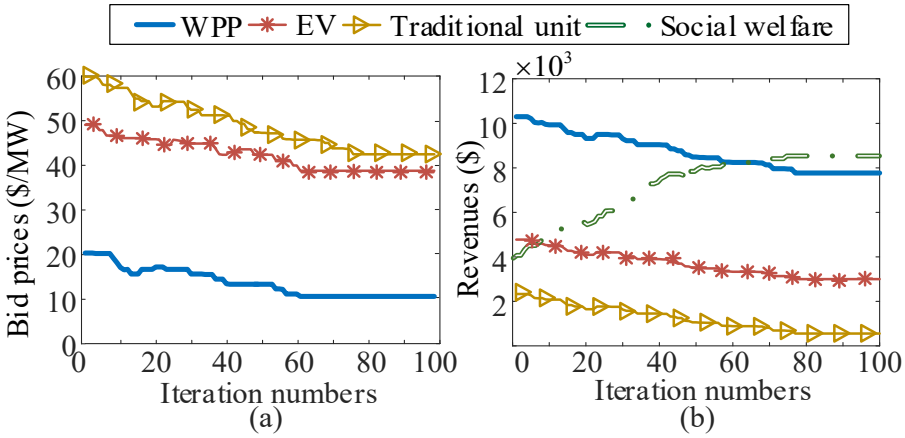

Fig. 5.9 Market clearing results of 3 players for total demand less than total generation capacity in 6-bus system

(3) The total load demand is further reduced to 322.5MW, which is equal to the total capacity of the WPP and the EV aggregator. The converged bid prices and revenues of these three players as well as the social welfare are shown in Fig. 5.10. In this way, the total load demand can be covered just by two generation units with lower cost prices. The traditional supplier with the relatively higher cost price has little

chances to sell products and earn profits. It is obvious in Fig. 5.10 that none has the interest to buy from the traditional supplier although its bid price has been reduced to its cost price. Meanwhile, WPP and EV aggregator have raised their prices to earn more with the WPP being the first to run out due to its lower bid prices. Afterward, if the bid price of the EV aggregator exceeds the traditional generator, the market becomes competitive. As a result, the EV aggregator would ensure its bid price slightly lower than that of the traditional supplier, which is consistent with curves in Fig. 5.10. The computation time is 255.78s.

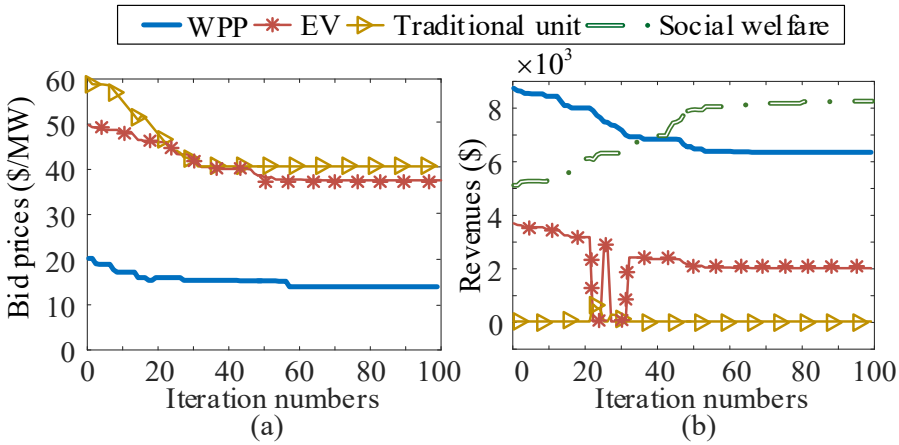

Fig. 5.10 Market clearing results of 3 players for total demand equal to the total generation capacity of WPP and EV aggregator in 6-bus system

(4) The total load demand is further reduced to below total capacity of the WPP and EV aggregator to form a competitive relationship between these two suppliers. Bid prices combined with social welfare are shown in Fig. 5.11 and the computation time is 251.38s. Similar to the previous case shown in Fig. 5.10, the traditional generator bids according to its cost price and has no revenue. The competition drives the EV aggregator and the WPP to lower its bid price than that in Fig. 5.10.

5.4.3 Case 3

Loads are reset as elastic with curtailed parts and considered as a load aggregator. In order to expand the model for more participants, four strategic players consisting of an elastic load, a traditional generator, a WPP and an EV aggregator are investigated in

this case. Fig. 5.12 shows the bid prices and revenues of these four strategic players as well as the social welfare. The computation time is 265.23s and the convergence performance is good. These imply that the proposed model is suitable for traditional units to participate in strategically bidding and works well for different typical strategic players participated in the market.

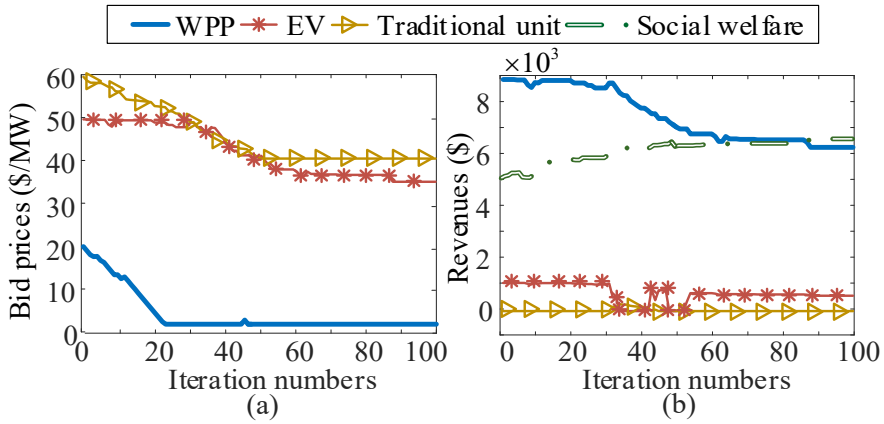

Fig. 5.11 Market clearing results of 3 players for total demand less than the total generation capacity of WPP and EV aggregator in 6-bus system

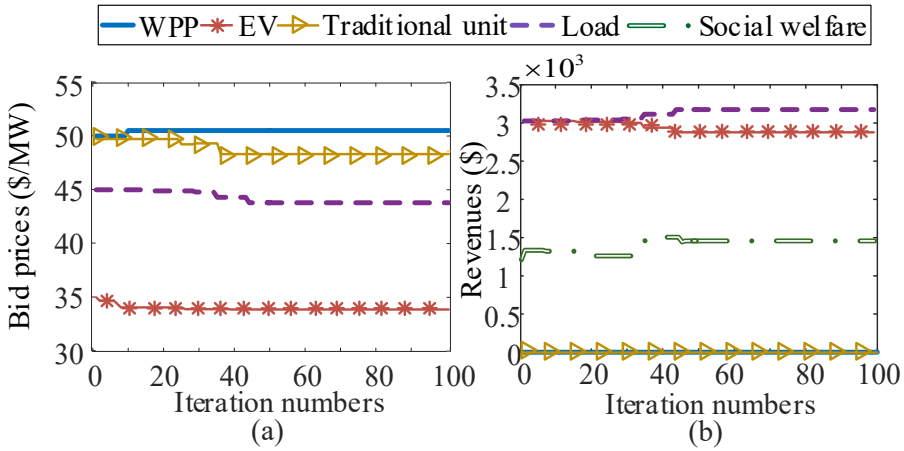

Fig. 5.12 Market clearing results for 4 players in 6-bus system

Next, three energy suppliers remain the same as before, and the load demand is split into three agents with the capacity equal to1/3 of total capacity of the original load. The computation time is 289.72s. Bidding results of these six players and the social welfare are plotted in Fig. 5.13. The resulted bid prices are much lower compared with the ones with four players in Fig. 5.12. This implies that players would adopt a relatively conservative behavior in a more competitive environment. Also noted is that WPP and

traditional generator with higher bid prices will have little chance to sell their power generation and the load demand can be preferentially supported by the EV aggregator with lower price.

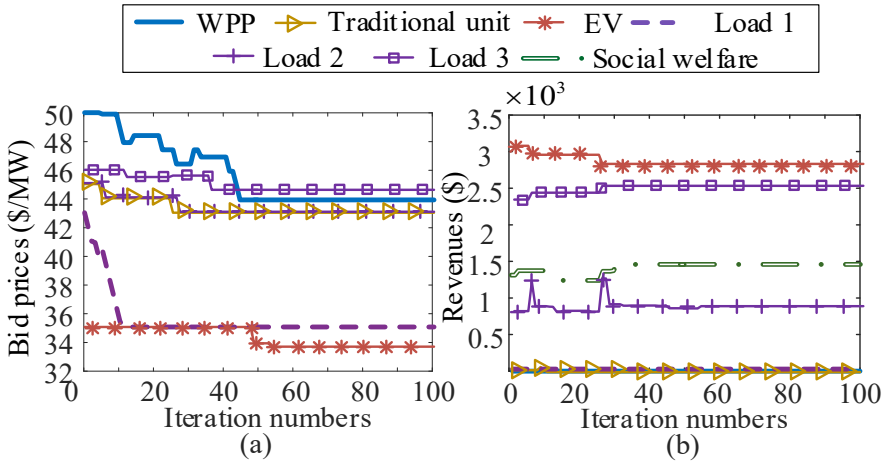

Fig. 5.13 Market clearing results for 6 players in 6-bus system

5.4.4 Case 4

The model of four strategic players in Case 3 is applied to a modified IEEE 118-bus system, in which the WPP, EV aggregator and traditional generator are located at nodes 32, 49 and 94, respectively, and loads are considered as a load aggregator. Both the bid prices and the social welfare are nicely converged as shown in Fig. 5.14. It shows that *WoLF-PHC* could successfully obtain the optimal bid price for every strategic player in a larger fully competitive electricity market.

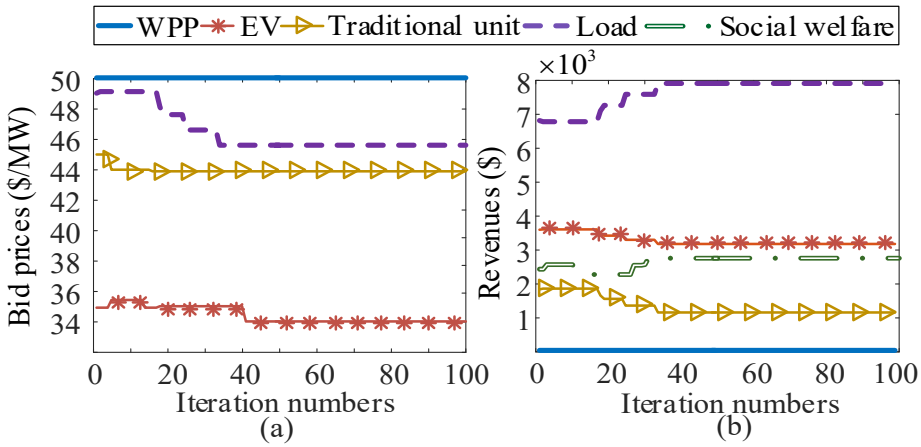

Fig. 5.14 The market clearing results for 4 players in 118-bus system

Each of these four strategic players is then duplicated to become three identical players at the same location while loads are equally assigned to three load aggregators, and thereby there are twelve strategic players in total. The game of these twelve strategic players in the modified IEEE 118-bus system converges to its equilibrium with bid prices and the social welfare plotted in Fig. 5.15. It confirms that the model with *WoLF-PHC* could be successfully used for more players to strategically bid in a large scale market. In addition, the overall bid prices of twelve strategic makers are kept at lower level than the case with four strategic players, which is consistent with Case 3 that bid prices would be reduced in a more competitive environment. With the use of the afore mentioned *WoLF-PHC* pre-learning process and 6 parallel computation threads running on a 6-core 3.2 GHz Intel Core i7-8700 computer, the computation times for market clearing with four and twelve strategic players are reduced to 735.09s and 946.72s respectively, and would satisfactorily meet the offline market clearing requirement for the proposed DA market model.

The objective of the proposed model is to maximize the social welfare as the priority, while with the LMP $\varphi_{n,\alpha,t}^{DA}$ interacted by the market-clearing in the lower level, the WPP and EV aggregator participants in the upper level make strategic biddings for increasing their respective revenues. As can be observed from Fig 5.6-5.15, the social welfare is increased on different levels, while the revenues of WPP and EV aggregator participants in some case studies would increase during the iteration process while others would reduce. Furthermore, the revenue of a particular market player would go up or down depending on the position of the final solution relative to the initial point of the *WoLF-PHC* algorithm. And the revenues of a group of market players, such as WPPs, EV aggregators, generators and loads, are not necessary always going up or down together, as demonstrated in Fig.5.15(b) of Case 4 where the revenue of Load 1 is reduced while those of Load 2 and 3 are increased.

Although the *WoLF-PHC* cannot be mathematically proved to be convergent, many examples have represented that the *WoLF-PHC* could converge to best-response policies for two multi-state stochastic games, one is a general-sum grid world domain

used by Hu and Wellman and the other is a zero-sum soccer game introduced by Littman [136]. In addition, the *WoLF-PHC* is also used in the engineering field for smart generation control of interconnected complex power grids and results show the algorithm is convergent [137]. From case studies of Chapter V, it is clear to see bidding prices are convergent with using the *WoLF-PHC*.

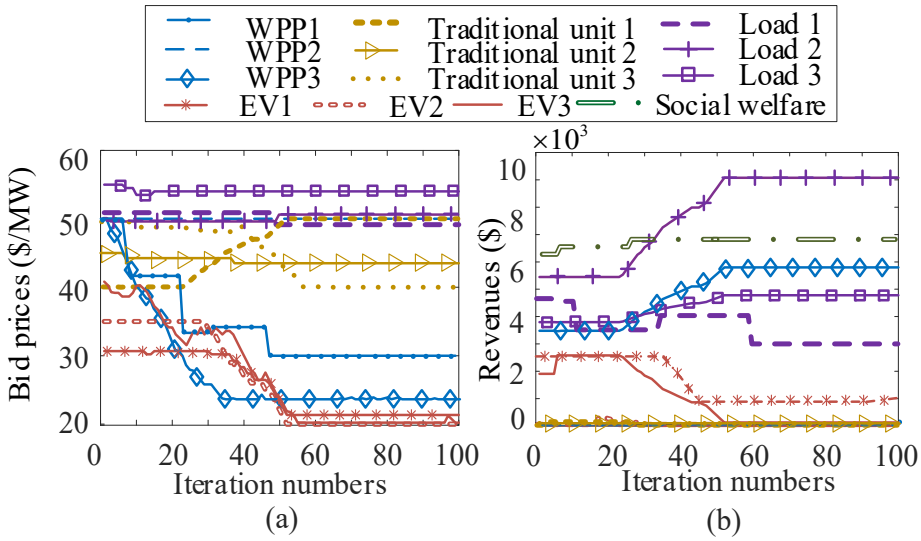

Fig. 5.15 Market clearing results for 12 players in 118-bus system

5.5 Summary

A new competitive bidding market model with incomplete information for considering the uncertainties in bid prices of non-strategic participants and available power productions of WPPs and EV aggregators is presented in this Chapter. A recently developed MARL algorithm named *WoLF-PHC* is adopted to successfully solve the proposed model for strategic players to optimize their bidding in an oligopoly electricity market with personal privacy protection and respecting the autonomy of strategic suppliers. The market is simulated as a multi-agent based system, with three test cases built on a modified IEEE 6-bus system and a larger case study based on a modified IEEE 118-bus system, the bid result in four cases is nicely converged to the equilibrium. Promising conclusions drawn from these case studies include 1) multiple participants could respectively optimize their bids by learning using the *WoLF-PHC* algorithm in

competitive electricity markets; 2) compared with the cooperated model of the WPP and EV aggregator in Chapter III, the proposed competitive model is able to adapt to a more flexible market environment in which every strategic player has full autonomy in biddings with incomplete information to maximize its own profit; 3) bid prices of market players would be reduced with more competition brought from either the decreased demand or the increased number of strategic participants.

Chapter VI

Conclusions and Future Work

6.1 Conclusions

With the rapid growth in the capacity of DERs, it is worthy of developing an effective approach to model bidding strategies for these large-scaled DERs. Bidding strategies of a large number of DERs bring both challenges and opportunities to the electricity market. On one hand, the power output of these aggregated DERs is uncertain and thereby may affect their own incomes. On the other hand, these DERs can be cooperated or competed to improve their interests. This thesis covers the development of bidding strategies on cooperative WPPs and EV aggregators, cooperative WPPs and NGG-P2G units, and competitive WPPs and EV aggregators. The primary conclusions and contributions of this research are summarized as follows:

i) Risk-Constrained Offering Strategy for a Hybrid Power Plant (HPP) Consisting of Wind Power Producer and Electric Vehicle Aggregator

This scheme schedules a stochastic optimization model to derive the offering strategy for the aggregated HPP consisting of the WPP and EV aggregator to be a price-maker in the DA pool-based market. The effectiveness and adaptability of the proposed model are evaluated. Firstly, large-scale renewable WPPs could be cooperated with EV aggregators for strategical bidding and setting electricity prices according to their and the grid's interests. The aggregated HPP has improved the common interests of EVs and WPPs on account of their energy coordination during different time slots. In addition, the profit volatility caused by uncertainties could be coped more effectively with the consideration of risk in the proposed model.

ii) Bidding Strategy for the Coordinated Operation of Wind Power Plants and NGG-P2G Units in Electricity Market

In the multi-energy system, a bidding strategy of the cooperative WPP and NGG-P2G unit is proposed. The cooperative unit participates in DA market and RT market as well as providing auxiliary services employed in real-time. Simulation results have demonstrated that large-scaled WPP can cooperate with the integrated NGG-P2G unit in a VMP for strategically bidding to improve their interests in DA electricity market, in which uncertainties of the WPP are mitigated with flexible control of NGG-P2G unit and the waste of wind resources is also reduced. Besides, most revenues of the proposed model are from the WPP in DA market, and the integrated P2G-G2P unit helps to gain common profits mainly through providing auxiliary services.

iii) A Multi-agent Competitive Bidding Strategy in a Pool-Based Electricity Market with Price-Maker Participants of WPPs and EV Aggregators

A new competitive bidding strategy is formulated for WPPs and EV aggregators. Different from the previous cooperative HPP model depending highly on the centralized control and scheduling of a central aggregator who owns lots of bidding information of EVs and WPPs, a recently developed MARL algorithm named *WoLF-PHC* is adopted to successfully solve the bidding problem with incomplete information for strategic players increasing their respective profits with great respect for personal privacy and their autonomy. Simulation results have shown that multiple participants could respectively optimize their bids by learning using the *WoLF-PHC* algorithm in competitive electricity markets. Besides, bid prices of market players would be reduced with more competition brought from either the decreased demand or the increased number of strategic participants.

6.2 Future Work

This thesis has proposed the cooperative and competitive model for large-scaled DERs in the transmission grid, such as WPPs, EV aggregators and NGG-P2G units, strategically bidding in the electricity market. To enrich the current work, the following topics should be investigated in the future.

(1) With the rapid growth of the distributed renewable generation, micro grids have attracted more attention. Micro grids can not only call on prosumers to take part in electricity market, but also offer more flexible choices for customers to island from the main grid. Micro grid users can choose the reliability services they prefer on the basis of the availability and price of DERs. Thus, the energy transaction mechanism of customers in distribution markets behaving strategically deserves to be studied as it becomes important with the deployment of smart grids.

(2) The potential bi-directional energy trading imposes the stronger physical and economic dependence relationship between gas and power systems, which inspires the research on the synchronized gas-electricity markets. Compared with the current research in Chapter IV, in which DERs in the integrated gas and electricity network behave strategically only in electricity market. Strategically bidding of DERs can be extended to both gas and electricity markets. Therefore, it is worth to study the equilibrium of the coupled gas and electricity markets.

Appendix

Solution Methodology

1) MPEC Formulation

To obtain the optimal value, the proposed bi-level model can be transformed to a single-level model by transforming the lower level model using KKT (Karush-Kuhn-Tucker) constraints. After transformation, the objective function in the lower level can be replaced by corresponding constraints. Therefore, all deformed constraints in lower level are added to constraints in upper level to limit the upper objective function. And the original bi-level model has become a single-level MPEC problem described as follows.

Maximize

$$\sum_{t\in T}(\varphi_{n,t}\cdot P_{c,t}^{CO,DA}+\sum_{\beta\in N_\beta}\sum_{\alpha\in N_\alpha}\tau_\beta\cdot\tau_\alpha\cdot(\varphi_\alpha^{RT}\cdot P_{\alpha,\beta,c,t}^{CO,RT}-\lambda_{gas}\cdot P_{\alpha,\beta,i,t}^{IN}+\lambda_{reg,i,t}^{IN,up}\cdot P_{\alpha,\beta,i,t}^{IN,up}+\lambda_{reg,i,t}^{IN,dn}\cdot P_{\alpha,\beta,i,t}^{IN,dn})) \tag{7.1}$$

Subject to

Constrains (4.1.1)-(4.1.20), (4.2.1)-(4.2.20) (7.1.1)

$$\lambda_s^{S,DA}-\varphi_{n,t}+\mu_{s,t}^{U,DA}-\mu_{s,t}^{L,DA}=0,\forall s,t \tag{7.1.2}$$

$$\lambda_b^{B,DA}-\varphi_{n,t}+\mu_{b,t}^{U,DA}-\mu_{b,t}^{L,DA}=0,\forall b,t \tag{7.1.3}$$

$$\lambda_{c,t}^{CO,bid}-\varphi_{n,t}+\mu_{c,t}^{U}-\mu_{c,t}^{L},=0,\forall c,t \tag{7.1.4}$$

$$-\lambda_{le}^{Int,DA}+\varphi_{n,t}+\mu_{le,t}^{int,L,DA}-\mu_{le,t}^{int,L,DA}=0,\forall le,t \tag{7.1.5}$$

$$-\lambda_{let}^{et,DA}+\varphi_{n,t}+\mu_{let,t}^{et,L,DA}-\mu_{let,t}^{et,L,DA}=0,\forall let,t \tag{7.1.6}$$

$$\sum_{m\in\Omega_n^N}B_{nm}\cdot(\varphi_{n,t}-\varphi_{m,t})+\sum_{m\in\Omega_n^N}B_{nm}\cdot(\mu_{n,t}^{U,DA}-\mu_{m,t}^{U,DA}) \tag{7.1.7}$$

$$-\sum_{m\in\Omega_n^N} B_{nm}\cdot\left(\mu_{n,t}^{L,DA}-\mu_{m,t}^{L,DA}\right)-\ \mu_{\theta,t}^{DA}=0, n{:}\,ref,\forall t$$

$$\sum_{m\in\Omega_n^N} B_{nm}\cdot\left(\varphi_{n,t}-\varphi_{m,t}\right)+\sum_{m\in\Omega_n^N} B_{nm}\cdot\left(\mu_{n,t}^{U,DA}-\mu_{m,t}^{U,DA}\right) \tag{7.1.8}$$

$$-\sum_{m\in\Omega_n^N} B_{nm}\cdot\left(\mu_{n,t}^{L,DA}-\mu_{m,t}^{L,DA}\right)+\mu_{\theta,t}^{L,DA}-\ \mu_{\theta,t}^{U,DA}$$

$$=0,\forall n\backslash ref,\forall t$$

$$0\le f_{nm}^{max}-B_{nm}\cdot(\theta_{n,t}^{DA}-\theta_{m,t}^{DA})\perp\mu_{\theta,t}^{U,DA}\ge 0,\forall m,n\ \in\Omega_n^N,t \tag{7.1.9}$$

$$0\le f_{nm}^{max}+B_{nm}\cdot(\theta_{n,t}^{DA}-\theta_{m,t}^{DA})\perp\mu_{\theta,t}^{L,DA}\ge 0,\forall m,n\ \in\Omega_n^N,t \tag{7.1.10}$$

$$0\le P_s^{max}-P_{s,t}^{S,DA}\perp\mu_{s,t}^{U,DA}\ge 0,\ \ \forall s\,,t \tag{7.1.11}$$

$$0\le P_{s,t}^{S,DA}\perp\mu_{s,t}^{L,DA}\ge 0,\forall s\,,t \tag{7.1.12}$$

$$0\le P_b^{max}-P_{b,t}^{B,DA}\perp\mu_{b,t}^{U,DA}\ge 0,\ \ \forall b\,,t \tag{7.1.13}$$

$$0\le P_{b,t}^{B,DA}\perp\mu_{b,t}^{U,DA}\ge 0,\forall b\,,t \tag{7.1.14}$$

$$0\le P_{le}^{Int,max}-P_{le,t}^{Int,DA}\ \perp\mu_{le,t}^{int,U,DA}\ge 0,\forall le,t \tag{7.1.15}$$

$$0\le P_{le,t}^{Int,DA}\perp\mu_{le,t}^{int,L,DA}\ge 0,\forall le,t \tag{7.1.16}$$

$$0\le P^{The}-P^{The,min}-P_{let,t}^{et,DA}\ \perp\mu_{let,t}^{et,U,DA}\ge 0,\forall let,t \tag{7.1.17}$$

$$0\le P_{let,t}^{et,DA}\perp\mu_{let,t}^{et,L,DA}\ge 0,\forall let,t \tag{7.1.18}$$

$$0\le P_{c,t}^{CO,bid}-P_{c,t}^{CO,DA}\ \perp\mu_{c,t}^{U}\ge 0,\ \ \forall c,t \tag{7.1.19}$$

$$0\le P_{c,t}^{CO,DA}\perp\mu_{c,t}^{L}\ge 0,\forall k,t \tag{7.1.20}$$

$$0\le\mu_{\theta,t}^{U,DA}\perp\pi-\theta_{n,t}^{DA}\ge 0,\ \ \forall n\ \backslash n{:}\,ref,\forall t \tag{7.1.21}$$

$$0\le\ \mu_{\theta,t}^{L,DA}\perp\pi+\theta_{n,t}^{DA}\ge 0,\ \ \forall n\ \backslash n{:}\,ref,\forall t \tag{7.1.22}$$

The MPEC model described above contains two terms of nonlinearities. The first part is $\varphi_{n,t}\cdot P_{c,t}^{CO,DA}$ in objective function (7.1), the second part is complementary constraints (7.1.9) - (7.1.22). By replacing these two non-linear terms using strong duality theorem (SDT) and the Fortuny-Amat transformation [31], the MPEC model is

easily transformed to a MILP model.

2) MILP Formulation

Firstly, the objective function is transformed into a linear function. According to SDT, there exists the same optimized solution for the primal and dual objective problem. As a result, the objective function in lower level can also be written as equation (7.2).

Minimize

$$\begin{aligned}
&\sum_{t\in T}\Big(\sum_{s\in\Omega_n^S}\lambda_s^{S,DA}\cdot P_{s,t}^{S,DA}+\sum_{b\in\Omega_n^B}\lambda_b^{B,DA}\cdot P_{b,t}^{B,DA}+\lambda_{c,t}^{CO,bid}\cdot P_{c,t}^{CO,DA}\\
&\qquad-\sum_{le\in\Omega_n^{Le}}\lambda_{le}^{Int,DA}\cdot P_{le,t}^{Int,DA}-\sum_{let\in\Omega_n^{Let}}\lambda_{let}^{et,DA}\cdot P_{let,t}^{et,DA}\\
&=-\sum_{m\in\Omega_n^N}f_{nm}^{max}\cdot\left(\mu_{nm,t}^{L,DA}+\mu_{nm,t}^{U,DA}\right)-\sum_{s\in\Omega_n^S}P_s^{max}\cdot\mu_{s,t}^{U,DA}\\
&\qquad-\sum_{b\in\Omega_n^B}P_b^{max}\cdot\mu_{b,t}^{U,DA}-\sum_{le\in\Omega_n^{Le}}P_{le}^{Int,max}\cdot\mu_{le,t}^{int,U,DA}\\
&\qquad-\sum_{let\in\Omega_n^{Let}}(P^{The}-P^{The,min})\cdot\mu_{let,t}^{et,U,DA}\\
&-P_{c,t}^{CO,bid}\cdot\mu_{c,t}^{U}-\sum_{n\in\Omega_n^N\setminus n:ref}\pi\cdot(\mu_{\theta,t}^{L,DA}+\mu_{\theta,t}^{U,DA}),\qquad\forall t
\end{aligned}\tag{7.2}$$

From constraints (7.1.4), the offer price for the coordinated supplier can be written as (7.3).

$$\lambda_{c,t}^{CO,bid}=\varphi_{n,t}-\mu_{c,t}^{U}+\mu_{c,t}^{L},\forall c,t \tag{7.3}$$

Therefore,

$$\lambda_{c,t}^{CO,bid}\cdot P_{c,t}^{CO,DA}=(\varphi_{n,t}-\mu_{c,t}^{U}+\mu_{c,t}^{L})\cdot P_{c,t}^{CO,DA},\forall c,t \tag{7.4}$$

From (7.1.19) to (7.1.20),

$$P_{c,t}^{CO,bid}\cdot\mu_{c,t}^{U}=P_{c,t}^{CO,DA}\cdot\mu_{c,t}^{U},\ \ \forall c,t \tag{7.5}$$

$$P_{c,t}^{CO,DA} \cdot \mu_{c,t}^{L} = 0, \forall c, t \tag{7.6}$$

Using (7.5) and (7.6) to simplify (7.4), then (7.7) can be obtained.

$$\lambda_{c,t}^{CO,bid} \cdot P_{c,t}^{CO,DA} = \varphi_{n,t} \cdot P_{c,t}^{CO,DA} - \mu_{c,t}^{U} \cdot P_{c,t}^{CO,bid}, \forall c, \forall t \tag{7.7}$$

Substitute $\lambda_{c,t}^{CO,bid} \cdot P_{c,t}^{CO,DA}$ in (7.2), then (7.8) can be obtained.

$$\begin{aligned} \varphi_{n,t} \cdot P_{c,t}^{CO,DA} = & \sum_{le \in \Omega_n^{Le}} \lambda_{le}^{Int,DA} \cdot P_{le,t}^{Int,DA} + \sum_{let \in \Omega_n^{Let}} \lambda_{let}^{et,DA} \cdot P_{let,t}^{et,DA} \\ & - \sum_{s \in \Omega_n^{S}} \lambda_{s}^{S,DA} \cdot P_{s,t}^{S,DA} - \sum_{b \in \Omega_n^{B}} \lambda_{b}^{B,DA} \cdot P_{b,t}^{B,DA} \\ & - \sum_{m \in \Omega_n^{N}} f_{nm}^{max} \cdot \left(\mu_{nm,t}^{L,DA} + \mu_{nm,t}^{U,DA} \right) - \sum_{s \in \Omega_n^{S}} P_{s}^{max} \cdot \mu_{s,t}^{U,DA} \\ & - \sum_{b \in \Omega_n^{B}} P_{b}^{max} \cdot \mu_{b,t}^{U,DA} - \sum_{le \in \Omega_n^{Le}} P_{le}^{Int,max} \cdot \mu_{le,t}^{int,U,DA} \\ & - \sum_{let \in \Omega_n^{Let}} (P^{The} - P^{The,min}) \cdot \mu_{let,t}^{et,U,DA} \\ & - \sum_{n \in \Omega_n^{N} \setminus n:ref} \pi \cdot \left(\mu_{\theta,t}^{L,DA} + \mu_{\theta,t}^{U,DA} \right), \forall t \end{aligned} \tag{7.8}$$

As a result, the proposed model can be transformed to a MILP problem, which includes the objective function (7.9) and constraints (7.9.1)-(7.9.29).

$$\begin{aligned} & \textstyle\sum_{t \in T} \big(\sum_{le \in \Omega_n^{Le}} \lambda_{le}^{Int,DA} \cdot P_{le,t}^{Int,DA} + \sum_{let \in \Omega_n^{Let}} \lambda_{let}^{et,DA} \cdot P_{let,t}^{et,DA} - \\ & \textstyle\sum_{s \in \Omega_n^{S}} \lambda_{s}^{S,DA} \cdot P_{s,t}^{S,DA} - \sum_{b \in \Omega_n^{B}} \lambda_{b}^{B,DA} \cdot P_{b,t}^{B,DA} - \sum_{m \in \Omega_n^{N}} f_{nm}^{max} \cdot \\ & \left(\mu_{nm,t}^{L,DA} + \mu_{nm,t}^{U,DA} \right) - \textstyle\sum_{s \in \Omega_n^{S}} P_{s}^{max} \cdot \mu_{s,t}^{U,DA} - \sum_{b \in \Omega_n^{B}} P_{b}^{max} \cdot \\ & \mu_{b,t}^{U,DA} - \textstyle\sum_{le \in \Omega_n^{Le}} P_{le}^{Int,max} \cdot \mu_{le,t}^{int,U,DA} - \sum_{let \in \Omega_n^{Let}} (P^{The} - \\ & P^{The,min}) \cdot \mu_{let,t}^{et,U,DA} - \textstyle\sum_{n \in \Omega_n^{N} \setminus n:ref} \pi \cdot \left(\mu_{\theta,t}^{L,DA} + \mu_{\theta,t}^{U,DA} \right) + \end{aligned} \tag{7.9}$$

$$\sum_{\beta\in N_\beta}\sum_{\alpha\in N_\alpha}\tau_\beta\cdot\tau_\alpha\cdot(\varphi_\alpha^{RT}\cdot P_{\alpha,\beta,c,t}^{CO,RT}-\lambda_{gas}\cdot P_{\alpha,\beta,i,t}^{IN}+\lambda_{reg,i,t}^{IN,up}\cdot$$

$$P_{\alpha,\beta,i,t}^{IN,up}+\lambda_{reg,i,t}^{IN,dn}\cdot P_{\alpha,\beta,i,t}^{IN,dn}))$$

Subject to

Constraints(7.1.1)-(7.1.8) (7.9.1)

$$0\le\mu_{nm,t}^{U,DA}\le Q^{max}\cdot\sigma_{nm,t}^{max},\forall m\in\Omega_n^N,t \quad (7.9.2)$$

$$0\le\mu_{nm,t}^{L,DA}\le Q^{min}\cdot\sigma_{n,m,t}^{min},\forall m\in\Omega_n^N,t \quad (7.9.3)$$

$$0\le\mu_{b,t}^{U,DA}\le Q^{max}\cdot\sigma_{b,t}^{max},\forall b\in\Omega_n^B,t \quad (7.9.4)$$

$$0\le\ \mu_{b,t}^{L,DA}\le Q^{min}\cdot\sigma_{b,t}^{min}\ ,\forall b\in\Omega_n^B,t \quad (7.9.5)$$

$$0\le\mu_{s,t}^{U,DA}\le Q^{max}\cdot\sigma_{s,t}^{max},\forall s\in\Omega_n^S,t \quad (7.9.6)$$

$$0\le\ \mu_{s,t}^{L,DA}\le Q^{min}\cdot\sigma_{s,t}^{min}\ ,\forall s\in\Omega_n^S,t \quad (7.9.7)$$

$$0\le\mu_{le,t}^{int,U,DA}\le Q^{max}\cdot\sigma_{le,t}^{max}\ \ ,\forall le\in\Omega_n^{Le},t \quad (7.9.8)$$

$$0\le\ \mu_{le,t}^{int,L,DA}\le Q^{min}\cdot\sigma_{le,t}^{min},\forall le\in\Omega_n^{Le},t \quad (7.9.9)$$

$$0\le\mu_{c,t}^{U}\le Q^{max}\cdot\sigma_{c,t}^{max},\forall c\in\Omega_n^C,t \quad (7.9.10)$$

$$0\le\mu_{c,t}^{L}\le Q^{min}\cdot\sigma_{c,t}^{min}\ ,\forall c\in\Omega_n^C,t \quad (7.9.11)$$

$$0\le\mu_{let,t}^{et,U,DA}\le Q^{max}\cdot\sigma_{let,t}^{max}\ ,\forall let\in\Omega_n^{Let},t \quad (7.9.12)$$

$$0\le\ \mu_{let,t}^{et,L,DA}\le Q^{min}\cdot\sigma_{let,t}^{min}\ ,\forall let\in\Omega_n^{Let},t \quad (7.9.13)$$

$$0\le\mu_{\theta,t}^{U,DA}\le Q^{max}\cdot\sigma_{\theta,t}^{max}\ ,\forall n\setminus n{:}ref,t \quad (7.9.14)$$

$$0\le\ \mu_{\theta,t}^{L,DA}\le Q^{min}\cdot\sigma_{\theta,t}^{min},\forall n\setminus n{:}ref,t \quad (7.9.15)$$

$$0\le f_{nm}^{max}-B_{nm}\cdot(\theta_{n,t}^{DA}-\theta_{m,t}^{DA})\le Q^{max}\cdot(1-\sigma_{n,m,t}^{max}),\forall m\in\Omega_n^N,t \quad (7.9.16)$$

$$0\le f_{nm}^{max}+B_{nm}\cdot(\theta_{n,t}^{DA}-\theta_{m,t}^{DA})\le Q^{min}\cdot(1-\sigma_{n,m,t}^{min}),\forall m\in\Omega_n^N,t \quad (7.9.17)$$

$$0\le P_b^{max}-P_{b,t}^{B,DA}\le Q^{max}\cdot(1-\sigma_{b,t}^{max}),\forall b\ \in\Omega_n^B,t \quad (7.9.18)$$

$$0\le P_{b,t}^{B,DA}\le Q^{min}\cdot(1-\sigma_{b,t}^{min}),\forall b\in\Omega_n^B,t \quad (7.9.19)$$

$$0 \le P_s^{max} - P_{s,t}^{S,DA} \le Q^{max} \cdot (1 - \sigma_{s,t}^{max}), \forall s \in \Omega_n^S, t \quad (7.9.20)$$

$$0 \le P_{s,t}^{S,DA} \le Q^{min} \cdot (1 - \sigma_{s,t}^{min}), \forall s \in \Omega_n^S, t \quad (7.9.21)$$

$$0 \le P_{le}^{Int,max} - P_{le,t}^{Int,DA} \le Q^{max} \cdot (1 - \sigma_{le,t}^{max}), \forall le \in \Omega_n^{Le}, t \quad (7.9.22)$$

$$0 \le P_{le,t}^{Int,DA} \le Q^{min} \cdot (1 - \sigma_{le,t}^{min}), \forall le \in \Omega_n^{Le}, t \quad (7.9.23)$$

$$0 \le (P^{The} - P^{The,min} - P_{let,t}^{et,DA} \le Q^{max} \cdot (1 - \sigma_{let,t}^{max}), \quad (7.9.24)$$

$$\forall let \in \Omega_n^{Let}, t$$

$$0 \le P_{let,t}^{et,DA} \le Q^{min} \cdot (1 - \sigma_{let,t}^{min}), \ \ \forall let \in \Omega_n^{Let}, t \quad (7.9.25)$$

$$0 \le P_{c,t}^{CO,bid} - \ P_{c,t}^{CO,DA} \le Q^{max} \cdot (1 - \sigma_{c,t}^{max}), \forall c \in \Omega_n^C, t \quad (7.9.26)$$

$$0 \le P_{c,t}^{CO,DA} \le Q^{min} \cdot (1 - \sigma_{c,t}^{min}), \forall c \in \Omega_n^c, t \quad (7.9.27)$$

$$0 \le \pi - \theta_{n,t}^{DA} \le Q^{max} \cdot (1 - \sigma_{n,t}^{max}), \ \ \forall n \setminus n{:}\, ref, t \quad (7.9.28)$$

$$0 \le \ \pi + \theta_{n,t}^{DA} \le Q^{min} \cdot (1 - \sigma_{n,t}^{min}), \ \ \forall n \setminus n{:}\, ref, t \quad (7.9.29)$$

In constraints (7.9.1)-(7.9.29), Q^{max} and Q^{min} are large enough constants. Besides, $\mu_{c,t}^{L}$, $\mu_{c,t}^{U}$, $\mu_{s,t}^{L,DA}$, $\mu_{s,t}^{U,DA}$, $\mu_{b,t}^{L,DA}$, $\mu_{b,t}^{U,DA}$, $\mu_{le,t}^{int,L,DA}$, $\mu_{le,t}^{int,U,DA}$, $\mu_{let,t}^{et,L,DA}$, $\mu_{let,t}^{et,U,DA}$, $\varphi_{n,t}$, $\mu_{nm,t}^{L,DA}$, $\mu_{nm,t}^{U,DA}$, $\mu_{\theta,t}^{DA}$, $\mu_{\theta,t}^{L,DA}$, $\mu_{\theta,t}^{U,DA}$ are auxiliary binary variables. ”

References

[1] J. Pinho, J. Resende, and I. Soares, "Capacity investment in electricity markets under supply and demand uncertainty," Energy, vol. 150, pp. 1006-1017, 2018/05/01/ 2018.

[2] E. Samani and F. Aminifar, "Tri-level robust investment planning of DERs in distribution networks with AC constraints," IEEE Transactions on Power Systems, vol. 34, no. 5, pp. 3749-3757, 2019.

[3] M. Z. Jacobson et al., "100% Clean and Renewable Wind, Water, and Sunlight All-Sector Energy Roadmaps for 139 Countries of the World," Joule, vol. 1, no. 1, pp. 108-121, 2017/09/06/ 2017.

[4] L. Chinmoy, S. Iniyan, and R. Goic, "Modeling wind power investments, policies and social benefits for deregulated electricity market–A review," Applied energy, vol. 242, pp. 364-377, 2019.

[5] P. Jain, Wind energy engineering. New York: McGraw-Hill, 2011.

[6] L. Baringo and A. J. Conejo, "Strategic Offering for a Wind Power Producer," IEEE Transactions on Power Systems, vol. 28, no. 4, pp. 4645-4654, 2013.

[7] J. C. Ketterer, "The impact of wind power generation on the electricity price in Germany," Energy Economics, vol. 44, pp. 270-280, 2014.

[8] Y. Xiao, X. Wang, X. Wang, C. Dang, and M. Lu, "Behavior analysis of wind power producer in electricity market," Applied Energy, vol. 171, pp. 325-335, 2016.

[9] M. Gonzalez Vaya and G. Andersson, "Self Scheduling of Plug-In Electric Vehicle Aggregator to Provide Balancing Services for Wind Power," IEEE Transactions on Sustainable Energy, vol. 7, no. 2, pp. 886-899, 2016.

[10] A. A. S. d. l. Nieta, J. Contreras, J. I. Muñoz, and M. O. Malley, "Modeling the Impact of a Wind Power Producer as a Price-Maker," IEEE Transactions on Power Systems, vol. 29, no. 6, pp. 2723-2732, 2014.

[11] M. Shafie-khah and J. P. S. Catalao, "A Stochastic Multi-Layer Agent-Based Model to Study Electricity Market Participants Behavior," IEEE Transactions on Power Systems, vol. 30, no. 2, pp. 867-881, 2015.

[12] D. J. Crow, P. Balcombe, N. Brandon, and A. D. Hawkes, "Assessing the impact of future greenhouse gas emissions from natural gas production," Science of the total environment, vol. 668, pp. 1242-1258, 2019.

[13] R. Zhang, Z. Y. Dong, Y. Xu, K. Meng, and K. P. Wong, "Short-term load forecasting of Australian National Electricity Market by an ensemble model of extreme learning machine," IET Generation, Transmission & Distribution, vol. 7, no. 4, pp. 391-397, 2013.

[14] H. Daneshi, M. Shahidehpour, and A. L. Choobbari, "Long-term load forecasting in electricity market," in 2008 IEEE International Conference on Electro/Information Technology, 2008, pp. 395-400: IEEE.

[15] A. T. Lora, J. M. R. Santos, A. G. Expósito, J. L. M. Ramos, and J. C. R. Santos, "Electricity market price forecasting based on weighted nearest neighbors techniques," IEEE Transactions on Power Systems, vol. 22, no. 3, pp. 1294-1301, 2007.

[16] X. Yan and N. A. Chowdhury, "Mid-term electricity market clearing price forecasting: A hybrid LSSVM and ARMAX approach," International Journal of Electrical Power & Energy Systems, vol. 53, pp. 20-26, 2013.

[17] M. Dicorato, G. Forte, M. Pisani, and M. Trovato, "Planning and operating combined wind-storage system in electricity market," IEEE Transactions on Sustainable Energy, vol. 3, no. 2, pp. 209-217, 2012.

[18] R. K. Mallick, R. Agrawal, and P. K. Hota, "Bidding strategies of Gencos and large consumers in competitive electricity market based on TLBO," in 2016 IEEE 6th International Conference on Power Systems (ICPS), 2016, pp. 1-6.

[19] T. Chung, S. Zhang, C. Yu, and K. Wong, "Electricity market risk management using forward contracts with bilateral options," IEE Proceedings-Generation, Transmission and Distribution, vol. 150, no. 5, pp. 588-594, 2003.

[20] M. Liu and F. F. Wu, "Risk management in a competitive electricity market," International Journal of Electrical Power & Energy Systems, vol. 29, no. 9, pp. 690-697, 2007.

[21] Y.-p. Zhang et al., "A survey of transmission congestion management in electricity markets," Power System Technology, vol. 8, pp. 1-9, 2003.

[22] A. K. David and F. Wen, "Strategic bidding in competitive electricity markets: a literature survey," in 2000 Power Engineering Society Summer Meeting (Cat. No. 00CH37134), 2000, vol. 4, pp. 2168-2173: IEEE.

[23] F. S. Gazijahani and J. Salehi, "IGDT-Based Complementarity Approach for Dealing With Strategic Decision Making of Price-Maker VPP Considering Demand Flexibility," IEEE Transactions on Industrial Informatics, vol. 16, no. 4, pp. 2212-2220, 2019.

[24] J. Arteaga and H. Zareipour, "A price-maker/price-taker model for the operation of battery storage systems in electricity markets," IEEE Transactions on Smart Grid, vol. 10, no. 6, pp. 6912-6920, 2019.

[25] A. Barbry, M. F. Anjos, E. Delage, and K. R. Schell, "Robust self-scheduling of a price-maker energy storage facility in the New York electricity market," Energy Economics, vol. 78, pp. 629-646, 2019.

[26] J. Iria, F. Soares, and M. Matos, "Optimal bidding strategy for an aggregator of prosumers in energy and secondary reserve markets," Applied Energy, vol. 238, pp. 1361-1372, 2019.

[27] M. Shahidehpour, H. Yamin, and Z. Li, Market operations in electric power systems: forecasting, scheduling, and risk management. John Wiley & Sons, 2003.

[28] M. H. Abbasi, M. Taki, A. Rajabi, L. Li, and J. Zhang, "Coordinated operation of electric vehicle charging and wind power generation as a virtual power plant: A multi-stage risk constrained approach," Applied Energy, vol. 239, pp. 1294-1307, 2019.

[29] B. Li, X. Wang, M. Shahidehpour, C. Jiang, and Z. Li, "DER Aggregator's Data-Driven Bidding Strategy Using the Information Gap Decision Theory in a Non-Cooperative Electricity Market," IEEE Transactions on Smart Grid, vol. 10, no. 6, pp. 6756-6767, 2019.

[30] B. Li, X. Wang, M. Shahidehpour, C. Jiang, and Z. Li, "Robust bidding strategy and profit allocation for cooperative DSR aggregators with correlated wind power generation," IEEE Transactions on Sustainable Energy, vol. 10, no. 4, pp. 1904-1915, 2018.

[31] D. Csercsik, "Competition and cooperation in a bidding model of electrical energy trade," Networks and Spatial Economics, vol. 16, no. 4, pp. 1043-1073, 2016.

[32] O. Ben-Moshe and O. D. Rubin, "Does wind energy mitigate market power in deregulated electricity markets?," Energy, vol. 85, pp. 511-521, 2015/06/01/ 2015.

[33] H. Wu, M. Shahidehpour, A. Alabdulwahab, and A. Abusorrah, "A Game Theoretic Approach to Risk-Based Optimal Bidding Strategies for Electric Vehicle Aggregators in Electricity Markets With Variable Wind Energy Resources," IEEE Transactions on Sustainable Energy, vol. 7, no. 1, pp. 374-385, 2016.

[34] M. Rahimiyan and L. Baringo, "Strategic bidding for a virtual power plant in the day-ahead and real-time markets: A price-taker robust optimization approach," IEEE Transactions on Power Systems, vol. 31, no. 4, pp. 2676-2687, 2015.

[35] S. P. Mathur and A. Arya, "Impact of emission trading on optimal bidding of price takers in a competitive energy market," in Harmony Search and Nature Inspired Optimization Algorithms: Springer, 2019, pp. 171-180.

[36] A. J. Conejo, J. Contreras, J. M. Arroyo, and S. De la Torre, "Optimal response of an oligopolistic generating company to a competitive pool-based electric

power market," IEEE transactions on power systems, vol. 17, no. 2, pp. 424-430, 2002.

[37] L. P. Garces and A. J. Conejo, "Weekly self-scheduling, forward contracting, and offering strategy for a producer," IEEE Transactions on Power Systems, vol. 25, no. 2, pp. 657-666, 2009.

[38] C. G. Baslis and A. G. Bakirtzis, "Mid-term stochastic scheduling of a price-maker hydro producer with pumped storage," IEEE Transactions on Power Systems, vol. 26, no. 4, pp. 1856-1865, 2011.

[39] J. Aghaei, M. Barani, M. Shafie-khah, A. A. S. d. l. Nieta, and J. P. S. Catalão, "Risk-Constrained Offering Strategy for Aggregated Hybrid Power Plant Including Wind Power Producer and Demand Response Provider," IEEE Transactions on Sustainable Energy, vol. 7, no. 2, pp. 513-525, 2016.

[40] A. Botterud et al., "Wind power trading under uncertainty in LMP markets," IEEE Transactions on power systems, vol. 27, no. 2, pp. 894-903, 2011.

[41] J. M. Angarita and J. G. Usaola, "Combining hydro-generation and wind energy: Biddings and operation on electricity spot markets," Electric Power Systems Research, vol. 77, no. 5, pp. 393-400, 2007/04/01/ 2007.

[42] M. Black and G. Strbac, "Value of bulk energy storage for managing wind power fluctuations," IEEE transactions on energy conversion, vol. 22, no. 1, pp. 197-205, 2007.

[43] S. Ghavidel, M. J. Ghadi, A. Azizivahed, J. Aghaei, L. Li, and J. Zhang, "Risk-Constrained Bidding Strategy for a Joint Operation of Wind Power and CAES Aggregators," IEEE Transactions on Sustainable Energy, vol. 11, no. 1, pp. 457-466, 2019.

[44] A. Rabiee, A. Soroudi, B. Mohammadi-Ivatloo, and M. Parniani, "Corrective voltage control scheme considering demand response and stochastic wind power," IEEE Transactions on Power Systems, vol. 29, no. 6, pp. 2965-2973, 2014.

[45] J. Mohammadi, A. Rahimi-Kian, and M. S. Ghazizadeh, "Aggregated wind power and flexible load offering strategy," IET Renewable Power Generation, vol. 5, no. 6, pp. 439-447, 2011.

[46] E. Heydarian-Forushani, M. P. Moghaddam, M. K. Sheikh-El-Eslami, M. Shafie-khah, and J. P. S. Catalão, "Risk-Constrained Offering Strategy of Wind Power Producers Considering Intraday Demand Response Exchange," IEEE Transactions on Sustainable Energy, vol. 5, no. 4, pp. 1036-1047, 2014.

[47] M. H. Abbasi et al., "Risk-constrained offering strategies for a price-maker demand response aggregator," in 2017 20th International Conference on Electrical Machines and Systems (ICEMS), 2017, pp. 1-6.

[48] P. Cappers, C. Goldman, and D. Kathan, "Demand response in U.S. electricity markets: Empirical evidence," Energy, vol. 35, no. 4, pp. 1526-1535, 2010/04/01/ 2010.

[49] P. Hanemann and T. Bruckner, "Effects of electric vehicles on the spot market price," Energy, vol. 162, pp. 255-266, 2018/11/01/ 2018.

[50] E. A. M. Ceseña and P. Mancarella, "Energy systems integration in smart districts: robust optimisation of multi-energy flows in integrated electricity, heat and gas networks," IEEE Transactions on Smart Grid, vol. 10, no. 1, pp. 1122-1131, 2018.

[51] Y. Li et al., "Optimal Stochastic Operation of Integrated Low-Carbon Electric Power, Natural Gas, and Heat Delivery System," IEEE Transactions on Sustainable Energy, vol. 9, no. 1, pp. 273-283, 2018.

[52] T. Ma, J. Wu, L. Hao, W.-J. Lee, H. Yan, and D. Li, "The optimal structure planning and energy management strategies of smart multi energy systems," Energy, vol. 160, pp. 122-141, 2018.

[53] G. Li, R. Zhang, T. Jiang, H. Chen, L. Bai, and X. Li, "Security-constrained bi-level economic dispatch model for integrated natural gas and electricity systems considering wind power and power-to-gas process," Applied energy, vol. 194, pp. 696-704, 2017.

[54] D. Xu, Q. Wu, B. Zhou, C. Li, L. Bai, and S. Huang, "Distributed Multi-Energy Operation of Coupled Electricity, Heating and Natural Gas Networks," IEEE Transactions on Sustainable Energy, 2019.

[55] M. Yazdani-Damavandi, N. Neyestani, M. Shafie-khah, J. Contreras, and J. P. Catalao, "Strategic behavior of multi-energy players in electricity markets as aggregators of demand side resources using a bi-level approach," IEEE Transactions on Power Systems, vol. 33, no. 1, pp. 397-411, 2017.

[56] H. Cui, F. Li, Q. Hu, L. Bai, and X. Fang, "Day-ahead coordinated operation of utility-scale electricity and natural gas networks considering demand response based virtual power plants," Applied Energy, vol. 176, pp. 183-195, 2016/08/15/ 2016.

[57] Y. Li, W. Liu, M. Shahidehpour, F. Wen, K. Wang, and Y. Huang, "Optimal Operation Strategy for Integrated Natural Gas Generating Unit and Power-to-Gas Conversion Facilities," IEEE Transactions on Sustainable Energy, vol. 9, no. 4, pp. 1870-1879, 2018.

[58] V. Davatgaran, M. Saniei, and S. S. Mortazavi, "Optimal bidding strategy for an energy hub in energy market," Energy, vol. 148, pp. 482-493, 2018/04/01/ 2018.

[59] M. Jenabi, S. M. T. F. Ghomi, and Y. Smeers, "Bi-Level Game Approaches for Coordination of Generation and Transmission Expansion Planning Within a Market Environment," IEEE Transactions on Power Systems, vol. 28, no. 3, pp. 2639-2650, 2013.

[60] M. R. Salehizadeh and S. Soltaniyan, "Application of fuzzy Q-learning for electricity market modeling by considering renewable power penetration," Renewable and Sustainable Energy Reviews, vol. 56, pp. 1172-1181, 2016/04/01/ 2016.

[61] C. Dou, D. Yue, X. Li, and Y. Xue, "MAS-Based Management and Control Strategies for Integrated Hybrid Energy System," IEEE Transactions on Industrial Informatics, vol. 12, no. 4, pp. 1332-1349, 2016.

[62] M. Shafie-khah, E. Heydarian-Forushani, M. E. H. Golshan, M. P. Moghaddam, M. K. Sheikh-El-Eslami, and J. P. S. Catalão, "Strategic Offering for a Price-Maker Wind Power Producer in Oligopoly Markets Considering Demand Response Exchange," IEEE Transactions on Industrial Informatics, vol. 11, no. 6, pp. 1542-1553, 2015.

[63] J. Xiao, X. Kong, Q. Jin, H. You, K. Cui, and Y. Zhang, "Demand-Responsive Virtual Power Plant Optimization Scheduling Method Based on Competitive Bidding Equilibrium," Energy Procedia, vol. 152, pp. 1158-1163, 2018/10/01/ 2018.

[64] S. Najafi, M. Shafie-khah, P. Siano, W. Wei, and J. P. Catalão, "Reinforcement Learning Method for Plug-In Electric Vehicle Bidding," IET Smart Grid, 2019.

[65] Q. Huang, Q.-S. Jia, and X. Guan, "A multi-timescale and bilevel coordination approach for matching uncertain wind supply with EV charging demand," IEEE Transactions on Automation Science and Engineering, vol. 14, no. 2, pp. 694-704, 2016.

[66] S. I. Vagropoulos, C. K. Simoglou, and A. G. Bakirtzis, "Synergistic supply offer and demand bidding strategies for wind producers and electric vehicle aggregators in day-ahead electricity markets," in 2013 IREP Symposium Bulk Power System Dynamics and Control-IX Optimization, Security and Control of the Emerging Power Grid, 2013, pp. 1-13: IEEE.

[67] A. Tavakoli, M. Negnevitsky, and K. M. Muttaqi, "Pool strategy of a producer coordinated with vehicle-to-grid services to maximize profitability," in 2015 Australasian Universities Power Engineering Conference (AUPEC), 2015, pp. 1-6: IEEE.

[68] J. Qiu, J. Zhao, H. Yang, and Z. Y. Dong, "Optimal scheduling for prosumers in coupled transactive power and gas systems," IEEE Transactions on Power Systems, vol. 33, no. 2, pp. 1970-1980, 2017.

[69] S. Y. Kan, B. Chen, X. F. Wu, Z. M. Chen, and G. Q. Chen, "Natural gas overview for world economy: From primary supply to final demand via global supply chains," Energy Policy, vol. 124, pp. 215-225, 2019/01/01/ 2019.

[70] R. Zhang, T. Jiang, F. F. Li, G. Li, H. Chen, and X. Li, "Coordinated Bidding Strategy of Wind Farms and Power-to-Gas Facilities using a Cooperative Game Approach," IEEE Transactions on Sustainable Energy, 2020.

[71] Y. Yuan, F.-Y. Wang, and D. Zeng, "Competitive analysis of bidding behavior on sponsored search advertising markets," IEEE Transactions on Computational Social Systems, vol. 4, no. 3, pp. 179-190, 2017.

[72] A. González-Garrido, H. Gaztañaga, A. Saez-de-Ibarra, A. Milo, and P. Eguia, "Electricity and reserve market bidding strategy including sizing evaluation and a novel renewable complementarity-based centralized control for storage lifetime enhancement," Applied Energy, vol. 262, p. 114591, 2020.

[73] S. Yu, S. Yang, Y. Li, and J. Geng, "Distributed energy transaction mechanism design based on smart contract," in 2018 China International Conference on Electricity Distribution (CICED), 2018, pp. 2790-2793: IEEE.

[74] J. Bower and D. W. Bunn, "Model-based comparisons of pool and bilateral markets for electricity," The energy journal, pp. 1-29, 2000.

[75] A. Weidlich and D. Veit, "A critical survey of agent-based wholesale electricity market models," Energy Economics, vol. 30, no. 4, pp. 1728-1759, 2008.

[76] H. Nehrir, K. Dehghanpour, J. Sheppard, and N. Kelly, "Agent-Based Modeling of Retail Electrical Energy Markets with Demand Response," in 2018 IEEE Power & Energy Society General Meeting (PESGM), 2018, pp. 1-1.

[77] S. Najafi, M. Shafie-khah, P. Siano, W. Wei, and J. P. S. Catalão, "Reinforcement learning method for plug-in electric vehicle bidding," IET Smart Grid, vol. 2, no. 4, pp. 529-536, 2019.

[78] Y. Ye, D. Qiu, M. Sun, D. Papadaskalopoulos, and G. Strbac, "Deep Reinforcement Learning for Strategic Bidding in Electricity Markets," IEEE Transactions on Smart Grid, pp. 1-1, 2019.

[79] N. Rashedi, M. A. Tajeddini, and H. Kebriaei, "Markov game approach for multi-agent competitive bidding strategies in electricity market," IET Generation, Transmission & Distribution, vol. 10, no. 15, pp. 3756-3763, 2016.

[80] R. Hao, Q. Ai, and Z. Jiang, "Bilayer game strategy of regional integrated energy system under multi-agent incomplete information," The Journal of Engineering, vol. 2019, no. 16, pp. 1285-1291, 2019.

[81] I. Praça, C. Ramos, Z. Vale, and M. Cordeiro, "MASCEM: a multiagent system that simulates competitive electricity markets," IEEE Intelligent Systems, vol. 18, no. 6, pp. 54-60, 2003.

[82] H. Kebriaei, A. Rahimi-Kian, and M. N. Ahmadabadi, "Model-Based and Learning-Based Decision Making in Incomplete Information Cournot Games: A State Estimation Approach," IEEE Transactions on Systems, Man, and Cybernetics: Systems, vol. 45, no. 4, pp. 713-718, 2015.

[83] M. Bowling and M. Veloso, "Multiagent learning using a variable learning rate," Artificial Intelligence, vol. 136, no. 2, pp. 215-250, 2002/04/01/ 2002.

[84] X. Gao, K. W. Chan, S. Xia, B. Zhou, X. Lu, and D. Xu, "Risk-constrained offering strategy for a hybrid power plant consisting of wind power producer and electric vehicle aggregator," Energy, vol. 177, pp. 183-191, 2019/06/15/ 2019.

[85] J. A. Momoh, Electric power system applications of optimization. CRC press, 2017.

[86] V. Gabrel, C. Murat, and A. Thiele, "Recent advances in robust optimization: An overview," European journal of operational research, vol. 235, no. 3, pp. 471-483, 2014.

[87] A. Zare, C. Chung, J. Zhan, and S. O. Faried, "A distributionally robust chance-constrained MILP model for multistage distribution system planning with uncertain renewables and loads," IEEE Transactions on Power Systems, vol. 33, no. 5, pp. 5248-5262, 2018.

[88] H. Heitsch and W. Romisch, "Generation of multivariate scenario trees to model stochasticity in power management," in 2005 IEEE Russia Power Tech, 2005, pp. 1-7: IEEE.

[89] M. Dyer and L. Stougie, "Computational complexity of stochastic programming problems," mathematical programming, vol. 106, no. 3, pp. 423-432, 2006.

[90] D. Pozo and J. Contreras, "A chance-constrained unit commitment with an $ nK $ security criterion and significant wind generation," IEEE Transactions on Power systems, vol. 28, no. 3, pp. 2842-2851, 2012.

[91] K. Høyland and S. W. Wallace, "Generating scenario trees for multistage decision problems," Management science, vol. 47, no. 2, pp. 295-307, 2001.

[92] A. Papavasiliou, S. S. Oren, and R. P. O'Neill, "Reserve requirements for wind power integration: A scenario-based stochastic programming framework," IEEE Transactions on Power Systems, vol. 26, no. 4, pp. 2197-2206, 2011.

[93] P.-L. Liu and A. Der Kiureghian, "Multivariate distribution models with prescribed marginals and covariances," Probabilistic Engineering Mechanics, vol. 1, no. 2, pp. 105-112, 1986.

[94] N. Growe-Kuska, H. Heitsch, and W. Romisch, "Scenario reduction and scenario tree construction for power management problems," in 2003 IEEE Bologna Power Tech Conference Proceedings, 2003, vol. 3, p. 7 pp. Vol.3.

[95] J. M. Morales, S. Pineda, A. J. Conejo, and M. Carrion, "Scenario Reduction for Futures Market Trading in Electricity Markets," IEEE Transactions on Power Systems, vol. 24, no. 2, pp. 878-888, 2009.

[96] H. Heitsch and W. Römisch, "A note on scenario reduction for two-stage stochastic programs," Operations Research Letters, vol. 35, no. 6, pp. 731-738, 2007.

[97] L. Rao, X. Liu, L. Xie, and Z. Pang, "Hedging against uncertainty: A tale of internet data center operations under smart grid environment," IEEE Transactions on Smart Grid, vol. 2, no. 3, pp. 555-563, 2011.

[98] A. Baillo, M. Ventosa, M. Rivier, and A. Ramos, "Optimal offering strategies for generation companies operating in electricity spot markets," IEEE Transactions on Power Systems, vol. 19, no. 2, pp. 745-753, 2004.

[99] S. Moazeni, A. H. Miragha, and B. Defourny, "A risk-averse stochastic dynamic programming approach to energy hub optimal dispatch," IEEE Transactions on Power Systems, vol. 34, no. 3, pp. 2169-2178, 2018.

[100] Z. Ding, L. Xie, Y. Lu, P. Wang, and S. Xia, "Emission-aware stochastic resource planning scheme for data center microgrid considering batch workload scheduling and risk management," IEEE Transactions on Industry Applications, vol. 54, no. 6, pp. 5599-5608, 2018.

[101] C. Li, Y. Xu, X. Yu, C. Ryan, and T. Huang, "Risk-averse energy trading in multienergy microgrids: A two-stage stochastic game approach," IEEE Transactions on Industrial Informatics, vol. 13, no. 5, pp. 2620-2630, 2017.

[102] E. Borgonovo and L. Peccati, "Financial management in inventory problems: Risk averse vs risk neutral policies," International Journal of Production Economics, vol. 118, no. 1, pp. 233-242, 2009.

[103] J. Kettunen, A. Salo, and D. W. Bunn, "Optimization of electricity retailer's contract portfolio subject to risk preferences," IEEE Transactions on Power Systems, vol. 25, no. 1, pp. 117-128, 2009.

[104] M. K. AlAshery, D. Xiao, and W. Qiao, "Second-Order Stochastic Dominance Constraints for Risk Management of a Wind Power Producer's Optimal Bidding Strategy," IEEE Transactions on Sustainable Energy, 2019.

[105] D. Yu, A. G. Ebadi, K. Jermsittiparsert, N. H. Jabarullah, M. V. Vasiljeva, and S. Nojavan, "Risk-constrained stochastic optimization of a concentrating solar power plant," IEEE Transactions on Sustainable Energy, 2019.

[106] L. Guo, T. Sriyakul, S. Nojavan, and K. Jermsittiparsert, "Risk-Based Traded Demand Response Between Consumers' Aggregator and Retailer Using Downside Risk Constraints Technique," IEEE Access, vol. 8, pp. 90957-90968, 2020.

[107] M. Ghamkhari, H. Mohsenian-Rad, and A. Wierman, "Optimal risk-aware power procurement for data centers in day-ahead and real-time electricity markets," in 2014 IEEE Conference on Computer Communications Workshops (INFOCOM WKSHPS), 2014, pp. 610-615: IEEE.

[108] J. E. Hernandez, F. Kreikebaum, and D. Divan, "Flexible electric vehicle (EV) charging to meet renewable portfolio standard (RPS) mandates and minimize green house Gas emissions," in 2010 IEEE Energy Conversion Congress and Exposition, 2010, pp. 4270-4277: IEEE.

[109] M. Mahvi and M. M. Ardehali, Optimal bidding strategy in a competitive electricity market based on agent-based approach and numerical sensitivity analysis. 2011, pp. 6367–6374.

[110] S. Djørup, J. Z. Thellufsen, and P. Sorknæs, "The electricity market in a renewable energy system," Energy, vol. 162, pp. 148-157, 2018.

[111] Y. Gao et al., "Optimal operation modes of photovoltaic-battery energy storage system based power plants considering typical scenarios," Protection and Control of Modern Power Systems, vol. 2, no. 1, p. 36, 2017.

[112] M. H. Abbasi et al., "Risk-constrained offering strategies for a price-maker demand response aggregator," in Electrical Machines and Systems (ICEMS), 2017 20th International Conference on, 2017, pp. 1-6: IEEE.

[113] L. Baringo and A. J. Conejo, "Offering Strategy of Wind-Power Producer: A Multi-Stage Risk-Constrained Approach," IEEE Transactions on Power Systems, vol. 31, no. 2, pp. 1420-1429, 2016.

[114] C. Ruiz and A. J. Conejo, "Pool Strategy of a Producer With Endogenous Formation of Locational Marginal Prices," IEEE Transactions on Power Systems, vol. 24, no. 4, pp. 1855-1866, 2009.

[115] X. Wu, X. Wang, J. Li, J. Guo, K. Zhang, and J. Chen, "A joint operation model and solution for hybrid wind energy storage systems," Proceedings of the CSEE, vol. 33, no. 13, pp. 10-17, 2013.

[116] I. G. Sardou, M. E. Khodayar, and M. T. Ameli, "Coordinated operation of natural gas and electricity networks with microgrid aggregators," IEEE Transactions on Smart Grid, vol. 9, no. 1, pp. 199-210, 2016.

[117] Z. Ji and X. Huang, "Coordinated bidding strategy in synchronized electricity and natural gas markets," in 2017 Asian Conference on Energy, Power and Transportation Electrification (ACEPT), 2017, pp. 1-6: IEEE.

[118] Y. Li, Z. Li, F. Wen, and M. Shahidehpour, "Minimax-Regret Robust Co-Optimization for Enhancing the Resilience of Integrated Power Distribution and Natural Gas Systems," IEEE Transactions on Sustainable Energy, vol. 11, no. 1, pp. 61-71, 2018.

[119] S. D. Manshadi and M. E. Khodayar, "Coordinated operation of electricity and natural gas systems: a convex relaxation approach," IEEE Transactions on Smart Grid, vol. 10, no. 3, pp. 3342-3354, 2018.

[120] J. Qiu et al., "A linear programming approach to expansion co-planning in gas and electricity markets," IEEE Transactions on Power Systems, vol. 31, no. 5, pp. 3594-3606, 2015.

[121] B. Bahmani-Firouzi, S. Sharifinia, R. Azizipanah-Abarghooee, and T. Niknam, "Scenario-Based Optimal Bidding Strategies of GENCOs in the Incomplete Information Electricity Market Using a New Improved Prey—Predator Optimization Algorithm," IEEE Systems Journal, vol. 9, no. 4, pp. 1485-1495, 2015.

[122] H. Yang, S. Zhang, J. Qiu, D. Qiu, M. Lai, and Z. Dong, "CVaR-Constrained Optimal Bidding of Electric Vehicle Aggregators in Day-Ahead and Real-Time Markets," IEEE Transactions on Industrial Informatics, vol. 13, no. 5, pp. 2555-2565, 2017.

[123] B. Zhou et al., "Optimal Coordination of Electric Vehicles for Virtual Power Plants with Dynamic Communication Spectrum Allocation," IEEE Transactions on Industrial Informatics, 2020.

[124] E. Heydarian-Forushani, M. P. Moghaddam, M. K. Sheikh-El-Eslami, M. Shafie-khah, and J. P. Catalão, "Risk-constrained offering strategy of wind power producers considering intraday demand response exchange," IEEE Transactions on sustainable energy, vol. 5, no. 4, pp. 1036-1047, 2014.

[125] T. W. Hill and A. Ravindran, "On programming with absolute-value functions," Journal of Optimization Theory and Applications, vol. 17, no. 1, pp. 181-183, 1975.

[126] K. Hwang, W. Jiang, and Y. Chen, "Pheromone-Based Planning Strategies in Dyna-Q Learning," IEEE Transactions on Industrial Informatics, vol. 13, no. 2, pp. 424-435, 2017.

[127] A. C. Tellidou and A. G. Bakirtzis, "Multi-Agent Reinforcement Learning for Strategic Bidding in Power Markets," in 2006 3rd International IEEE Conference Intelligent Systems, 2006, pp. 408-413.

[128] T. Krause, E. V. Beck, R. Cherkaoui, A. Germond, G. Andersson, and D. Ernst, "A comparison of Nash equilibria analysis and agent-based modelling for power markets," International Journal of Electrical Power & Energy Systems, vol. 28, no. 9, pp. 599-607, 2006/11/01/ 2006.

[129] E. G. Kardakos, C. K. Simoglou, and A. G. Bakirtzis, "Short-Term Electricity Market Simulation for Pool-Based Multi-Period Auctions," IEEE Transactions on Power Systems, vol. 28, no. 3, pp. 2526-2535, 2013.

[130] L. Gallego, O. Duarte, and A. Delgadillo, "Strategic bidding in Colombian electricity market using a multi-agent learning approach," in 2008 IEEE/PES Transmission and Distribution Conference and Exposition: Latin America, 2008, pp. 1-7.

[131] L. Panait and S. Luke, "Cooperative Multi-Agent Learning: The State of the Art," Autonomous Agents and Multi-Agent Systems, vol. 11, no. 3, pp. 387-434, 2005.

[132] L. Xi, T. Yu, B. Yang, and X. Zhang, "A novel multi-agent decentralized win or learn fast policy hill-climbing with eligibility trace algorithm for smart

generation control of interconnected complex power grids," Energy Conversion and Management, vol. 103, pp. 82-93, 2015/10/01/ 2015.

[133] S. Xia, X. Luo, K. W. Chan, M. Zhou, and G. Li, "Probabilistic transient stability constrained optimal power flow for power systems with multiple correlated uncertain wind generations," IEEE Transactions on Sustainable Energy, vol. 7, no. 3, pp. 1133-1144, 2016.

[134] A. M. L. Da Silva, R. A. Fernandez, and C. Singh, "Generating capacity reliability evaluation based on Monte Carlo simulation and cross-entropy methods," IEEE Transactions on Power Systems, vol. 25, no. 1, pp. 129-137, 2010.

[135] Y. Guo, J. Xiong, S. Xu, and W. Su, "Two-stage economic operation of microgrid-like electric vehicle parking deck," IEEE Transactions on Smart Grid, vol. 7, no. 3, pp. 1703-1712, 2015.

[136] M. Bowling and M. Veloso, "Multiagent learning using a variable learning rate," Artificial Intelligence, vol. 136, no. 2, pp. 215-250, 2002/04/01/ 2002.

[137] L. Xi, T. Yu, B. Yang, and X. Zhang, "A novel multi-agent decentralized win or learn fast policy hill-climbing with eligibility trace algorithm for smart generation control of interconnected complex power grids," Energy Conversion and Management, vol. 103, pp. 82-93, 2015/10/01/ 2015.